The Effects of Initial Conditions and Liquid Composition on the One-Dimensional Consolidation Behaviour of Clay-Based Sealing Materials

NWMO TR-2008-06 March 2008

D. G. Priyanto[1]
J. A. Blatz[2]
G. A. Siemens[3]
R. Offman[2]
J. S. Boyle[3]
D. A. Dixon[1]

[1]Atomic Energy of Canada Limited
[2]University of Manitoba
[3]Royal Military College of Canada

nwmo
NUCLEAR WASTE MANAGEMENT ORGANIZATION
SOCIÉTÉ DE GESTION DES DÉCHETS NUCLÉAIRES

Nuclear Waste Management Organization
22 St. Clair Avenue East, 6th Floor
Toronto, Ontario
M4T 2S3
Canada

Tel: 416-934-9814
Web: www.nwmo.ca

The Effects of Initial Conditions and Liquid Composition on the One-Dimensional Consolidation Behaviour of Clay-Based Sealing Materials

NWMO TR-2008-06

March 2008

D. G. Priyanto[1]
J. A. Blatz[2]
G. A. Siemens[3]
R. Offman[2]
J. S. Boyle[3]
D. A. Dixon[1]

[1]Atomic Energy of Canada Limited;
[2]University of Manitoba;
[3]Royal Military College of Canada

ABSTRACT

Title: **The Effects of Initial Conditions and Liquid Composition on the One-Dimensional Consolidation Behaviour of Clay-Based Sealing Materials**
Report No.: NWMO TR-2008-06
Author(s): D. G. Priyanto[1], J. A. Blatz[2], G. A. Siemens[3], R. Offman[2], J. S. Boyle[3], and D. A. Dixon[1]
Company: [1]Atomic Energy of Canada Limited;
[2]University of Manitoba;
[3]Royal Military College of Canada
Date: March 2008

Abstract
Groundwaters at proposed repository depths of 500 to 1000 m can contain significant quantities of soluble salts (Gascoyne et al. 1987; Mazurek 2004). These salts have the potential to affect the hydraulic-mechanical behaviour of clay-based sealing materials installed in a Deep Geologic Repository (DGR) of the type presented by Russell and Simmons (2003) and Maak and Simmons (2005). As a result of the influence of liquid salinity on material behaviour, one of the design decisions for the engineering of a sealing system is whether to prepare the sealing materials with fresh or saline liquid (Baumgartner et al. 2008) and to determine if this will affect the performance of the barrier materials.

The results of one-dimensional (1D) consolidation tests conducted in 2007 on three clay-based sealing materials including: Highly Compacted Bentonite (HCB); Dense Backfill (DBF); and Light Backfill (LBF) are presented and discussed. Testing was conducted at three different laboratories: Atomic Energy of Canada Limited (AECL)'s geotechnical laboratory at the Underground Research Laboratory (URL) (HCB); the University of Manitoba (U of M) (DBF); and the Royal Military College of Canada (RMC) (LBF).

The 1D consolidation tests are used to examine the effects of: boundary conditions and applied load during initial saturation; and high pore liquid salinities (up to 250 g/L $CaCl_2$) used in specimen preparation and as a reservoir liquid. Parameters to define the mechanical behaviour (i.e., Compression Index (C_c) and Swelling Index (C_s)) of the HCB, DBF, and LBF have been determined from the results of these tests. The values of these parameters were found to decrease with an increase in concentration of calcium chloride ($CaCl_2$) solution in pore liquid. The relationship of these parameters to the pore liquid composition is suggested for use in defining the mechanical behaviour of clay-based sealing materials in THM numerical modelling.

TABLE OF CONTENTS

LIST OF TABLES

Page

LIST OF FIGURES

Page

1. INTRODUCTION

Several sealing-system components are proposed for use in an emplacement-room sealing system (e.g., the CTECH-type in-room placement method shown in Figure 1) in a deep geological repository (DGR) for used nuclear fuel (Russell and Simmons 2003; Gierszewski et al. 2004; Maak and Simmons 2005). For the clay-based portions of the repository sealing system, five sealing-system components are being considered.

1. Highly Compacted Bentonite (HCB) – 100% bentonite clay either installed at high dry density by in-situ compaction or prefabricated as blocks.
2. Bentonite-Sand Buffer (BSB) – a mixture of bentonite clay and silica sand either installed at high dry density by in-situ compaction or prefabricated as blocks (shown in Figure 1 as "Compacted Buffer").
3. Dense Backfill (DBF) – a mixture of lake clay, crushed host rock and bentonite clay, either installed at high dry density by in-situ compaction or prefabrication as blocks.
4. Light Backfill (LBF) – a mixture of bentonite clay and silica sand, likely installed in the form of dense pellets and installed at low-to-medium dry density.
5. Gapfill (GF) – either bentonite clay, possibly fabricated in the form of dense pellets, silica sand or some combination of the two, which are likely to be installed at low-to-medium average dry density.

Some suggested compositions and fundamental physical characteristics of these candidate sealing-system components are presented in Table 1.

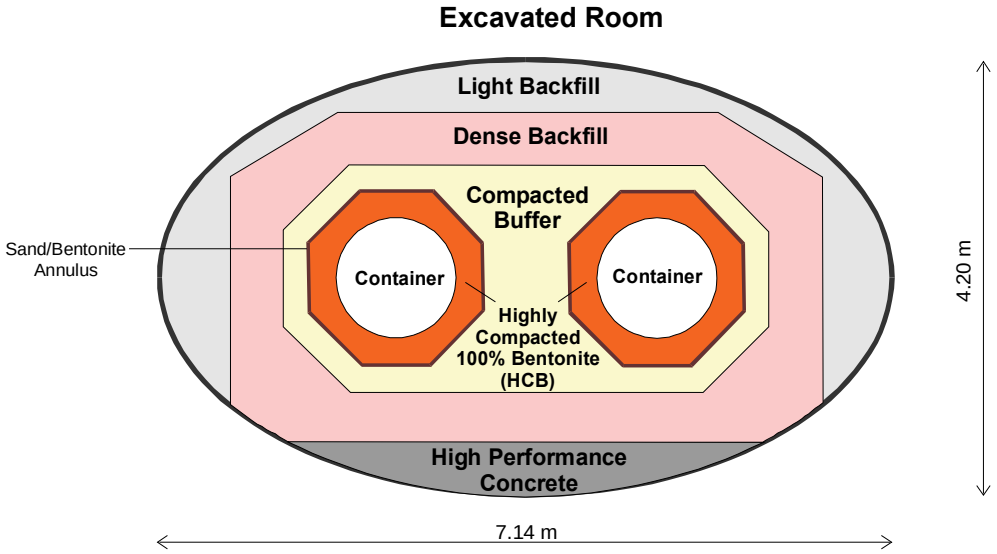

Figure 1: In-room Placement Cross-sectional Geometry (CTECH 2002)

Table 1: Physical Characteristics of Engineering Barriers System Components
(after Russell and Simmons 2003)

Property	HCB	BSB	GF	DBF	LBF
Composition (dry mass %)	100% bentonite	50% bentonite 50% sand	100% bentonite	5% bentonite 25% glacial lake clay 70% crushed granite	50% bentonite 50% sand
Initial Gravimetric Water Content (%)	17	18.5	2	8.5	15
As-Placed Saturation (%)	65	80	6	80	33
Dry Density (Mg/m^3)	1.61	1.69	1.40	2.12	1.24
EMDD (Mg/m^3)*	1.50	1.15	1.25	0.8	0.66

* assumes that all bentonites have a minimum 75% montmorillonite content

1.1 BACKGROUND

The chemistry of the pore liquid strongly affects the swelling potential and hydraulic conductivity of bentonite clay. Groundwaters at proposed repository depths of 500 to 1000 m can contain significant quantities of soluble salts and an increase in salinity is known to decrease the swelling potential and increase the hydraulic conductivity (Dixon 2000) of barrier materials containing a swelling clay mineral component.

Gascoyne et al. (1987) and Mazurek (2004) have collated data from the crystalline rock of the Canadian Shield and the sedimentary rock in southern Ontario, respectively, and very high concentrations of soluble salts can exist. Salt concentrations also typically vary with depth, tending to be low near the surface and increasing with depth. Salt concentrations also vary considerably throughout the Canadian Shield. Salinities, in terms of Total Dissolved Solids (TDS) at proposed repository depths, can vary from 8 to >100 g/L in the Canadian Shield to greater than 200 g/L in Ordovician-age sediments. Salt speciation is often Na-Ca-Cl at shallow depth trending to Ca-Na-Cl at greater depth.

The observation of the role that the chemistry of the pore liquid plays in the behaviour of bentonite clay has been largely limited to NaCl solutions using constant-volume load cells (Dixon 2000), which does not provide comparative data on Ca-rich groundwaters. The presence of $CaCl_2$ in groundwater makes testing of clay-based sealing materials with $CaCl_2$ solutions of importance in confirming their behaviour. One-dimensional (1D) consolidation tests have recently been completed at salinities up to 100 g/L $CaCl_2$ in order to start the process of increasing the behavioural database for sealing materials (Baumgartner et al. 2008). Baumgartner et al. (2008) observed that specimen preparation affected the behaviour of the clay-based sealing materials. One of the design decisions for the engineering of a sealing system is the choice for preparing the sealing materials with either fresh or saline water.

With identification of high salinity conditions (TDS > 200 g/L) in the Canadian Shield (Gascoyne et al. 1987, Mazurek 2004) the range of liquid concentrations examined by Baumgartner et al.

(2008) needs to be extended. This report investigates the effect of salinities up to 250 g/L $CaCl_2$ on the behaviour of HCB, DBF, and LBF using 1D consolidation tests. In response to potential effects of different methods of specimen preparation (mixing with saline solution (i.e., 250 g/L $CaCl_2$ solution) and mixing with Distilled Water (DW)), sample preparation with both liquids is examined.

In related studies, the results of the triaxial testing on unsaturated Bentonite-Sand-Buffer material have also shown that boundary conditions affect both the hydraulic (H) and mechanical (M) behaviour (Siemens 2006). In those tests, two types of boundary conditions (i.e., constant volume and constant pressure) were applied during the initial saturation to examine the effect of boundary conditions applied at the early stage of the tests. In the tests described in the current study, both constant pressure and constant volume conditions were also examined.

The primary goal of the stress-strain testing described in this report is to provide physically-measured parameter values. The values are used in Thermal-Hydraulic-Mechanical (THM) models to simulate the behaviour of clay-based sealing materials in a repository. THM numerical modelling requires the parameters of thermal (T), hydraulic (H) and mechanical (M) constitutive models. The results of 1D consolidation tests are used to interpret the parameters of mechanical (M) and hydraulic (H) constitutive models. Comparison of the results of 1D consolidation tests with various pore liquid concentrations provides a measure of to what degree the parameters of these constitutive models are affected by the pore liquid salinity.

1.2 OBJECTIVES

The objectives of the 1D consolidation tests done in 2007 are to:

1. examine the effect of higher pore liquid salinity (up to 250 g/L $CaCl_2$);
2. examine the effects of different mixing liquid used in specimen preparation and boundary conditions during initial saturation; and
3. define mechanical and hydraulics parameters interpreted from the 1D consolidation tests that include the effect of liquid composition in the pore liquid of clay-based sealing materials for use in THM modelling.

1.3 SCOPE OF THE WORK

1.3.1 1D Consolidation of HCB, DBF, and LBF in 2006

The work done during 2006 consisted of a series of laboratory 1D consolidation tests on three clay-based sealing materials (i.e., HCB, DBF, and LBF). Testing was divided between Atomic Energy of Canada Limited (AECL)'s geotechnical laboratory at the Underground Research Laboratory (URL), the Department of Civil Engineering at the University of Manitoba (U of M), and Department of Civil Engineering at Lakehead University (LHU). Each group was assigned a material-type to test. AECL tested the HCB, U of M tested the DBF, and LHU tested the LBF. The 2006 work investigated the effect of pore liquid concentration on the mechanical behaviour of HCB, DBF, and LBF using 1D consolidation tests (i.e., up to 100 g/L $CaCl_2$ for DBF and LBF specimens, and 75 g/L $CaCl_2$ for HCB specimens).

1.3.2 1D Consolidation of HCB, DBF, and LBF in 2007

During 2007 AECL continued testing of HCB specimens, and the U of M continued testing of DBF specimens. Due to resourcing issues at LHU in 2007, testing of LBF specimens was shifted to the Department of Civil Engineering at the Royal Military College of Canada (RMC) under the supervision of Dr. Siemens, who has worked previously in testing of swelling clay materials at the U of M. This report presents the results of 1D consolidation tests on HCB, DBF, and LBF conducted in 2007.

2. MATERIALS

The following three sealing-system components are tested in the series of consolidation tests.

- HCB, composed of 100% (by weight) Wyoming MX80 bentonite (montmorillonite content ~75%).
- LBF, composed of 50% (by weight) Avonlea (Saskatchewan) bentonite (montmorillonite content ~80%) and 50% (by weight) silica sand.
- DBF, composed of 75% (by weight) crushed granite, 18.75% crushed illite clay (Sealbond) and 6.25% (by weight) Avonlea bentonite (montmorillonite content ~80%). This DBF composition differs from that provided in Table 1 due to the desire to use a material consistent with that used in previous work on DBF.

3. EQUIPMENT

Three different sizes of cells are required since each material has very different swelling and mechanical properties. Conventional 50-mm-diameter consolidation rings that allow 19-thick specimens to be tested are used for the LBF. Larger cells, 101-mm-in-diameter and allowing a 101-mm-thick specimen, are used to test the DBF to accommodate the large size of the aggregate (i.e., up to 35-mm granite chips). Small-diameter oedometer cells (i.e., 28.1 mm diameter) are used to test the HCB, which permit application of high stress (i.e., maximum 16 MPa). All the cells are fabricated from non-corrosive material. No corrosion effects were observed in any of the tests conducted in 2007.

Conventional dead-weight-type oedometers are used to test the DBF and LBF and data are collected by manually monitoring the deformation of these two materials. The very high swelling capacity and associated high swelling pressure in HCB require a different type of testing system to be used for that material. In testing the HCB a small-diameter, thick-walled cell is used in a compression frame that has hydraulic rams installed. Each hydraulic ram is actuated by a high-pressure nitrogen-gas cylinder acting on a gas-over-oil accumulator. An LVDT is used to measure the displacement of the specimen and connected to a data logger. A second frame using a servo-hydraulic testing system manufactured by the MTS® (Materials Testing Services) added in 2007 to test the HCB. This additional equipment enables application of different boundary conditions in the tests (i.e., constant volume or constant pressure).

4. TESTING PROGRAM (2006 TO 2007)

4.1 ONE-DIMENSIONAL (1D) CONSOLIDATION TESTS IN 2006

Tables 2, 4, and 6 show the test matrices for the 1D consolidation tests conducted in 2006 on HCB, DBF, and LBF specimens, respectively. Baumgartner et al. (2008) summarized the results of these tests. The objectives of the testing program were: to determine H-M parameters from 1D consolidation test results; and to investigate the effect of pore liquid salinity (up to 75 g/L $CaCl_2$ for HCB specimens and 100 g/L $CaCl_2$ for LBF and DBF specimens).

4.2 ONE-DIMENSIONAL (1D) CONSOLIDATION TESTS IN 2007

Tables 2, 4, and 7 show the test matrices for the 1D consolidation tests conducted in 2007 on the HCB, DBF, and LBF specimens, respectively. The results of these tests are discussed in this report in Appendices A, B, and C for HCB, DBF, and LBF specimens respectively.

Four (4) tests on HCB were planned at AECL, four (4) tests on the DBF were planned at the U of M, and six (6) tests on LBF were planned at the RMC. AECL provided the material (i.e., DBF and LBF) and the specification of initial conditions, including target initial dry density, liquid used in specimen preparation, and liquid added to the tests.

Considering the availability of the equipment and additional work required to prepare additional specimens, HCB11 was added to provide more data defining the relationship of compression index (C_c) and swelling index (C_s) versus concentration of $CaCl_2$ in the pore liquid. This relationship can be used to include the effect of concentration of $CaCl_2$ in the pore liquid to the mechanical behaviour of sealing material.

The testing programs in the year of 2007 were designed to address the objectives presented in Section 1.2 and to compare these results to the results of 1D consolidation tests completed in 2006 (Baumgartner et al. 2008).

Table 2: Test Matrix for 1D Consolidation Test of HCB Material (2006 to 2007)

Test No.	Sample No.	Mixing Liquid	Reservoir Liquid	Dry Density (Mg/m^3)	Degree of Saturation (%)	Gravimetric Water Content (%)	Boundary Condition during Initial Water Uptake	Target Swelling on Initial Water Uptake (%)	Loading Sequence	Status	Testing Location	Reference
2006												
Effect of pore fluid concentration on mechanical behaviour of HCB (up to 75 g/L $CaCl_2$)												
1	HCB1	DW	DW	1.65	90	21.5	CP	100% at 1 MPa	Load to 1, 2, 4, 8, & 16 MPa; Unload to 8, 4, & 2 MPa	Completed	AECL	Baumgartner et al. (2008)
2	HCB2	DW	DW	1.65	90	21.5	CP	Attempt rigid confinement with no LVDT displcement beginning at 1 MPa	Load to 1 & 16 MPa; Unload to 8, 4, 2, & 1 MPa	Completed	AECL	Baumgartner et al. (2008)
3	HCB3	75 g/L $CaCl_2$	75 g/L $CaCl_2$	1.65	90	21.5	CP	100% at 1 MPa	Load to 1, 2, 4, & 8 MPa; Unload to 4, 2, & 1 MPa; Load to 4, 8, & 16 MPa	Completed	AECL	Baumgartner et al. (2008)
4	HCB4	75 g/L $CaCl_2$	75 g/L $CaCl_2$	1.65	90	21.5	CP	100% at 8 MPa	Load to 8 MPa; Unload to 4, 2, & 1 MPa; Load to 1, 2, 4, 8,& 16 MPa	Completed	AECL	Baumgartner et al. (2008)
5	HCB5	DW	DW	1.40	91	31	CP	100% at 1 MPa	Load to 1, 2, 4, 8, & 16 MPa; Unload to 8, 4, 2, & 1 MPa; Load to 2, 4, 8, & 16 MPa	Completed	AECL	Baumgartner et al. (2008)
6	HCB6	75 g/L $CaCl_2$	75 g/L $CaCl_2$	1.40	91	31	CP	100% at 1 MPa	Load to 1, 2, 4, 8, & 16 MPa; Unload to 8, 4, 2, & 1 MPa; Load to 2, 4, 8, & 16 MPa	Completed	AECL	Baumgartner et al. (2008)
2007												
Effect of pore fluid concentration, mixing liquid, initial boundary condition on mechanical behaviour of HCB (higher concentration: 250 g/L $CaCl_2$)												
7	HCB7	DW	250 g/L $CaCl_2$	1.65	95	23	CP	100% at 1 MPa	Load to 1, 2, 4, 8, & 16 MPa; Unload to 8, 4, 2, & 1 MPa.	Completed	AECL	Priyanto et al. (2008)
8	HCB8	250 g/L $CaCl_2$	250 g/L $CaCl_2$	1.65	95	20	CP	100% at 1 MPa	Load to 1, 2, 4, 8, & 16 MPa; Unload to 8, 4, 2, & 1 MPa.	Completed	AECL	Priyanto et al. (2008)
9	HCB9	DW	DW	1.65	95	23	CV	0	Load to 1, 2, 4, 8, & 16 MPa; Unload to 8, 4, 2, & 1 MPa.	Completed	AECL	Priyanto et al. (2008)
10	HCB10	250 g/L $CaCl_2$	250 g/L $CaCl_2$	1.65	95	20	CV	0	Load to 1, 2, 4, 8, & 16 MPa; Unload to 8, 4, 2, & 1 MPa.	Completed	AECL	Priyanto et al. (2008)
11	HCB11*	DW	150 g/L $CaCl_2$	1.65	95	23	CP	100% at 1 MPa	Load to 1, 2, 4, 8, & 16 MPa; Unload to 8, 4, 2, & 1 MPa.	Completed	AECL	Priyanto et al. (2008)

Note: *HCB11 was added to the original test matrix in 2007
CP = Constant Pressure; CV = Constant Volume; DW = Distilled Water

Table 3: Test Matrix Plan for 1D Consolidation Test of HCB Material (2008 and Beyond)

Test No.	Sample No.	Mixing Liquid	Reservoir Liquid	Dry Density (Mg/m^3)	Degree of Saturation (%)	Gravimetric Water Content (%)	Boundary Condition during Initial Water Uptake	Target Swelling on Initial Water Uptake (%)	Loading Sequence	Status	Testing Location	Reference
2008												
Effect of different fluid type (250 g/L NaCl)												
12	???	DW	250 g/L NaCl	1.65	95	23	CP	100% at 1 MPa	Load to 1, 2, 4, 8, & 16 MPa; Unload to 8, 4, 2, & 1 MPa.	Planned	AECL	NA
13	???	DW	250 g/L NaCl	1.65	95	23	CV	0	Load to 1, 2, 4, 8, & 16 MPa; Unload to 8, 4, 2, & 1 MPa.	Planned	AECL	NA
14	???	250 g/L NaCl	250 g/L NaCl	1.65	95	NA	CP	100% at 1 MPa	Load to 1, 2, 4, 8, & 16 MPa; Unload to 8, 4, 2, & 1 MPa.	Planned	AECL	NA
15	???	250 g/L NaCl	250 g/L NaCl	1.65	95	NA	CV	0	Load to 1, 2, 4, 8, & 16 MPa; Unload to 8, 4, 2, & 1 MPa.	Planned	AECL	NA
2009 - ….												
Alternative 1: More data to define the effect of NaCl concentration (Cc & Cs versus NaCl concentration)												
16	???	DW	150 g/L NaCl	1.65	95	23	CP	100% at 1 MPa	Load to 1, 2, 4, 8, & 16 MPa; Unload to 8, 4, 2, & 1 MPa.	Planned	AECL	NA
17	???	DW	150 g/L NaCl	1.65	95	23	CV	0	Load to 1, 2, 4, 8, & 16 MPa; Unload to 8, 4, 2, & 1 MPa.	Planned	AECL	NA
18	???	150 g/L NaCl	150 g/L NaCl	1.65	95	NA	CP	100% at 1 MPa	Load to 1, 2, 4, 8, & 16 MPa; Unload to 8, 4, 2, & 1 MPa.	Planned	AECL	NA
19	???	150 g/L NaCl	150 g/L NaCl	1.65	95	NA	CV	0	Load to 1, 2, 4, 8, & 16 MPa; Unload to 8, 4, 2, & 1 MPa.	Planned	AECL	NA
Alternative 2: Examining the effect of artificial ground water ($NaCl+CaCl_2$)												
20	???	DW	Artificial GW	1.65	95	23	CP	100% at 1 MPa	Load to 1, 2, 4, 8, & 16 MPa; Unload to 8, 4, 2, & 1 MPa.	Planned	AECL	NA
21	???	DW	Artificial GW	1.65	95	23	CV	0	Load to 1, 2, 4, 8, & 16 MPa; Unload to 8, 4, 2, & 1 MPa.	Planned	AECL	NA
22	???	Artificial GW	Artificial GW	1.65	95	NA	CP	100% at 1 MPa	Load to 1, 2, 4, 8, & 16 MPa; Unload to 8, 4, 2, & 1 MPa.	Planned	AECL	NA
23	???	Artificial GW	Artificial GW	1.65	95	NA	CV	0	Load to 1, 2, 4, 8, & 16 MPa; Unload to 8, 4, 2, & 1 MPa.	Planned	AECL	NA

Note: *HCB11 was added to the original test matrix in 2007
CP = Constant Pressure; CV = Constant Volume; DW = Distilled Water
Artificial GW = mixture of NaCl and $CaCl_2$ solution.

Table 4: Test Matrix for 1D Consolidation Test of DBF Material (2006 to 2007)

Test No.	Sample No.	Mixing Liquid	Reservoir Liquid	Bulk Density (Mg/m^3)	Degree of Saturation (%)	Gravimetric Water Content (%)	Boundary Condition during Initial Water Uptake	Target Swelling on Initial Water Uptake (%)	Loading Sequence	Status	Testing Location	Reference
2006												
Effect of pore fluid concentration on mechanical behaviour of DBF (up to 100 g/L $CaCl_2$)												
1	DBF1	DW	DW	2.3	NA	10.6	CP	20% at low load*	Load to 245, 490, 975, 1950, 3900 kPa; Unload to 975, 245 kPa	Completed	U of M	Baumgartner et al. (2008)
2	DBF2	DW	DW	2.3	NA	10.6	CV	Rigidly confined**	Load to 245, 490, 975, 1950, 3900 kPa; Unload to 975, 245 kPa	Completed	U of M	Baumgartner et al. (2008)
3	DBF3	100 g/L $CaCl_2$	100 g/L $CaCl_2$	2.3	NA	10.6	CP	20% at low load*	Load to 245, 490, 975, 1950, 3900 kPa; Unload to 975, 245 kPa	Completed	U of M	Baumgartner et al. (2008)
4	DBF4	100 g/L $CaCl_2$	100 g/L $CaCl_2$	2.3	NA	10.6	CV	Rigidly confined**	Load to 245, 490, 975, 1950, 3900 kPa; Unload to 975, 245 kPa	Completed	U of M	Baumgartner et al. (2008)
5	DBF5	DW	DW	2.3	NA	10.6	NA	Immediately loaded to 1 MPa	Load to 1, 2, and 4 MPa; Unload to 2, 1, and 0.5 MPa; Load to 1, 2, and 4 MPa	Completed	U of M	Baumgartner et al. (2008)
6	DBF6	100 g/L $CaCl_2$	100 g/L $CaCl_2$	2.3	NA	10.6	CP	Immediately loaded to 1 MPa	Load to 1, 2, and 4 MPa; Unload to 2, 1, and 0.5 MPa; Load to 1, 2, and 4 MPa	Completed	U of M	Baumgartner et al. (2008)
2007												
Effect of pore fluid concentration, mixing liquid, initial boundary condition on mechanical behaviour of DBF (higher concentration: 250 g/L $CaCl_2$)												
7	DBF1 (2007)	DW	250 g/L $CaCl_2$	2.3	NA	10.6	CP	100% at 1 MPa	Load to 1, 2, 4 MPa; Unload to 2, 1, and 0.5 MPa	In progress	U of M	Priyanto et al. (2008)
8	DBF2 (2007)	250 g/L $CaCl_2$	250 g/L $CaCl_2$	2.3	NA	10.6	CP	100% at 1 MPa	Load to 1, 2, 4 MPa; Unload to 2, 1, and 0.5 MPa	In progress	U of M	Priyanto et al. (2008)
9	DBF3 (2007)	DW	DW	2.3	NA	10.6	CV	0	Load to 1, 2, 4 MPa; Unload to 2, 1, and 0.5 MPa	In progress	U of M	Priyanto et al. (2008)
10	DBF4 (2007)	250 g/L $CaCl_2$	250 g/L $CaCl_2$	2.3	NA	10.6	CV	0	Load to 1, 2, 4 MPa; Unload to 2, 1, and 0.5 MPa	In progress	U of M	Priyanto et al. (2008)

Note: CP = Constant Pressure; CV = Constant Volume; DW = Distilled Water

Table 5: Test Matrix Plan for 1D Consolidation Test of DBF Material (2008 and Beyond)

Test No.	Sample No.	Mixing Liquid	Reservoir Liquid	Bulk Density (Mg/m^3)	Degree of Saturation (%)	Gravimetric Water Content (%)	Boundary Condition during Initial Water Uptake	Target Swelling on Initial Water Uptake (%)	Loading Sequence	Status	Testing Location	Reference
2008												
Effect of different fluid type (250 g/L NaCl)												
11	???	DW	250 g/L NaCl	2.3	NA	10.6	CP	100% at 1 MPa	Load to 1, 2, 4 MPa; Unload to 2, 1, and 0.5 MPa?	Planned	U of M	NA
12	???	DW	250 g/L NaCl	2.3	NA	10.6	CV	0	Load to 1, 2, 4 MPa; Unload to 2, 1, and 0.5 MPa?	Planned	U of M	NA
13	???	250 g/L NaCl	250 g/L NaCl	2.3	NA	10.6	CP	100% at 1 MPa	Load to 1, 2, 4 MPa; Unload to 2, 1, and 0.5 MPa?	Planned	U of M	NA
14	???	250 g/L NaCl	250 g/L NaCl	2.3	NA	10.6	CV	0	Load to 1, 2, 4 MPa; Unload to 2, 1, and 0.5 MPa?	Planned	U of M	NA
Alternative 1: More data to define the effect of NaCl concentration (Cc & Cs versus NaCl concentration)												
15	???	DW	150 g/L NaCl	1.65	95	23	CP	100% at 1 MPa	Load to 1, 2, 4 MPa; Unload to 2, 1, and 0.5 MPa?	Planned	U of M	NA
16	???	DW	150 g/L NaCl	1.65	95	23	CV	0	Load to 1, 2, 4 MPa; Unload to 2, 1, and 0.5 MPa?	Planned	U of M	NA
17	???	150 g/L NaCl	150 g/L NaCl	1.65	95	NA	CP	100% at 1 MPa	Load to 1, 2, 4 MPa; Unload to 2, 1, and 0.5 MPa?	Planned	U of M	NA
18	???	150 g/L NaCl	150 g/L NaCl	1.65	95	NA	CV	0	Load to 1, 2, 4 MPa; Unload to 2, 1, and 0.5 MPa?	Planned	U of M	NA
Alternative 2: Examining the effect of artificial ground water ($NaCl+CaCl_2$)												
19	???	DW	Artificial GW	1.65	95	23	CP	100% at 1 MPa	Load to 1, 2, 4 MPa; Unload to 2, 1, and 0.5 MPa?	Planned	U of M	NA
20	???	DW	Artificial GW	1.65	95	23	CV	0	Load to 1, 2, 4 MPa; Unload to 2, 1, and 0.5 MPa?	Planned	U of M	NA
21	???	Artificial GW	Artificial GW	1.65	95	NA	CP	100% at 1 MPa	Load to 1, 2, 4 MPa; Unload to 2, 1, and 0.5 MPa?	Planned	U of M	NA
22	???	Artificial GW	Artificial GW	1.65	95	NA	CV	0	Load to 1, 2, 4 MPa; Unload to 2, 1, and 0.5 MPa?	Planned	U of M	NA

Note: CP = Constant Pressure; CV = Constant Volume; DW = Distilled Water
Artificial GW = mixture of NaCl and $CaCl_2$ solution.

Table 6: Test Matrix for 1D Consolidation Test of LBF Material (2006)

Test No.	Sample No.	Mixing Liquid	Reservoir Liquid	Dry Density (Mg/m^3)	Degree of Saturation (%)	Gravimetric Water Content (%)	Boundary Condition during Initial Water Uptake	Swelling on Initial Water Uptake (%)	Loading Sequence	Status	Testing Location	Reference
2006												
Effect of pore fluid concentration on mechanical behaviour of LBF (up to 100 g/L $CaCl_2$)												
1	HB3	As supplied by AECL*	DW	1.24	NA	NA	NA	19.50%	After initial swelling; Load to , 111, 221, 332, 667, 1326 kPa; Unload to 668, 336, 166, 55 kPa	Completed	LHU	Baumgartner et al. (2008)
	HB6	As supplied by AECL*	DW	1.24	NA	NA	NA	20.80%	After initial swelling; Load to 166, 332, 664, 1326, 2652, 3986 kPa; Unload to 1326, 668, 336, 167, 57 kPa	Completed	LHU	Baumgartner et al. (2008)
	HB8	As supplied by AECL*	DW	1.24	NA	NA	NA	22.40%	After initial swelling; Load to 166, 332, 664, 1326, 2652 kPa; Unload to 1326, 668 kPa	Completed	LHU	Baumgartner et al. (2008)
2a	HB2	As supplied by AECL*	DW	1.24	NA	NA	NA	Rigidly confined	Load to 55, 81, 161, 332, 663, 1326, 2651 kPa	Completed	LHU	Baumgartner et al. (2008)
	HB4	As supplied by AECL*	DW	1.24	NA	NA	NA	Rigidly confined	Load to 55, 80, 166, 332, 665, 1328, 2654 kPa; Unload to 1328, 666 kPa	Completed	LHU	Baumgartner et al. (2008)
2b	HB7	As supplied by AECL*	DW	1.3	NA	NA	NA	Rigidly confined	Unload (let swell to 21.2%); Load to 167, 332, 664, 1326, 2652, 3986 kPa; Unload to 2652, 1326, and 664 kPa	Completed	LHU	Baumgartner et al. (2008)
	HB9	As supplied by AECL*	DW	1.3	NA	NA	NA	Rigidly confined	Unload (let swell to 21.2%); Load to 165, 331, 663, 1336, 2659 kPa; Unload to 1336, 663, 331, 165, and 55 kPa	Completed	LHU	Baumgartner et al. (2008)

Note: CP = Constant Pressure; CV = Constant Volume; DW = Distilled Water

Table 6: Test Matrix for 1D Consolidation Test of LBF Material (2006) (concluded)

Test No.	Sample No.	Mixing Liquid	Reservoir Liquid	Dry Density (Mg/m^3)	Degree of Saturation (%)	Gravimetric Water Content (%)	Boundary Condition during Initial Water Uptake	Swelling on Initial Water Uptake (%)	Loading Sequence	Status	Testing Location	Reference
2006												
Effect of pore fluid concentration on mechanical behaviour of LBF (up to 100 g/L $CaCl_2$)												
3	HB11	As supplied by AECL*	100 g/L $CaCl_2$	1.3	NA	NA	NA	10.40%	After initial swelling; Load to 25, 55, 166, 332, 664, 1326, 2661, 3990 kPa; Unload to 2661, 1326, 664, 166, 55 kPa	Completed	LHU	Baumgartner et al. (2008)
	HB12	As supplied by AECL*	100 g/L $CaCl_2$	1.3	NA	NA	NA	7.50%	After initial swelling; Load to 25, 55, 166, 336, 676, 1340, 2675 kPa; Unload to 1340, 676, 167, 57 kPa	Completed	LHU	Baumgartner et al. (2008)
	HB19	As supplied by AECL*	100 g/L $CaCl_2$	1.3	NA	NA	NA	6.30%	After initial swelling; Load to 1, 25, 55, 166, 332, 663, 1326, 2660 kPa; Unload to 1326, 668, 166, 55 kPa	Completed	LHU	Baumgartner et al. (2008)
4	HB14	As supplied by AECL*	100 g/L $CaCl_2$	1.3	NA	NA	NA	Rigidly confined	Unload, let swell to 3.6%; Load to 57, 167, 336, 668, 1343, 2673, 4000 kPa; Unload to 2673, 1343, 668, 336, 167, 57 kPa	Completed	LHU	Baumgartner et al. (2008)
5	HB13	100 g/L $CaCl_2$	100 g/L $CaCl_2$	1.3	NA	NA	NA	6.40%	After initial swelling, Load to 25, 55, 166, 332, 663, 1327, 2650 kPa; Unload to 1327, 663, 332, 166, and 55 kPa	Completed	LHU	Baumgartner et al. (2008)
	HB15	100 g/L $CaCl_2$	100 g/L $CaCl_2$	1.3	NA	NA	NA	7.10%	After initial swelling, Load to 25, 55, 166, 332, 664, 1327, 2656, 3985 kPa; Unload to 1327, 336, 166, 55 kPa	Completed	LHU	Baumgartner et al. (2008)
6	HB16	As supplied by AECL*	200 g/L $CaCl_2$	1.3	NA	NA	NA	6.10%	After initial swelling, Load to 25, 55, 166, 332, 663, 1327, 2650 kPa; Unload to 1327, 663, 332, 166, 55 kPa	Completed	LHU	Baumgartner et al. (2008)

Note: CP = Constant Pressure; CV = Constant Volume; DW = Distilled Water

Table 7: Test Matrix for 1D Consolidation Test of LBF Material (2007)

Test No.	Sample No.	Mixing Liquid	Reservoir Liquid	Dry Density (Mg/m^3)	Degree of Saturation (%)	Gravimetric Water Content (%)	Boundary Condition during Initial Water Uptake	Swelling on Initial Water Uptake (%)	Loading Sequence	Status	Testing Location	Reference
2007												
Effect of pore fluid concentration, mixing liquid, initial boundary condition on mechanical behaviour of LBF (higher concentration: 250 g/L $CaCl_2$)												
7	LBF_1	250 g/L $CaCl_2$	250 g/L $CaCl_2$	1.3	NA	19.1	CP	8.3% at 1 MPa	After initial swelling, Load to 55, 110, 220, 439, 878, 1702 kPa; Unload to 878, 439, 220, 110, 55 kPa.	Completed	RMC	Priyanto et al. (2008)
8	LBF_2	DW	250 g/L $CaCl_2$	1.3	NA	19.1	CP	4.2% at 1 MPa	After initial swelling, Load to 55, 110, 220, 441, 882, 1709 kPa; Unload to 882, 220, 110, and 55 kPa.	Completed	RMC	Priyanto et al. (2008)
9	LBF_3	250 g/L $CaCl_2$	250 g/L $CaCl_2$	1.3	NA	19.1	CV	Rigidly confined	After initial swelling, Load to 55, 110, 220, 441, 879, 1703 kPa; Unload to 879, 440, 220, 110 and 55 kPa.	Completed	RMC	Priyanto et al. (2008)
10	LBF_4	DW	250 g/L $CaCl_2$	1.3	NA	19.1	CV	Rigidly confined	After initial swelling, Load to 55, 110, 220, 441, 882, 1709 kPa; Unload to 882, 441, 220, 110 and 55 kPa.	Completed	RMC	Priyanto et al. (2008)
11	LBF_5B	100 g/L $CaCl_2$	100 g/L $CaCl_2$	1.3	NA	19.1	CP	7.7% at 1 MPa	After initial swelling, Load to 55, 110, 220, 439, 878, 1701 kPa; Unload to 878, 439, 220, 110 and 55 kPa.	Completed	RMC	Priyanto et al. (2008)
12	LBF_6	DW	100 g/L $CaCl_2$	1.3	NA	19.1	CV	Rigidly confined	After initial swelling, Load to 55, 110, 220, 441, 883, 1711 kPa; Unload to 883, 441, 220, 110 and 55 kPa.	Completed	RMC	Priyanto et al. (2008)

Note: CP = Constant Pressure; CV = Constant Volume; DW = Distilled Water

Table 8: Test Matrix Plan for 1D Consolidation Test of LBF Material (2008 and Beyond)

Test No.	Sample No.	Mixing Liquid	Reservoir Liquid	Dry Density (Mg/m^3)	Degree of Saturation (%)	Gravimetric Water Content (%)	Boundary Condition during Initial Water Uptake	Swelling on Initial Water Uptake (%)	Loading Sequence	Status	Testing Location	Reference
2008												
Effect of different fluid type (250 g/L NaCl)												
13	???	DW	250 g/L NaCl	1.3	NA	19.1	CP	NA?	Load to 1700 kPa; Unload to 55 kPa?	Planned	RMC	NA
14	???	DW	250 g/L NaCl	1.3	NA	19.1	CV	NA?	Load to 1700 kPa; Unload to 55 kPa?	Planned	RMC	NA
15	???	250 g/L NaCl	250 g/L NaCl	1.3	NA	19.1	CP	NA?	Load to 1700 kPa; Unload to 55 kPa?	Planned	RMC	NA
16	???	250 g/L NaCl	250 g/L NaCl	1.3	NA	19.1	CV	NA?	Load to 1700 kPa; Unload to 55 kPa?	Planned	RMC	NA
2009 - ….												
Alternative 1: More data to define the effect of NaCl concentration (Cc & Cs versus NaCl concentration)												
17	???	DW	150 g/L NaCl	1.3	NA	19.1	CP	100% at 1 MPa	Load to 1, 2, 4, 8, & 16 MPa; Unload to 8, 4, 2, & 1 MPa?	Planned	AECL	NA
18	???	DW	150 g/L NaCl	1.3	NA	19.1	CV	0	Load to 1, 2, 4, 8, & 16 MPa; Unload to 8, 4, 2, & 1 MPa?	Planned	AECL	NA
19	???	150 g/L NaCl	150 g/L NaCl	1.3	NA	19.1	CP	100% at 1 MPa	Load to 1, 2, 4, 8, & 16 MPa; Unload to 8, 4, 2, & 1 MPa?	Planned	AECL	NA
20	???	150 g/L NaCl	150 g/L NaCl	1.3	NA	19.1	CV	0	Load to 1, 2, 4, 8, & 16 MPa; Unload to 8, 4, 2, & 1 MPa?	Planned	AECL	NA
Alternative 2: Examining the effect of artificial ground water ($NaCl+CaCl_2$)												
21	???	DW	Artificial GW	1.3	NA	19.1	CP	100% at 1 MPa	Load to 1, 2, 4, 8, & 16 MPa; Unload to 8, 4, 2, & 1 MPa?	Planned	AECL	NA
22	???	DW	Artificial GW	1.3	NA	19.1	CV	0	Load to 1, 2, 4, 8, & 16 MPa; Unload to 8, 4, 2, & 1 MPa?	Planned	AECL	NA
23	???	Artificial GW	Artificial GW	1.3	NA	19.1	CP	100% at 1 MPa	Load to 1, 2, 4, 8, & 16 MPa; Unload to 8, 4, 2, & 1 MPa?	Planned	AECL	NA
24	???	Artificial GW	Artificial GW	1.3	NA	19.1	CV	0	Load to 1, 2, 4, 8, & 16 MPa; Unload to 8, 4, 2, & 1 MPa?	Planned	AECL	NA

Note: CP = Constant Pressure; CV = Constant Volume; DW = Distilled Water
Artificial GW = mixture of NaCl and $CaCl_2$ solution.

5. SUMMARY OF THE RESULTS

5.1 MECHANICAL CONSTITUTIVE MODEL PARAMETERS

Mechanical constitutive model parameters for the HCB, DBF, and LBF are interpreted from the results of 1D consolidation tests. Log-linear relationships are used to interpret the mechanical behaviour of the soils. The parameters C_c and C_s are the slope in loading and reloading , respectively, obtained from the void ratio (e) versus vertical stress (σ_v) plot as illustrated in Figure 2. Figures 3, 4, and 5 show the void ratio (e) versus vertical stress (σ_v) of the HCB, DBF, and LBF, respectively. Currently, a total of thirty-nine (39) 1D consolidation tests have been completed: 11 tests on the HCB; 8 tests on the DBF; and 20 tests on the LBF. Figure 6 shows the comparison of the HCB, DBF, and LBF. The compression index (C_c) and swelling index (C_s) are interpreted from the results of 1D consolidation tests. The parameters C_c and C_s for the HCB, DBF, and LBF are presented in Tables 9, 10, and 11, respectively. A discussion of the testing program for each type of material is presented in Appendices A, B, and C.

Combined with the results of triaxial tests that define the behaviour of soil during shearing and the failure criteria, these parameters can be used to evaluate soil behaviour using a critical state model (e.g., modified cam-clay (MCC) (Roscoe and Burland 1968)).

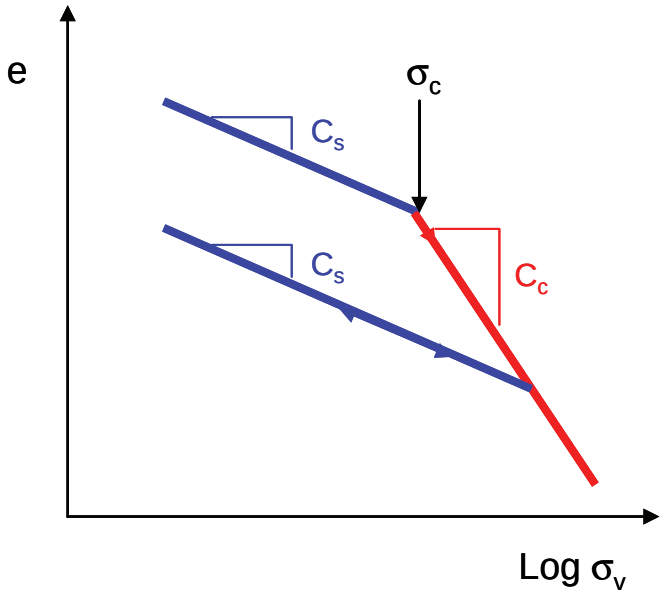

Figure 2: Definition of Parameters C_c and C_s

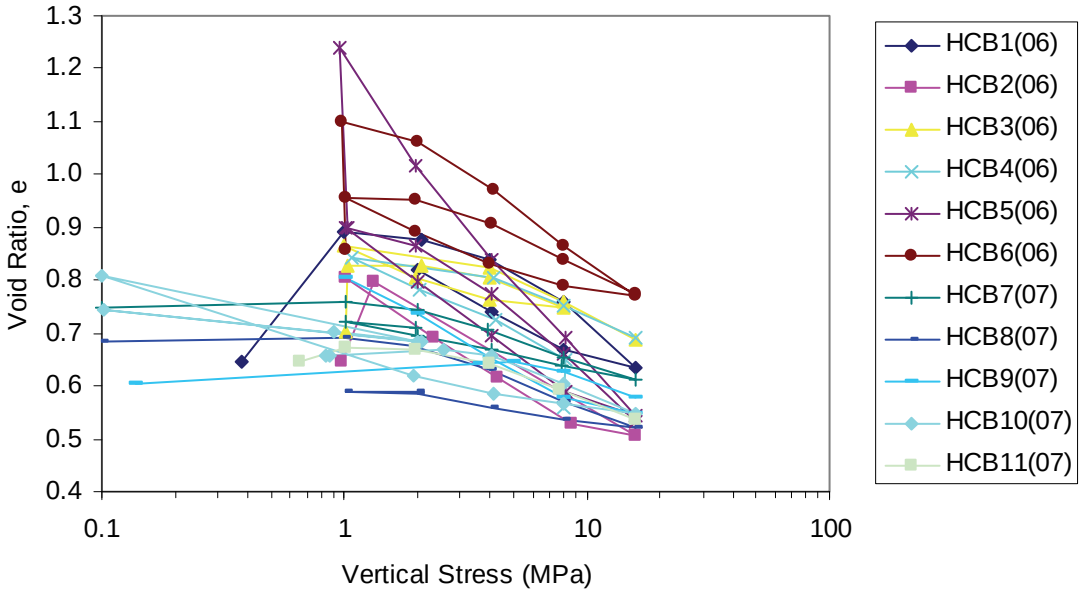

Figure 3: Void Ratio (e) versus Vertical Stress for HCB Specimens (11 Tests)

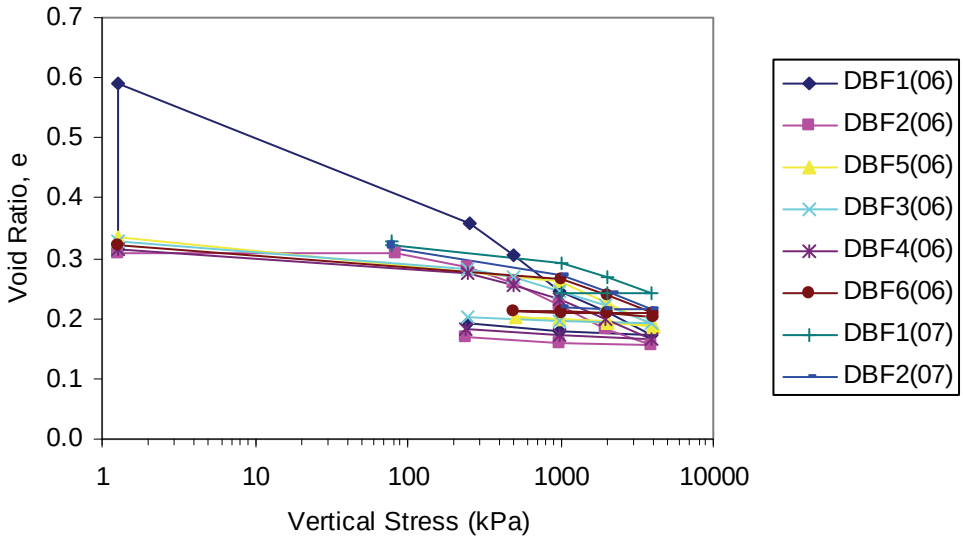

Figure 4: Void Ratio (e) versus Vertical Stress for LBF Specimens (8 Tests)

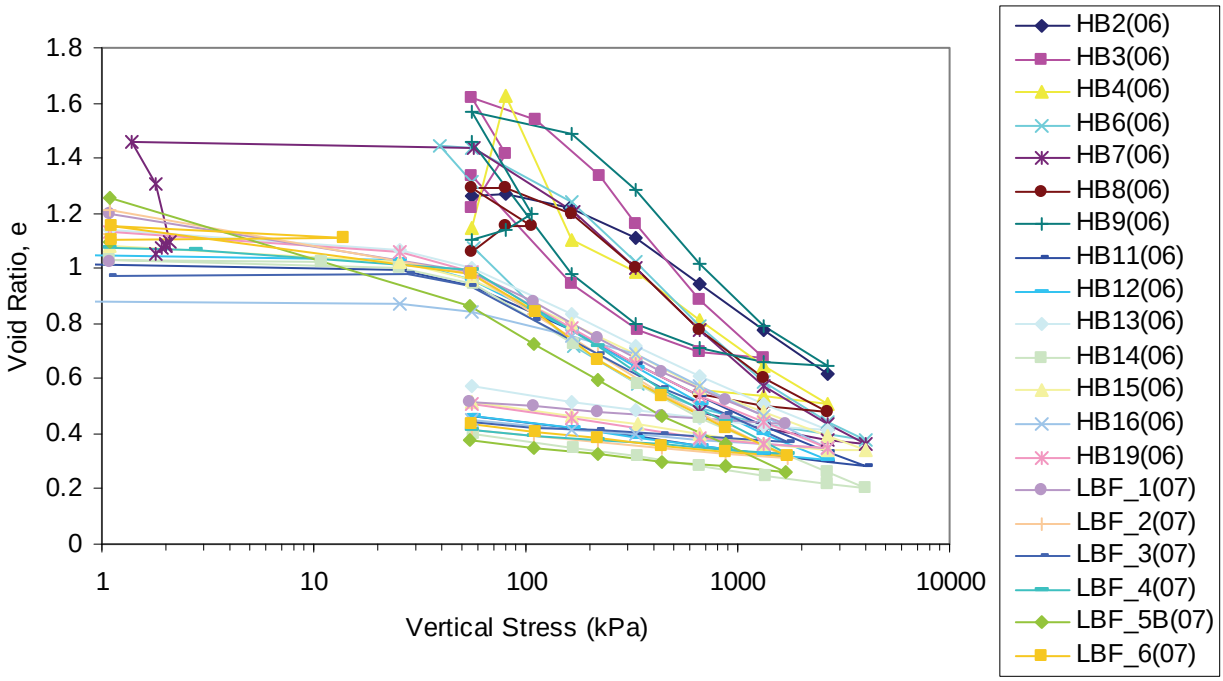

Figure 5: Void Ratio (e) versus Vertical Stress for LBF Specimens (20 Tests)

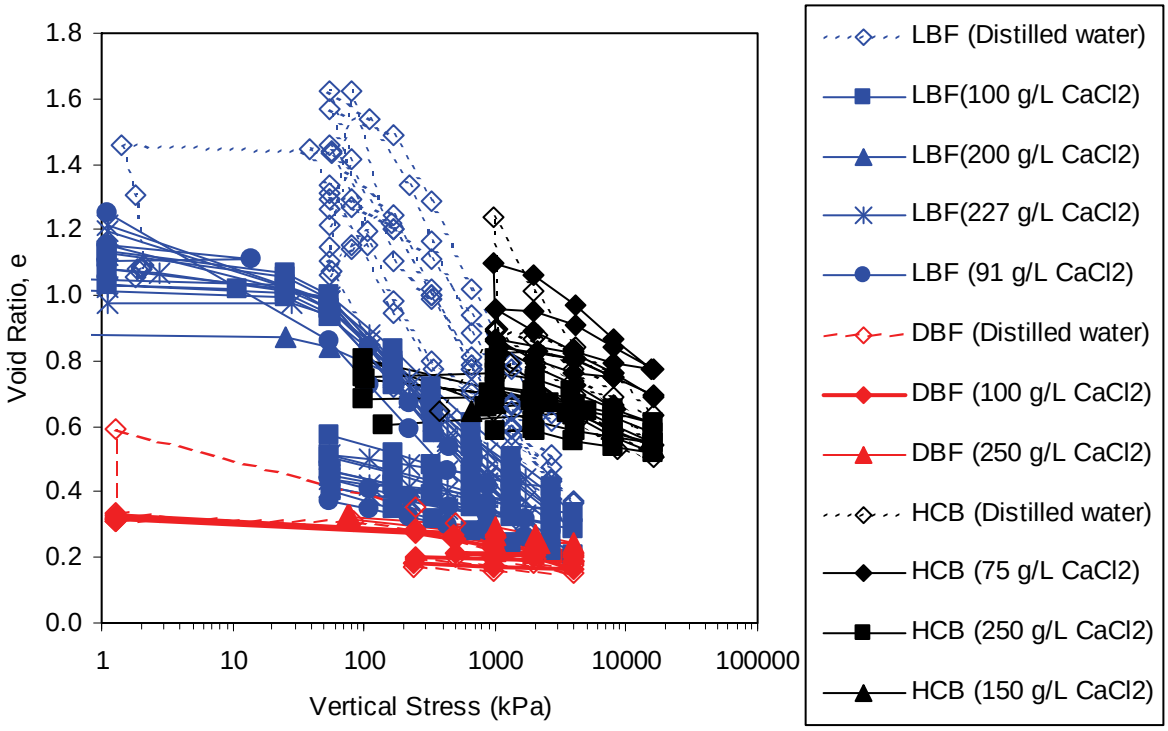

Figure 6: Comparison of the Void Ratio (e) versus Vertical Stress for the HCB, DBF, and LBF Specimens

Table 9: Compression Indices (C_c) and Swelling Indices (C_s) of the Highly Compacted Bentonite (HCB) Specimens

No.	Sample No.	Mixing Liquid	Reservoir Liquid	Cc	Cs	References
1	HCB1(06)	DW	DW	0.42	0.11	Baumgartner et al. 2008
2	HCB2(06)	DW	DW	0.27	0.09	Baumgartner et al. 2008
3	HCB3(06)	75 g/L $CaCl_2$	75 g/L $CaCl_2$	0.15	0.09	Baumgartner et al. 2008
4	HCB4(06)	75 g/L $CaCl_2$	75 g/L $CaCl_2$	0.19	0.07	Baumgartner et al. 2008
5	HCB5(06)	DW	DW	0.57	0.30	Baumgartner et al. 2008
6	HCB6(06)	75 g/L $CaCl_2$	75 g/L $CaCl_2$	0.32	0.15	Baumgartner et al. 2008
7	HCB7(07)	DW	250 g/L $CaCl_2$	0.16	0.09	Priyanto et al. 2008
8	HCB8(07)	250 g/L $CaCl_2$	250 g/L $CaCl_2$	0.18	0.06	Priyanto et al. 2008
9	HCB9(07)	DW	DW	0.16	0.09	Priyanto et al. 2008
10	HCB10(07)	250 g/L $CaCl_2$	250 g/L $CaCl_2$	0.19	0.06	Priyanto et al. 2008
11	HCB11(07)	DW	150 g/L $CaCl_2$	0.18	0.02	Priyanto et al. 2008

Table 10: Compression Indices (C_c) and Swelling Indices (C_s) of the Dense Backfill (DBF) Specimens

No.	Sample No.	Mixing Liquid	Reservoir Liquid	Cc	Cs	Reference
1	DBF1(06)	DW	DW	0.153	0.013	Baumgartner et al. 2008
2	DBF2(06)	DW	DW	0.116	0.013	Baumgartner et al. 2008
3	DBF5(06)	DW	DW	0.116	0.014	Baumgartner et al. 2008
4	DBF3(06)	100 g/L CaCl2	100 g/L CaCl2	0.091	0.008	Baumgartner et al. 2008
5	DBF4(06)	100 g/L CaCl2	100 g/L CaCl2	0.106	0.013	Baumgartner et al. 2008
6	DBF6(06)	100 g/L CaCl2	100 g/L CaCl2	0.095	0.001	Baumgartner et al. 2008
7	DBF1(07)	250 g/L CaCl2	250 g/L CaCl2	0.085	0.002	Priyanto et al. 2008
8	DBF2(07)	DW	250 g/L CaCl2	0.094	0.004	Priyanto et al. 2008

Table 11: Compression Indices (C_c) and Swelling Indices (C_s) of the Light Backfill (LBF) Specimens

Test No.	Sample No.	Mixing Liquid	Reservoir Liquid	Cc	Cs	References
1	HB2(06)	Distilled Water	Distilled Water	0.537	NA	Baumgartner et al. 2008
2	HB3(06)	Distilled Water	Distilled Water	0.851	0.169	Baumgartner et al. 2008
3	HB4(06)	Distilled Water	Distilled Water	0.531	0.077	Baumgartner et al. 2008
4	HB6(06)	Distilled Water	Distilled Water	0.629	0.158	Baumgartner et al. 2008
5	HB7(06)	Distilled Water	Distilled Water	0.608	0.149	Baumgartner et al. 2008
6	HB8(06)	Distilled Water	Distilled Water	0.600	0.113	Baumgartner et al. 2008
7	HB9(06)	Distilled Water	Distilled Water	0.713	0.114	Baumgartner et al. 2008
8	HB11(06)	Distilled water	100 g/L $CaCl_2$	0.353	0.097	Baumgartner et al. 2008
9	HB12(06)	Distilled water	100 g/L $CaCl_2$	0.387	0.095	Baumgartner et al. 2008
10	HB13(06)	100 g/L $CaCl_2$	100 g/L $CaCl_2$	0.351	0.097	Baumgartner et al. 2008
11	HB14(06)	Distilled water	100 g/L $CaCl_2$	0.398	0.105	Baumgartner et al. 2008
12	HB15(06)	100 g/L $CaCl_2$	100 g/L $CaCl_2$	0.334	0.095	Baumgartner et al. 2008
13	HB16(06)	Distilled water	200 g/L $CaCl_2$	0.380	0.062	Baumgartner et al. 2008
14	HB19(06)	Distilled water	100 g/L CaCl2	0.379	0.094	Baumgartner et al. 2008
15	LBF_1(07)	227 g/L $CaCl_2$	227 g/L $CaCl_2$	0.366	0.050	Priyanto et al. 2008
16	LBF_2(07)	Distilled water	227 g/L $CaCl_2$	0.446	0.065	Priyanto et al. 2008
17	LBF_3(07)	227 g/L $CaCl_2$	227 g/L $CaCl_2$	0.378	0.046	Priyanto et al. 2008
18	LBF_4(07)	Distilled water	227 g/L $CaCl_2$	0.445	0.056	Priyanto et al. 2008
19	LBF_5B(07)	91 g/L $CaCl_2$	91 g/L $CaCl_2$	0.400	0.074	Priyanto et al. 2008
20	LBF_6(07)	Distilled water	91 g/L $CaCl_2$	0.446	0.081	Priyanto et al. 2008

5.2 HYDRAULIC CONSTITUTIVE MODELS

Coefficient of consolidation (c_v) for each load increment can be interpreted from the results of 1D consolidation. The coefficient of consolidation (c_v) is a parameter that couples hydraulic and mechanical behaviour of the soil. Assuming soil has linear-elastic behaviour for each load increment, the hydraulic conductivity (K) can be calculated from the coefficient of consolidation (c_v) using the relationships developed by Terzhagi (1943). The assumption of linear-elastic behaviour for each load increment is reasonable, because constant load for each load increment was used during the 1D consolidation test. The coefficient of consolidation (c_v) and hydraulic conductivity (K) of HCB material have been interpreted from the results and shown in Figure 7. Detailed discussion on the result is presented in Appendix A. The 1D consolidation tests of DBF and LBF specimens are still in progress, complete test results are required to calculate the coefficient of consolidation (c_v) and hydraulic conductivity (K). These values for DBF and LBF will be presented in the report for the final report.

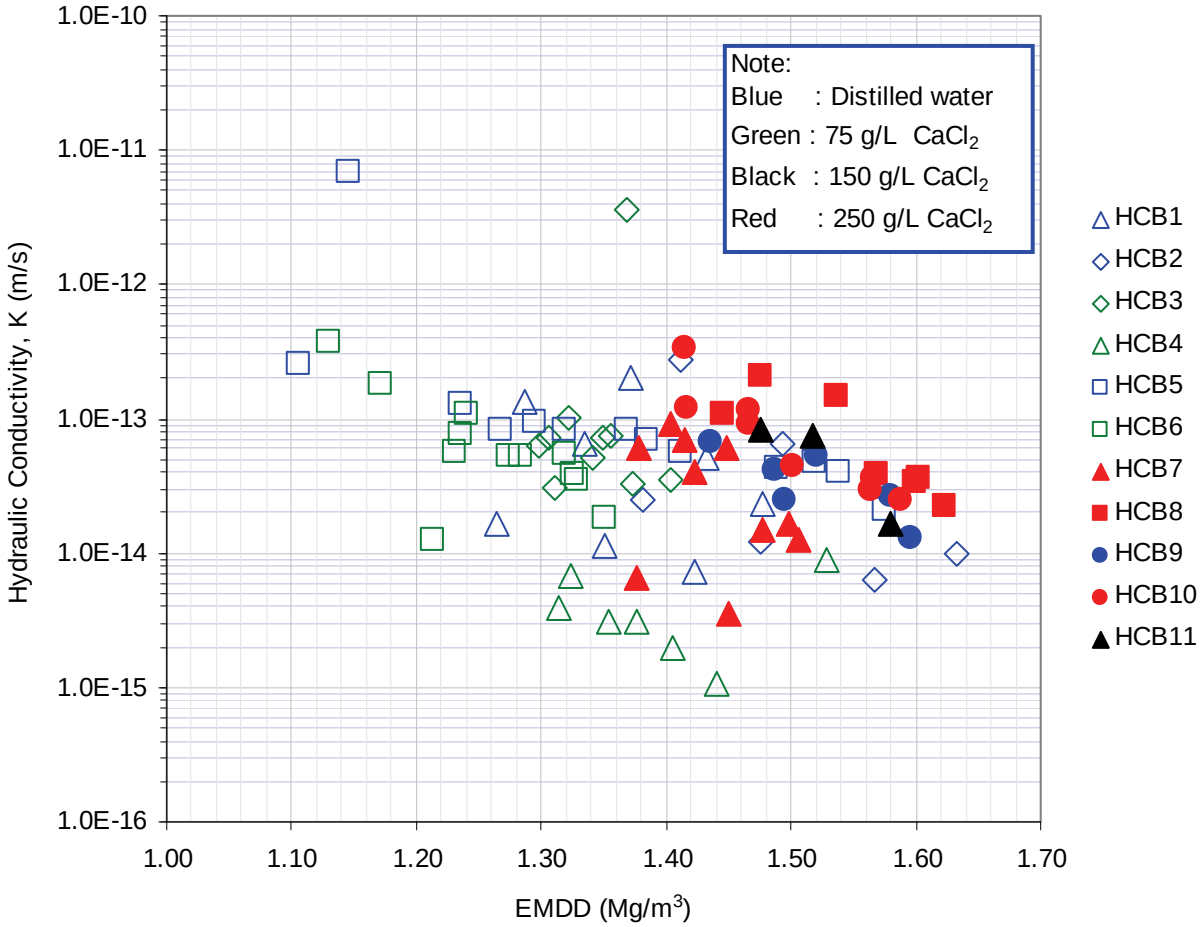

Figure 7: Hydraulic Conductivity (K) of the HCB Interpreted from the 1D Consolidation Test Results

5.3 EFFECTS OF CONCENTRATION OF THE SOLUTION IN THE PORE LIQUID, MIXING LIQUID USED IN SPECIMEN PREPARATION AND BOUNDARY CONDITIONS DURING INITIAL SATURATION

The effects of pore liquid concentration, mixing liquid used in specimen preparation and boundary condition during initial saturation for each type of material are discussed in Appendices A, B, and C. The results show that parameters C_c and C_s decrease (i.e., the soil becomes stiffer) with increasing of pore-liquid concentration for all materials. This relationship can be used to include the effect of pore liquid salinity on the mechanical behaviour of the clay-based sealing materials using THM numerical models. The relationship of the concentration of Calcium Chloride ($CaCl_2$) in the pore liquid and the compression indices (C_c) and swelling indices (C_s) for the three clay-based sealing materials are illustrated in Figures 8 and 9 respectively, which indicates that the compression indices (C_c) and swelling indices (C_s) decrease with an increase in the concentration of $CaCl_2$ in the pore liquid for the three clay-based sealing material. A decrease in the compression index (C_c) indicates that the materials become stiffer and less compressible; while a decrease of the swelling index (C_s) indicates a reduction in the ability of the material to swell. The effects of the concentration of the solution in the pore liquid and mixing liquid used in specimen preparation, and the boundary condition during initial saturation are discussed in Appendices A, B, and C for each material.

Under constant volume boundary conditions during initial saturation, the vertical stress increases up to a certain pressure required to maintain constant volume. Figure 10 shows the swelling pressure for specimen HCB9 prepared with distilled water is higher than specimen HCB10 with 250 g/L $CaCl_2$ (5 MPa versus 2.5 MPa). This result shows a reduction of 2.5 MPa of swelling pressure of the Highly Compacted Bentonite (HCB) specimen with an increase of concentration of Calcium Chloride ($CaCl_2$) from 0 g/L to 250 g/L in pore liquid.

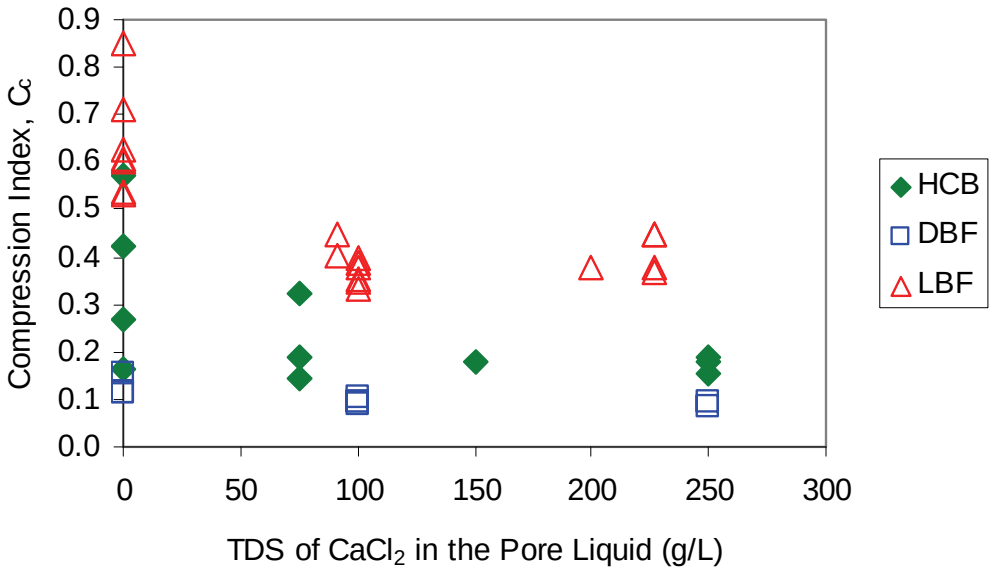

Figure 8: Relationship of the Compression Index (C_c) to the Concentration (in TDS) of Calcium Chloride ($CaCl_2$) in the Pore Liquid

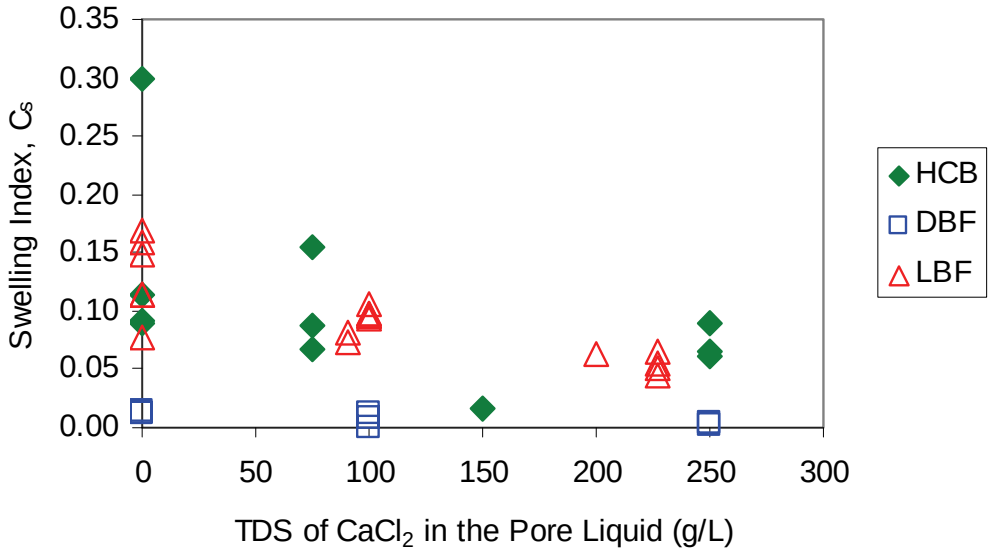

Figure 9: Relationship of the Compression Index (C_c) to the Concentration (in TDS) of Calcium Chloride ($CaCl_2$) in the Pore Liquid

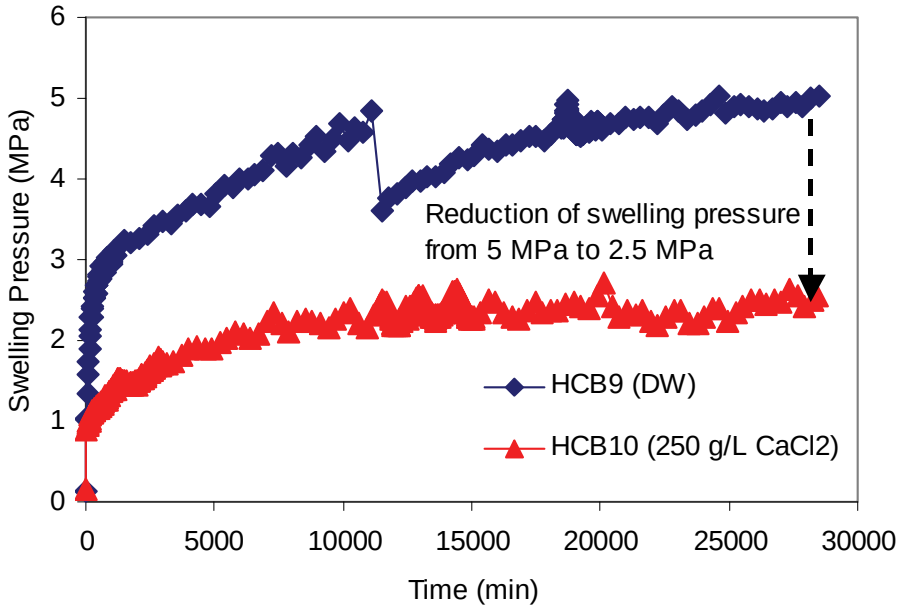

Figure 10: The Effect of $CaCl_2$ Concentration in Pore Liquid on the Swelling Pressure of Highly Compacted Bentonite (HCB)

6. PLANS FOR FUTURE WORKS

6.1 PLAN FOR 1D CONSOLIDATION TESTS IN 2008

The placement of a repository will likely be a ground water environment that consists of a mixture of $CaCl_2$ and NaCl as the dominant dissolved species that will vary with location and depth (Gascoyne et al. 1987; Mazurek 2004). As most of the initial 1D-consolidation testing was done using fresh water or calcium chloride solutions, there is a need to establish what the effects of sodium dominated solutions will have on system behaviour and ultimately a limited number of tests should be done using mixed cation solutions. The focus of the 1D-consolidation testing in 2008 is investigation of the sodium chloride solutions as shown in Tables 3, 5, and 8. Variation of liquid used in the specimen mixing and initial boundary condition applied during initial saturation will be included to allow a comparison with the previous work (2006 and 2007).

The 1D consolidation tests of the DBF materials with various sand contents (i.e., 70% to 85%) (N. Chandler, personal communication, 2007) show that the swelling index (C_s) increases significantly during unloading under low pressure resulting in hysteretic behaviour. The same behaviours have also been observed for HCB material (Appendix A) and suggest the need to modify the currently used constitutive models for these clay-based sealing materials. Unloading to lower pressure than is currently done is included in 2008 test plan to allow for evaluation of this phenomenon.

6.2 PLAN FOR 1D CONSOLIDATION TESTS (2009 and beyond)

Two potential test plans have been identified for work in 2009 and beyond. The option selected will depend on the results obtained in the work from 2006 through 2008 and identification of what parameters are most important to evaluate. The two alternatives are described below.

Alternative 1: Establish the relationship of C_c and C_s to concentration of NaCl and $CaCl_2$ in the pore liquid. Currently, the THM numerical modelling assumes that the pore liquid salinity is constant during the analysis. Mass transport formulation is used to define the flow of fluid (i.e., liquid and gas). Addition of mass transport formulation describing the flow of solvent in the pore liquid in the THM numerical modelling may be used to incorporate the change of pore liquid concentration. The relationship of C_c and C_s to pore liquid concentration can be used to incorporate the effect of pore liquid concentration to the mechanical behaviour of clay-based sealing material in the THM numerical modelling. This relationship of C_c and C_s to pore liquid concentration may also be used to consider the change of salt type (i.e., NaCl and $CaCl_2$) and their concentration. Additional data are still required to define this relationship. Tables 3, 5, and 8 show alternative 1 for 2009 to include 150 g/L NaCl in 1D consolidation tests.

Alternative 2: Examine the effect of artificial groundwater (e.g., mixture of NaCl and $CaCl_2$). Natural groundwater consists of mixtures of various types of salts at different concentrations. Examining the effect of artificial groundwater on the mechanical behaviour of sealing materials is important if the mechanical behaviour of sealing materials is dependent on the types of salts or their ratios (i.e., NaCl and $CaCl_2$). Table 3, 5, and 8 shows alternative 2 for 2009 to include artificial water in 1D consolidation test.

6.3 PROJECTED RESULTS AT THE END OF TESTING PROGRAM

In the end of the outlined testing program it is hoped that the following relationships can be generated from the results of 1D consolidation tests of HCB, DBF, and LBF.

- The effects of salt types and their concentrations used as mixing and reservoir liquids, and boundary conditions during initial saturation on the mechanical behaviour of HCB, DBF, and LBF.
- Parameters C_c, C_s, and c_v for each test.
- Parameters C_c and C_s as a function of pore liquid concentration and salt type to incorporate the effect of pore liquid salinity in numerical modelling for each material (i.e., HCB, DBF, and LBF). Examples of the type of relationship that may be developed from the tests are shown in Figure 11. These relationships for the specimens with Calcium Chloride ($CaCl_2$) in the pore liquid are shown in Figures 8 and 9.

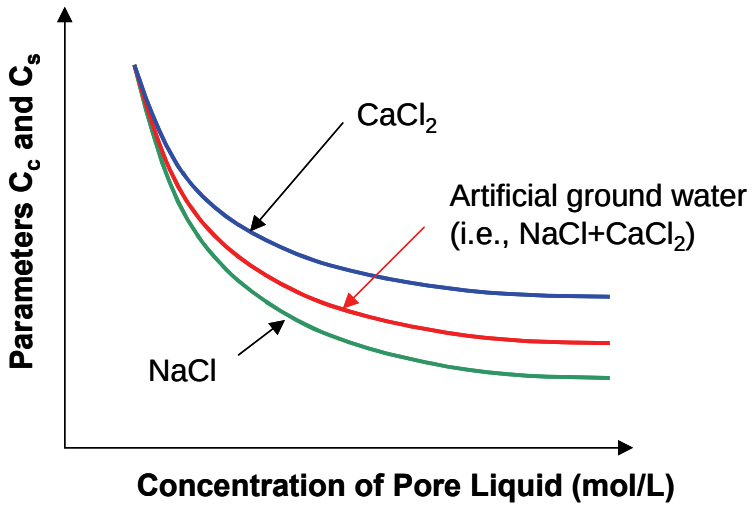

Figure 11: Possible Relationship of Parameters C_c and C_s and the Concentration of Solution in the Pore Liquid

7. CONCLUDING REMARKS

- Based on the results of the 1D-consolidation tests of the three clay-based sealing materials, the following conclusions can be made.

- The compression indices (C_c) and swelling indices (C_s) decrease with increasing concentration of $CaCl_2$ in the pore liquid for the three clay-based sealing materials (i.e., HCB, DBF, and LBF). A decrease in the compression index (C_c) indicates that the materials become stiffer and less compressible; while a decrease of the swelling index (C_s) indicates a reduction of the ability of the material to swell.

- The results of the 1D consolidation tests of the Highly Compacted Bentonite (HCB) show a loss of 2.5 MPa in its swelling pressure with an increase of concentration of Calcium Chloride ($CaCl_2$) solution from 0 g/L to 250 g/L in pore liquid.

REFERENCES

Baumgartner. P, D. G. Priyanto, J. R. Baldwin, J .A. Blatz, B. H. Kjartanson, and H. Batenipour. 2008. Preliminary Results of One-Dimensional Consolidation Testing on Bentonite Clay-Based Sealing Components Subjected to Two Pore-Fluid Chemistry Conditions. Nuclear Waste Management Organization (NWMO) Technical Report No. TR-2008-04. Toronto, Canada.

CTECH (CTECH Radioactive Materials Management). 2002. Conceptual design for a deep geologic repository for used nuclear fuel. CTECH Report 1106/MD18085/REP/01, Nuclear Waste Management Organization, Toronto, Canada (www.nwmo.ca).

Dixon, D.A. 2000. Porewater salinity and the development of swelling pressure in bentonite-based buffer and backfill materials. Helsinki, Posiva Report, POSIVA 2000-04 (ISBN 951-652-090-1).

Gascoyne, M., C.C. Davison, J.D. Ross and R. Pearson. 1987. Saline groundwaters and brines in plutons in the Canadian Shield. In Saline Water and Gases in Crystalline Rocks. Editors: Fritz, P. and Frape, S.K.; Geological Association of Canada Special Paper 33, Ottawa.

Gierszewski, P., J. Avis, N. Calder, A. D'Andrea, F. Garisto, C. Kitson, T. Melnyk, K. Wei and L. Wojciechowski. 2004. Third case study – Postclosure safety assessment. Ontario Power Generation, Nuclear Waste Management Division Report 06819-REP-01200-10109-R00. Toronto, Ontario.

Maak P and Simmons G R. 2005. Deep geologic repository concepts for isolation of used fuel in Canada, Canadian Nuclear Society, Waste Management, Decommissioning and Environmental Restoration for Canada's Nuclear Activities: Current Practices and Future Needs, Ottawa May 8-11 2005.

Mazurek, M. 2004. Long-term used nuclear fuel waste management – Geoscientific review of the sedimentary sequence in southern Ontario. Institute of Geological Sciences, Univ. of Bern, Technical Report TR 04-01, Bern, Switzerland, available from Nuclear Waste Management Organization, Toronto, Canada (www.nwmo.ca).

Russell, S.B. and G.R. Simmons. 2003. Engineered barrier system for a deep geologic repository. Presented at the 2003 International High-Level Radioactive Waste Management Conference. 2003 March 30-April 2, Las Vegas, NV.

Siemens, G. A. 2006. Influence of Boundary Conditions on the Hydraulic-Mechanical Behaviour of an Unsaturated Swelling Soil. Ph.D Thesis, University of Manitoba, Canada.

Terzhagi, K. 1943. Theoretical Soil Mechanics. Wiley, New York.

APPENDIX A:
HIGHLY COMPACTED BENTONITE

D. G. Priyanto and D. A. Dixon
Atomic Energy of Canada Limited

CONTENTS

LIST OF TABLES

Page

LIST OF FIGURES

Page

A1. HIGHLY COMPACTED BENTONITE (HCB)

Highly Compacted Bentonite (HCB) is a clay-based sealing-system component proposed for use in either full contact or very close proximity to the used-fuel container (Maak and Simmons 2005). HCB is composed of 100% bentonite (Russell and Simmons 2003), compacted to high dry densities. The test specimens are fabricated from 80-mesh granules of Wyoming bentonite (MX80) with an assumed minimum Na-montmorillonite content of 75%. The 1D consolidation tests of HCB specimens are conducted at the Atomic Energy of Canada Limited (AECL)'s geotechnical engineering laboratory.

A2. EQUIPMENT

A2.1 OEDOMETER CELL AND FILTER STONE

Small-diameter oedometer cells (28.1-mm diameter) are used in this test series to permit high stresses to be applied (i.e., maximum 16 MPa). Similar diameter filter stones (28.1 mm) are used in the tests to allow liquid to enter or leave the faces of the specimens. All components of the oedometer cells were fabricated from stainless steel to avoid corrosion, which can be a problem, particularly in those done using the saline solution. No corrosion was observed during the test series and so interaction of iron with the HCB is assumed to be a non-issue in these tests.

A2.2 COMPRESSION FRAME AND LOADING SYSTEM

Standard dead weight oedometers are unable to apply the high loads needed to generate stresses exceeding the expected swelling pressures for HCB. In order to complete these tests, two custom-built loading systems were constructed; each uses a different method to achieve the testing goals.

1. A compression frame similar to that used by Baumgartner et al. (2008) is used. This system has a double-action hydraulic ram (e.g., a 222 kN spring-return ram and a 445 kN double acting ram) to produce the required loads. Each hydraulic ram is actuated by a high-pressure nitrogen-gas cylinder acting on a gas-over-oil accumulator rather than the conventional mechanical hydraulic pumps. This allows the most stable possible loading condition to be achieved.
2. A new frame using a servo-hydraulic testing system manufactured by the MTS® (Materials Testing Services) was added in 2007 to test HCB. This equipment enables an application of different boundary conditions during initial saturation in tests (i.e., constant volume or constant pressure).

A2.3 STRAIN AND PRESSURE MEASUREMENT

Displacements are measured with calibrated linear variable differential transformers (LVDT). Loads are measured with calibrated strain-gauge load cells (i.e., 17.8-kN capacity). All instruments are connected to a data logger and logger scan rates are set at 5 minutes for the

first 24 hours of a load/unload increment and every hour thereafter until the load/unload increment is deemed complete. The laboratory seasonal temperature ranges between 19°C and 24°C, producing maximum dimensional variance of 0.011 mm or about a 0.1% variation for 10-mm-thick specimen (Baumgartner et al. 2008). This small variation is considered insignificant and no thermal compensation is included in any calculation.

A3. TEST PROCEDURE

A3.1 TEST MATRIX FOR HCB SPECIMENS

The test matrix for HCB specimens is shown in Table A1. Four specimens are initially planned for 1D consolidation of the HCB (i.e., Specimens HCB7, 8, 9, and 10). One additional specimen with 150 g/L $CaCl_2$ is added to the specimen matrix (i.e., Specimen HCB11) to define the relationship of the pore liquid concentration and the mechanical behaviour of the HCB. The availability of a load frame and only minor additional work in preparing specimen HCB11 are also the reasons of this additional specimen. Combined with the previous tests (Baumgartner et al. 2008), this test matrix examines the effect of the $CaCl_2$ concentration, different mixing liquid (Distilled Water (DW) or $CaCl_2$), and different boundary conditions during initial saturation on the mechanical behaviour of HCB.

Table A1: 1-D Consolidation Test Matrix for HCB Specimens in 2007

Specimen No.	Mixing Liquid	Reservoir Liquid	Target Initial Dry Density (kg/m^3)	Target Initial Degree of Saturation (%)	Initial Boundary Condition During Saturation	Load Sequence
HCB7	Distilled water	250 g/L $CaCl_2$	1650	95	Constant pressure at 1 MPa	Load to 1, 2, 4, 8, & 16 MPa Unload to 8, 4, 2, & 1 MPa
HCB8	250 g/L $CaCl_2$	250 g/L $CaCl_2$	1650	95	Constant pressure at 1 MPa	Load to 1, 2, 4, 8, & 16 MPa Unload to 8, 4, 2, & 1 MPa
HCB9	Distilled water	Distilled water	1650	95	Constant volume	Load to 1, 2, 4, 8, & 16 MPa Unload to 8, 4, 2, & 1 MPa
HCB10	250 g/L $CaCl_2$	250 g/L $CaCl_2$	1650	95	Constant volume	Load to 1, 2, 4, 8, & 16 MPa Unload to 8, 4, 2, & 1 MPa
HCB11*	Distilled water	150 g/L $CaCl_2$	1650	95	Constant pressure at 1 MPa	Load to 1, 2, 4, 8, & 16 MPa Unload to 8, 4, 2, & 1 MPa

* This specimen was added to the test plan at the end of 2007.

A3.2 SPECIMEN PREPARATION

Two different mixing liquids are used in the tests to examine the type of liquid that should be considered in the preparation of sealing-system components for a placement-room in a Deep Geological Repository (DGR). All the specimens are compacted with the target dry density of ~1650 kg/m^3 with a target degree of saturation of ~95%. This result in a target gravimetric water content (w) of 23% for specimens mixed with distilled water and 27% for specimens mixed with 250 g/L $CaCl_2$. The salt remaining in the specimen during the oven-dry process changes the value of gravimetric water content. Baumgartner et al. (2008) discussed the pore-liquid concentration affecting the volume-mass relationships.

The HCB specimens are fabricated from 80-mesh granules of Wyoming bentonite (MX80). Dry Wyoming bentonite (MX80) is mixed with the liquid in a small beaker. Liquid is added slowly with a syringe to achieve uniform gravimetric water content and avoid lumps during the mixing process. The mixing of the HCB with 250 g/L $CaCl_2$ is easier as compared to mixing with

distilled water with less formation of lumps. Heat is generated in the mixing of the HCB with 250 g/L $CaCl_2$, which is not observed when mixing with distilled water. This may be due to a reaction between the salt solution and the bentonite.

The target mass to be compacted in the cell is calculated based on the target dry density and degree of saturation. This calculated mass is added to the cell and the gravimetric water content analysis is made from the remaining specimen mixture. Filter papers and filter stones are installed on top and bottom of the specimen, and the specimen assembly is installed in the oedometer. The specimen is compacted in one lift in the oedometer ring with a hydraulic press (target thickness ~10-mm). The compaction piston has a scribed mark on its outer surface, which permits the technologist to observe when the specimen has reached its required initial density. The actual initial thickness is measured using calipers by measuring the piston stick-up of the cell.

For specimens HCB7, HCB8, and HCB11 a constant pressure load of 1 MPa was applied to settle the specimen assembly. The specified liquid was added to the reservoir after that. For specimens HCB9 and HCB10 with the initial constant volume boundary condition during initial saturation, the servo-hydraulic testing system was set to zero strain and a small vertical stress of approximately 0.1 MPa was initially applied. After liquid is added to the reservoir, the pressure increases due to the constrained swelling of the specimen.

A3.3 SPECIMEN LOADING, RESERVOIR LIQUID MAINTENANCE, AND DISMANTLING

The specimen load is adjusted with the regulator on the nitrogen (N_2) cylinder. The duration of the load increment is dependent on the response of the tests and specimens. Plastic shrouding encloses the assembly and reservoir to minimize evaporation. Three different liquids are used as the reservoir liquid in the tests: distilled water, 250 g/L $CaCl_2$, and 150 g/L $CaCl_2$. Due to evaporation of the reservoir liquid over the period of the test, liquid levels need to be replenished periodically. During the evaporation, only water is removed from the cell, the amount of the salt within the cell is constant. Therefore, distilled water is periodically added in the cell during the test to maintain a relatively constant salt concentration in the liquid reservoir.

At the end of the test the thickness and the gravimetric water content of the specimen are measured. The values of gravimetric water content, dry density, and Effective Montmorillonite Dry Density (EMDD) upon the installation are summarized in Table A2. Considering the high concentration of the pore liquid (i.e., 250 g/L $CaCl_2$), the four-component soil system volume-mass relationships (Baumgartner et al. 2008) are used to calculate these values. The definition of the 'apparent' gravimetric water ($w_{(app)}$), the 'true' gravimetric water content (w_w), and the gravimetric liquid content (w_l) in the four-component soil system are summarized as follows.

The 'apparent' gravimetric water content ($w_{(app)}$) is:

$$w_{(app)} = \frac{M_{wet} - M_{dry}}{M_{dry}} = \frac{M_w}{M_s + M_{salt}} \quad \text{(A1)}$$

where: M_{wet} - mass of wet specimen;
M_{dry} - the mass of oven-dry specimen;
M_w - the mass of water;
M_{salt} - mass of salt;
M_s - mass of solid.

The 'true' gravimetric water content (w_w) is:

$$w_w = \frac{M_w}{M_s} \tag{A2}$$

The gravimetric liquid content (w_l) is:

$$w_l = \frac{M_l}{M_s} = \frac{M_w + M_{salt}}{M_s} \tag{A3}$$

The relationships of all three gravimetric water contents are presented in Baumgartner et al. (2008). These relationships and the required formulas to calculate volume-mass relationships of soil with saline pore liquid are summarized in Table A3.

The smectite minerals dominate the behaviour of the clay fraction in the bentonites and the smectite content varies in bentonite from different global sources. The term effective montmorillonite dry density (EMDD) was derived (Baumgartner and Snider 2002, JNC 2000) to single out the role of montmorillonite in soil behaviour and is expressed as follows:

$$EMDD = \frac{M_m}{(V_m + V_v)} = \frac{f_m \cdot f_c \cdot \rho_d}{1 - \frac{(1-f_c)\cdot\rho_d}{G_a \cdot \rho_w} - \frac{(1-f_m)\cdot f_c \cdot \rho_d}{G_n \cdot \rho_w}} \tag{A4}$$

where M_m = mass of montmorillonite component (kg);
V_m = volume occupied by montmorillonite component (m^3);
V_v = volume of void (m^3);
f_m = mass fraction of montmorillonite in clay fraction f_c (e.g., > 75% in MX80);
f_c = mass fraction of clay in dry solids (e.g., ~100% in bentonite clay);
G_a = relative density of aggregate solid (e.g., quartz sand = 2.65);
G_n = relative density of non-montmorillonite component in clay (e.g., 2.645);
ρ_w = density of water (kg/m^3); and
ρ_d = dry density of soil (kg/m^3).

Tables A4 and A5 shows the properties of the HCB and the liquid to calculate the EMDD of HCB, respectively.

Table A2: Dimension, Mass Composition, Liquid Properties, Water Contents, Densities, Void Ratio, and Porosity of Specimens HCB7, HCB8, HCB9, HCB10, and HCB11 at Installation

Specimen No.	HCB7	HCB8	HCB9	HCB10	HCB11
DIMENSION					
Thickness (mm)	10.45	10.27	9.60	10.38	9.74
Diameter (mm)	28.20	28.19	28.12	28.1	28.17
Volume (cm^3)	6.53	6.41	5.96	6.44	6.07
LIQUID PROPERTIES					
Liquid	Distilled Water	$CaCl_2$ Solution	Distilled Water	$CaCl_2$ Solution	Distilled Water
TDS (g/L)	0	250	0	250	0
Concentration (mol/L)	0	2.253	0	2.253	0
Density of liquid (Mg/m^3)	1	1.1879	1	1.1879	1
VOLUME-MASS PROPERTIES					
"Apparent" gravimetric water content, $w_{(app)}$ (%)	22.5	18.60	23.10	19.1	23.10
Gravimetric liquid content, w_l (%)	22.5	24.79	23.10	25.49	23.10
Gravimetric water content, w_w (%)	22.5	19.57	23.10	20.13	23.10
Bulk density (Mg/m^3)	1.92	2.03	2.10	2.02	2.07
Dry density (Mg/m^3)	1.57	1.63	1.71	1.61	1.68
Effective Montmorillonite Dry Density (EMDD) (Mg/m^3)	1.38	1.44	1.529	1.425	1.499
Void ratio, e	0.75	0.69	0.606	0.704	0.633
Porosity, n	0.43	0.41	0.377	0.413	0.388
MASS COMPOSITION					
Bulk Mass (g)	12.55	13.03	12.55	13.01	12.56
Mass of Soil Solids (g)	10.25	10.44	10.20	10.37	10.20
Mass of Liquid (g)	2.30	2.59	2.35	2.64	2.36
Mass of Water (g)	2.30	2.04	2.35	2.09	2.36
Mass of $CaCl_2$ (g)	0.00	0.54	0.00	0.56	0.00

Table A3: Summary of Equations for Calculation of Mass-Volume Relationships of Soil with Saline Pore Liquid

Input Data

Data measured in the laboratory test:
M_{wet} = Mass of wet soil specimen;
M_{dry} = Mass of dry soil specimen; and
V_{total} = total volume.

Data required to calculate mass-volume relationship:
G_s = specific gravity of the soil solid phase;
TDS = total dissolved solid of the solution (g/L); and
ρ_l = density of the solution (liquid phase) (Mg/m^3)

Ratio of mass of solute to the mass of solution (C_m)

$$C_m = \frac{\text{TDS}\,(g/L)}{\rho_l\,(Mg/m^3)\times 1000}$$

"Apparent" gravimetric water content ($w_{(app)}$), gravimetric water content (w_w), and gravimetric liquid content (w_l)

"Apparent" gravimetric water content ($w_{(app)}$)

$$w_{(app)} = \frac{M_{wet} - M_{dry}}{M_{dry}} \times 100\% = \frac{M_w}{M_s + M_{salt}} \times 100\%$$

Gravimetric water content (w)

$$w = \frac{M_w}{M_s} \times 100\% = \frac{w_{(app)} \cdot (1 - C_m)}{1 - C_m (1 + w_{(app)})}$$

Gravimetric liquid content (w_l)

$$w_l = \frac{M_l}{M_s} \times 100\% = \frac{w_{(app)}}{1 - C_m (1 + w_{(app)})}$$

Summary of Equations for Calculation of Mass-Volume Relationships of Soil with Saline Pore Liquid (Table A3 Continued)

Bulk Density (ρ_{bulk})

$$\rho_{bulk} = \frac{M_{wet}}{V_{total}} = \frac{M_s + M_w + M_{salt}}{V_{total}}$$

Dry Density (ρ_{dry})

$$\rho_{dry} = \frac{\rho_{bulk}}{1 + w_l}$$

Void ratio (e) and porosity (n)

$$e = \frac{G_s \cdot \rho_w}{\rho_{dry}} - 1$$

$$n = \frac{e}{1 + e}$$

Degrees of saturation (S)

Degree of saturation (S_l)

$$S = \frac{V_l}{V_v} \times 100\% = \frac{V_w + V_{salt}}{V_v} \times 100\% = \frac{w_l \cdot G_s \cdot \rho_w}{e \cdot \rho_l} \times 100\%$$

Saturated density (ρ_{sat})

$$\rho_{sat} = \frac{G_s \cdot \rho_w + e \cdot \rho_l}{1 + e}$$

Summary of Equations for Calculation of Mass-Volume Relationships of Soil with Saline Pore Liquid (Table A3 Concluded)

List of symbols

ρ_{bulk}	= bulk density	[Mg/m^3]
ρ_{dry}	= dry density	[Mg/m^3]
ρ_l	= density of the solution (liquid phase)	[Mg/m^3]
ρ_{sat}	= density of specimen at 100% saturation	[Mg/m^3]
ρ_w	= density of water	[Mg/m^3]
C_m	= ratio of the mass of solute to the mass of solution	[no unit]
e	= void ratio (i.e., ratio of the volume of void (V_v) to the volume of solid (V_s))	[no unit]
G_s	= specific gravity of the soil solid phase	[no unit]
M_{wet}	= mass of wet soil specimen, before oven-drying process	[Mg]
M_{dry}	= mass of dry soil specimen, after oven-drying process	[Mg]
M_w	= mass of water	[Mg]
M_{salt}	= mass of salt	[Mg]
M_s	= mass of solid phase	[Mg]
n	= porosity	[no unit]
S	= degree of saturation (i.e., ratio of the volume of liquid phase to the volume of void)	[%]
TDS	= total dissolved solid of the solution (liquid phase)	[g/L]
V_l	= volume of liquid phase	[m^3]
V_{salt}	= volume of salt	[m^3]
V_s	= volume of solid	[m^3]
V_{total}	= total volume of soil specimen	[m^3]
V_v	= Volume of void	[m^3]
V_w	= volume of water	[m^3]
w_{app}	= “Apparent” gravimetric water content (i.e., the gravimetric water content measured directly from the oven-drying process)	[%]
w	= gravimetric water content (i.e., ratio of the mass of water to the mass of solid)	[%]
w_l	= gravimetric liquid content (i.e., ratio of the mass of liquid phase to the mass of solid)	[%]

Table A4: Properties of Highly Compacted Bentonite (HCB)

Material	HCB (Highly Compacted Bentonite)
Material Composition	100% Wyoming Bentonite
Relative density of solid, G_s	2.745
Relative density of aggregate, G_a	1
Relative density of non-montmorillonite component in clay, G_n	2.645
Mass fraction of clay in dry solids, f_c	100%
Mass fraction of montmorillonite in clay fraction, f_m	75%
Density of water, r_w (g/cm^3) =	1

Table A5: Properties of the Liquid

Liquid	Distilled water (H_2O)	Calcium Chloride ($CaCl_2$)	
TDS (g/L)	0	150	250
Salt concentration, c (mol/L)	0	1.352	2.253
Density of liquid, ρ_l (Mg/m^3)	1	1.1147*	1.1879*

* Lide (2007)

A4. RESULTS

A4.1 THICKNESS AND VERTICAL STRESS VERSUS TIME

Figures A1 to A5 show the applied vertical stress and thickness of the specimens HCB7, 8, 9, 10, and 11. Some issues experienced during the tests that cannot be avoided include the unintended pressure loss due to the depletion of nitrogen-gas cylinder (i.e., Specimens HCB7, 8, 9, 10, and 11). A two-cylinder set up will be employed in the future tests to eliminate this problem. During the testing of HCB11, the LVDT was found to stick periodically during the unload portion of the test, resulting in a less-smooth plot of displacement than would otherwise have been anticipated. This stick-release of the sensor did not affect the ability of the data to be analysed.

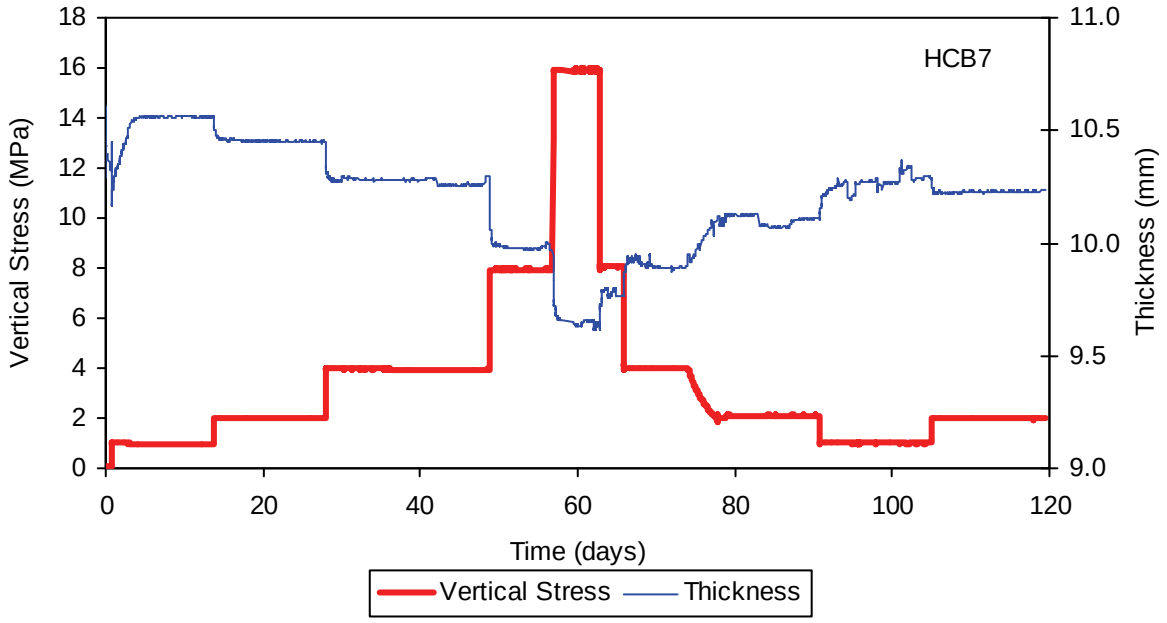

Figure A1: Loading and Displacement History of Specimen HCB7 (Mixing Liquid = Distilled Water; Reservoir Liquid = 250 g/L $CaCl_2$)

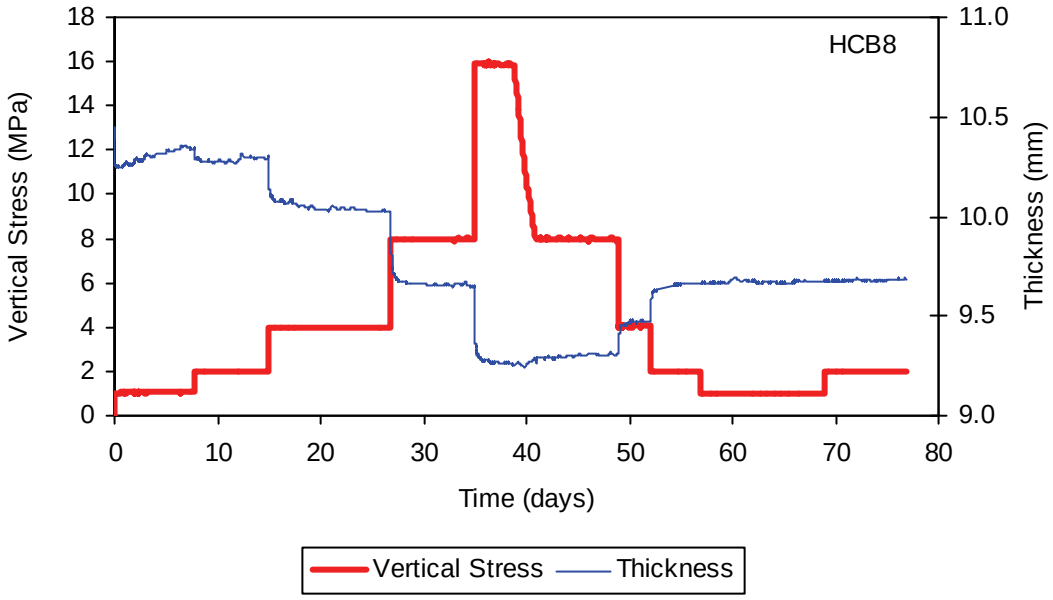

Figure A2: Loading and Displacement History of Specimen HCB8 (Mixing Liquid = Reservoir Liquid = 250 g/L $CaCl_2$)

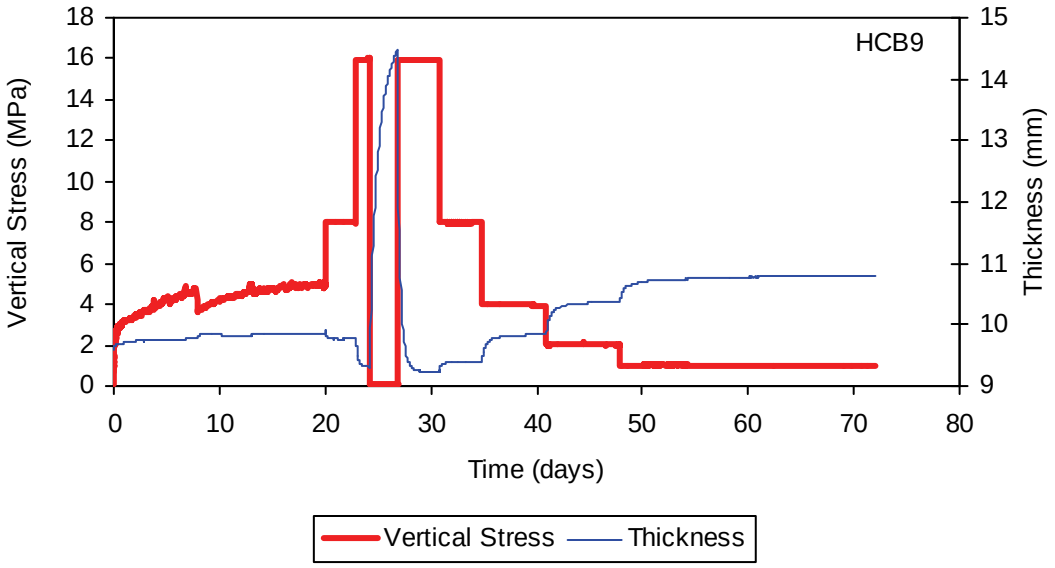

Figure A3: Loading and Displacement History of Specimen HCB9 (Mixing Liquid = Reservoir Liquid = Distilled Water)

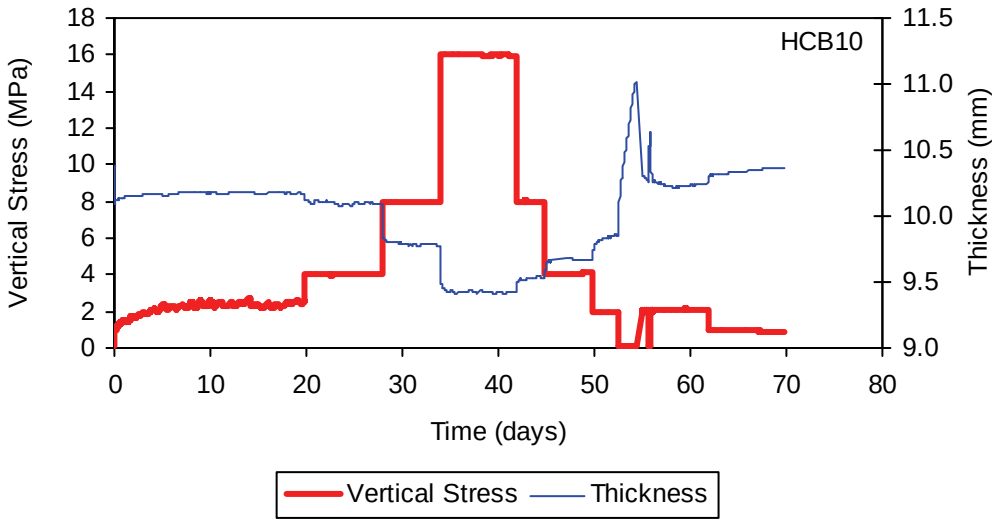

Figure A4: Loading and Displacement History of Specimen HCB10 (Mixing Liquid = Reservoir Liquid = 250 g/L $CaCl_2$)

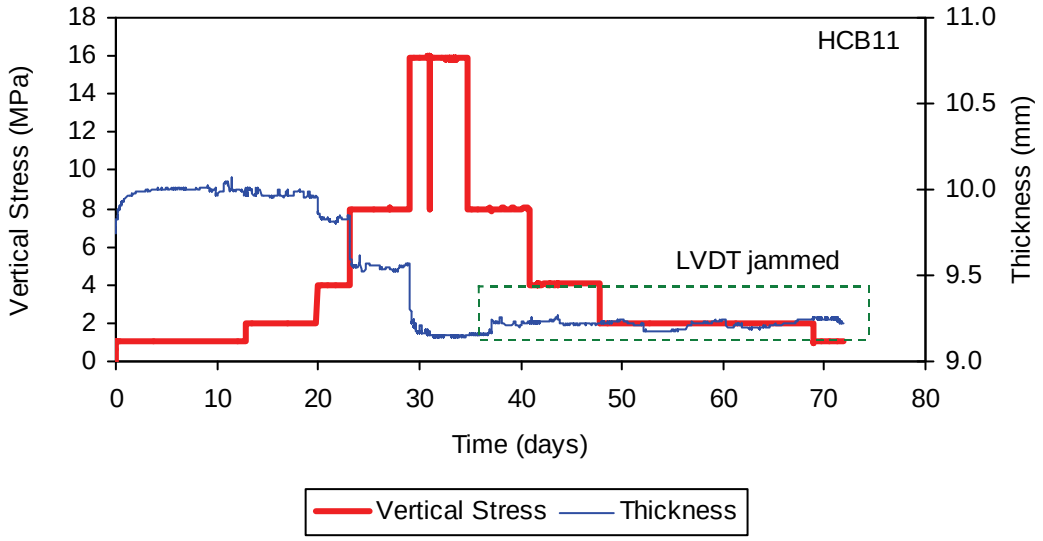

Figure A5: Loading and Displacement History of Specimen HCB11 (Mixing Liquid = Distilled Water; Reservoir Liquid = 150 g/L $CaCl_2$)

A4.2 VOID RATIO (E), DRY DENSITY (ρ_{DRY}), AND EMDD VERSUS VERTICAL STRESS (σ_v)

A4.2.1 HCB7

Specimen HCB7 was prepared with distilled water as a mixing liquid and 250 g/L $CaCl_2$ as a reservoir liquid. Figure A6 shows the void ratio (e) versus vertical stress (σ_v) of Specimen HCB7. Constant pressure of 1 MPa was applied to Specimen HCB7 at the initial saturation. The vertical stress was increased up to maximum 16 MPa and decreased back to 1 MPa. This vertical stress was increased to 2 MPa before the test was ended. The corresponding dry density (ρ_{dry}) versus vertical stress (σ_v) is illustrated in Figures A7.

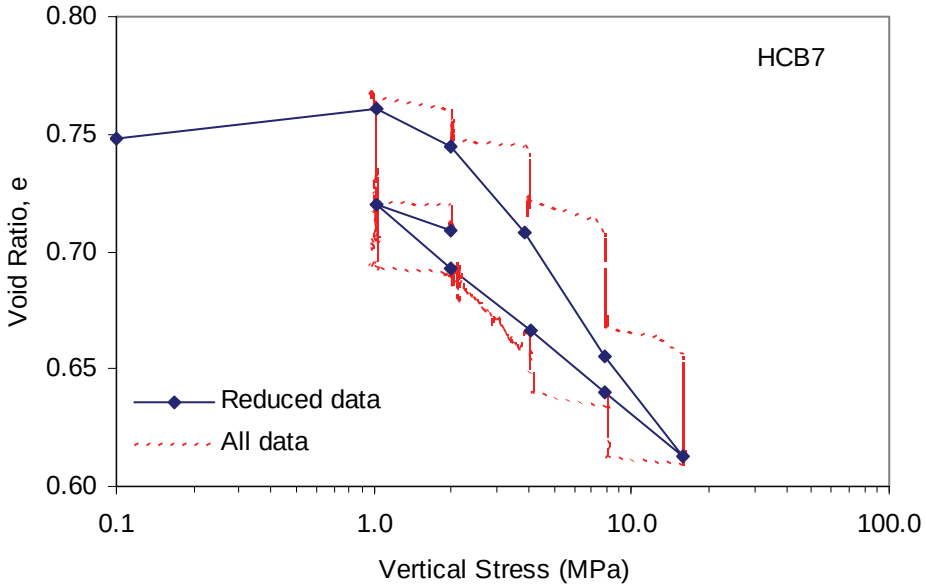

Figure A6: Void Ratio versus Vertical Stress of Specimen HCB7
(Reduced data = data point at the end of each load increment)

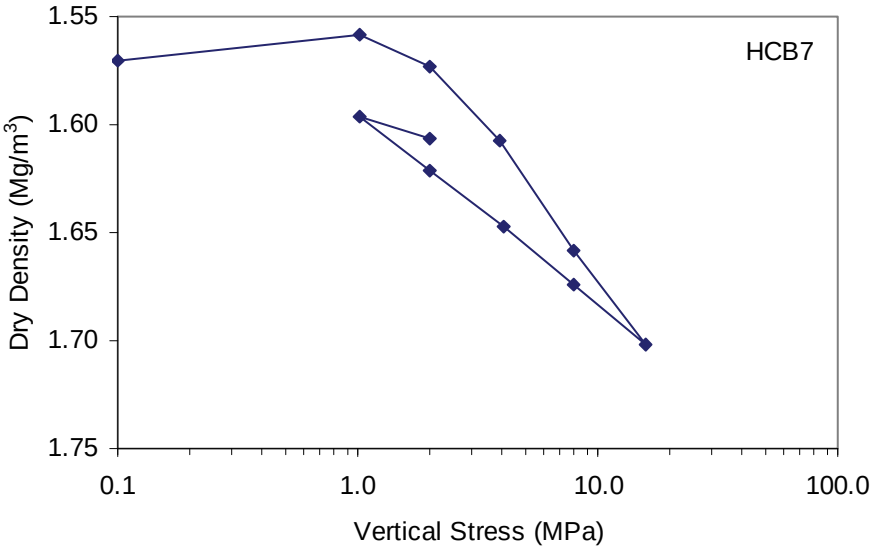

Figure A7: Dry Density versus Vertical Stress of Specimen HCB7

A4.2.2 HCB8

Specimen HCB8 was prepared with distilled water containing 250 g/L $CaCl_2$ as mixing liquid and reservoir liquid. Figure A8 shows the void ratio (e) versus vertical stress (σ_v) of Specimen HCB8. Constant pressure of 1 MPa is applied on Specimen HCB8 at the initial saturation. The specimen HCB8 has a similar loading sequence as Specimen HCB7. The corresponding dry density (ρ_{dry}) versus vertical stress (σ_v) is illustrated in Figure A9.

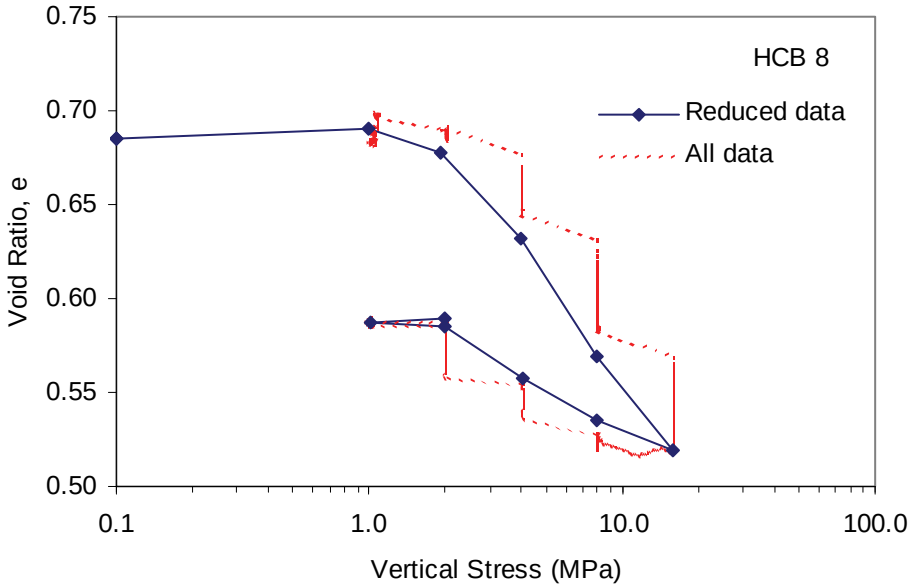

Figure A8: Void Ratio versus Vertical Stress of Specimen HCB8
(Reduced data = data point at the end of each load increment)

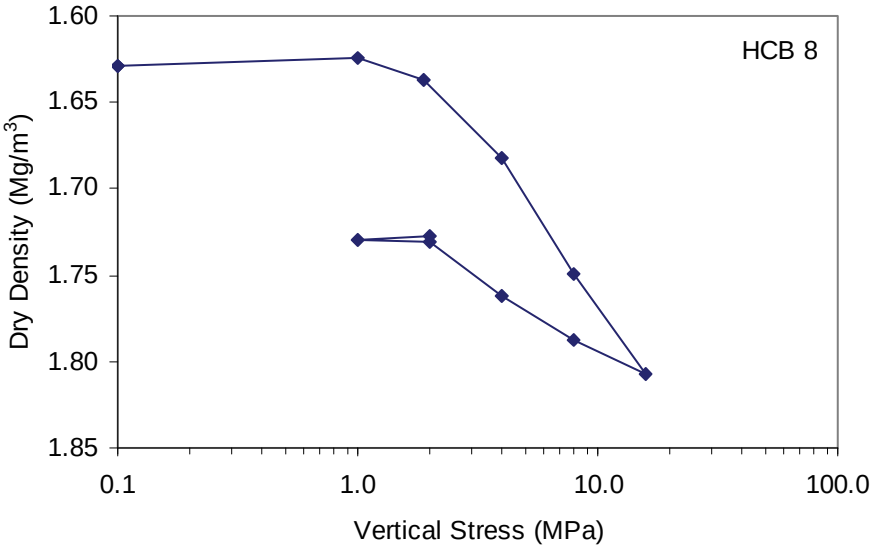

Figure A9: Dry Density versus Vertical Stress of Specimen HCB8

A4.2.3 HCB9

Specimen HCB9 was prepared with distilled water as mixing and reservoir liquids. Figure A10 shows the void ratio (e) versus vertical stress (σ_v) for Specimen HCB9. The corresponding dry density versus vertical stress for Specimen HCB9 is shown in Figures A11. The numbers in Figures A10 and A11 indicate the load sequence of the test. A constant volume boundary condition was applied during the initial saturation (i.e., load sequence no 1 to 2 in Figures A10 and A11). The change of the vertical stress during initial saturation is shown in Figure A12 with a maximum vertical stress of approximately 5 MPa applied. The vertical stress was increased up to 16 MPa (i.e., load sequence no 2 to 3 in Figure A10 and A11). An unintended pressure loss occurred due to the depletion of nitrogen-gas cylinder after the vertical stress of 16 MPa was reached (i.e., load sequence no 3 to 4 in Figure A10 and A11). It was decided to continue the test, despite of the pressure loss, considering the length of the test. The vertical stress was decreased up to 1 MPa before removal of the specimen from the apparatus (i.e., load sequence no 4 to 5 in Figure A10 and A11). The data during the pressure loss section are not included in Figures A10 and A11.

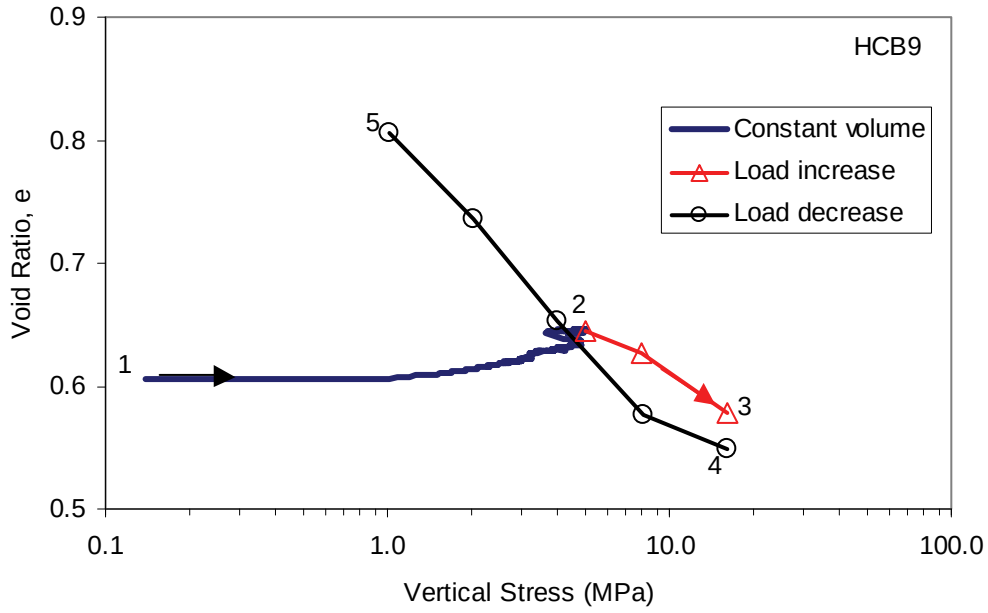

Figure A10: Void Ratio versus Vertical Stress of Specimen HCB9
(Note: numbers show load sequence)

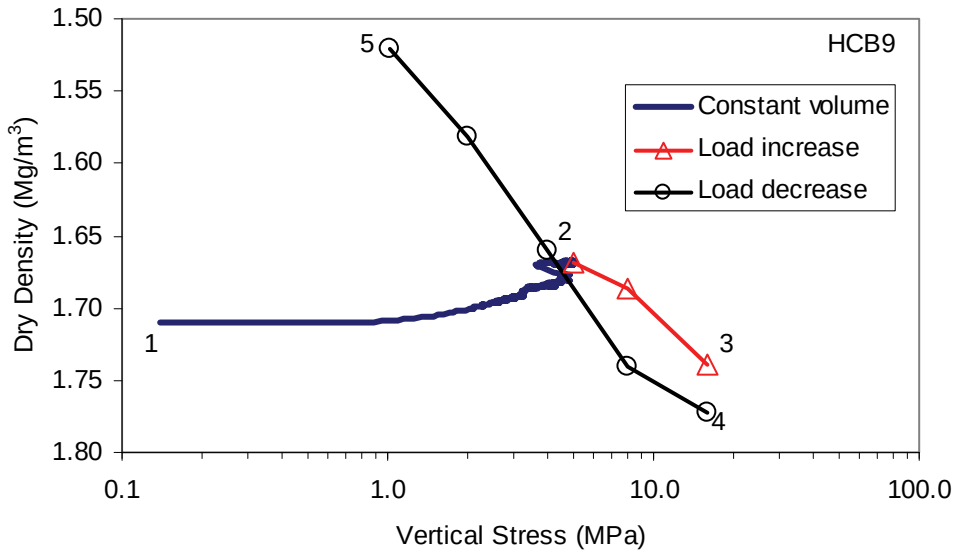

Figure A11: Dry Density versus Vertical Stress of Specimen HCB9
(Note: numbers show load sequence)

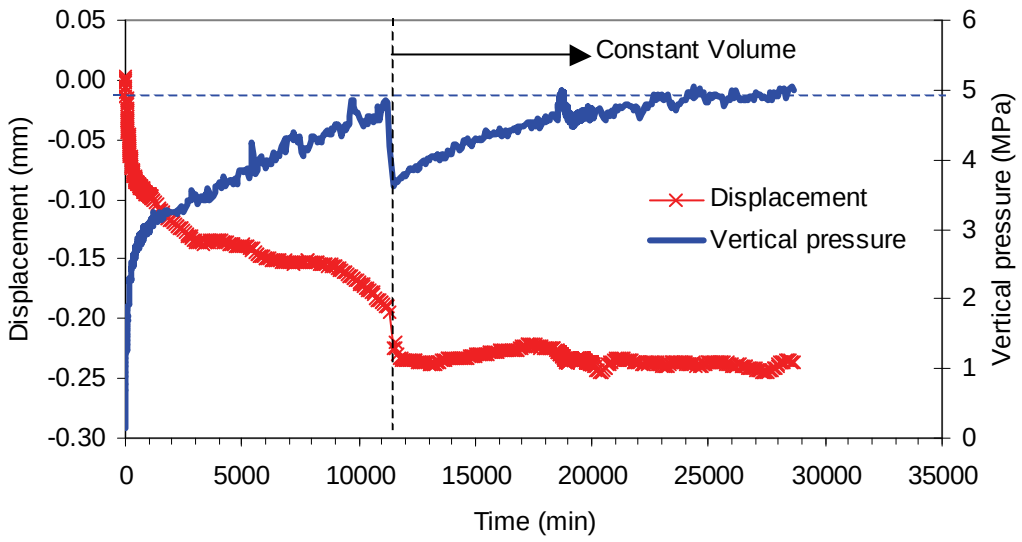

Figure A12: The Displacement and Vertical Stress during Initial Saturation of Specimen HCB9

A4.2.4 HCB10

Specimen HCB10 was prepared with distilled water containing 250 g/L $CaCl_2$ as mixing and reservoir liquids. Figure A13 shows the void ratio (e) versus vertical stress (σ_v) for Specimen HCB10. The corresponding dry density versus vertical stress of Specimen HCB10 is shown in Figure A14. A constant volume boundary condition was applied during the initial saturation. The maximum vertical stress at the initial saturation was approximately 2.3 MPa as shown in Figure A15. The vertical stress is increased up to 16 MPa and then decreased up to 2 MPa. Unintended pressure loss occurred in this test after the 2 MPa increment and so the data associated with this event are not included in Figures A13 and A14.

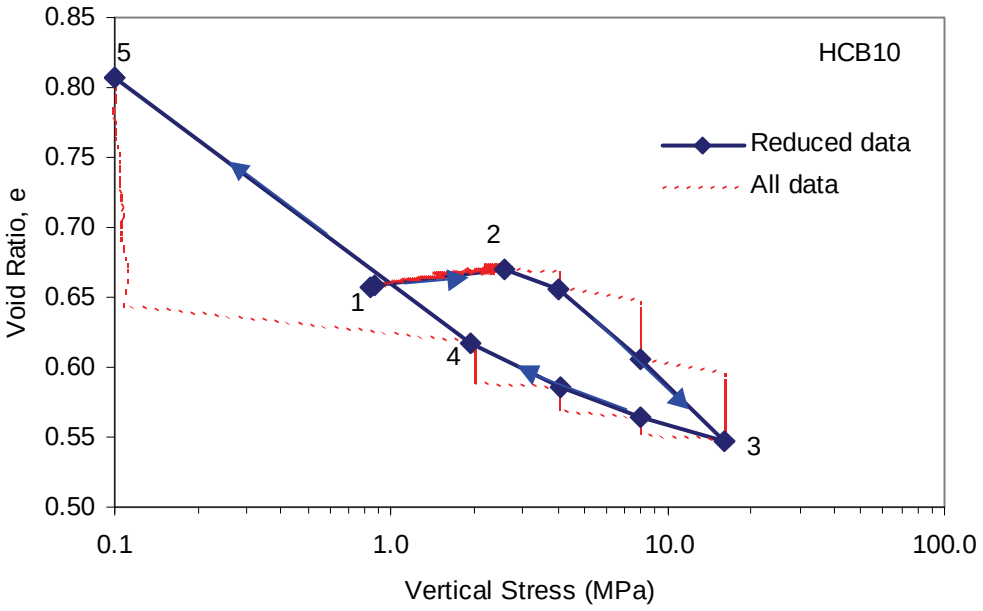

Figure A13: Void Ratio versus Vertical Stress of Specimen HCB10
(Note: numbers show load sequence;
reduced data = data point at the end of each load increment)

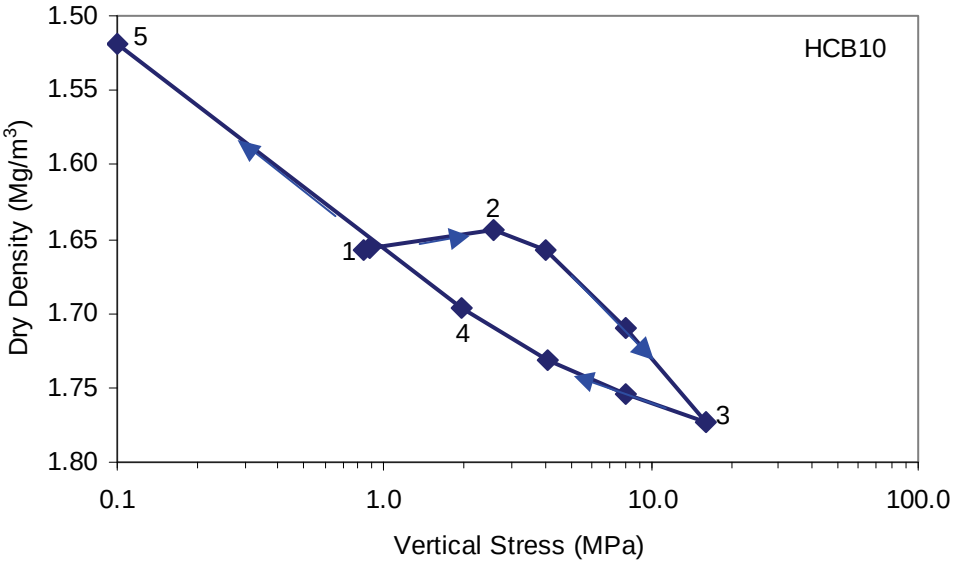

Figure A14: Dry Density versus Vertical Stress of Specimen HCB10
(Note: numbers show load sequence)

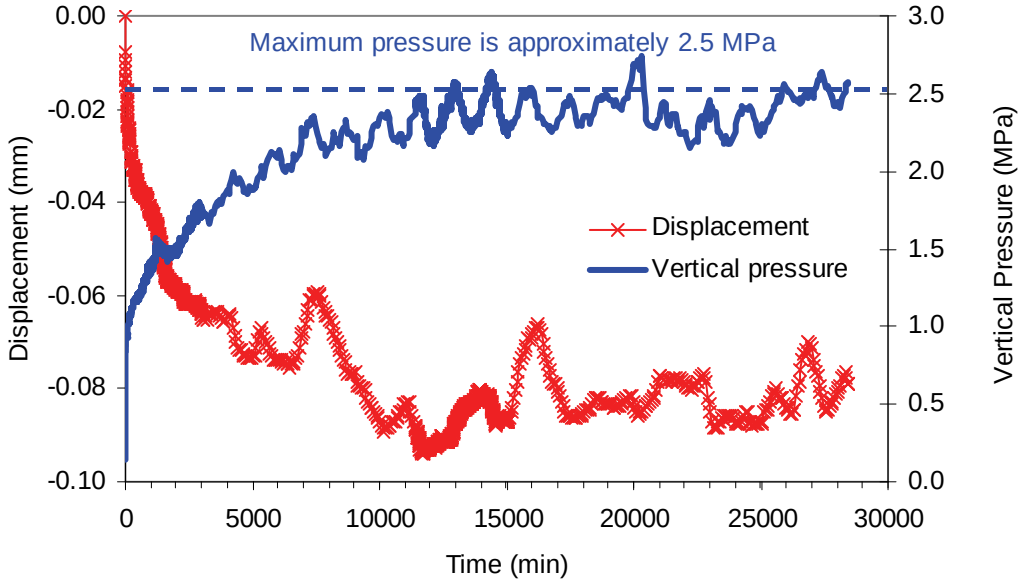

Figure A15: The Displacement and Vertical Stress during Initial Saturation of Specimen HCB10

A4.2.5 HCB11

Specimen HCB11 was prepared with distilled water as the mixing liquid and 150 g/L $CaCl_2$ as the reservoir liquid. Figures A17 and A18 show the void ratio (e) and dry density versus vertical stress (σ_v) of Specimen HCB11, respectively. A constant pressure of 1 MPa was applied during the initial saturation. The vertical stress was increased up to 16 MPa and then stepwise decreased to 1 MPa. The LVDT did not move during the decrease of vertical stress stage of testing. It was discovered at the end of this test that the LVDT was jammed. Data from this unloading portion of the experiment therefore cannot be used for consolidation calculations.

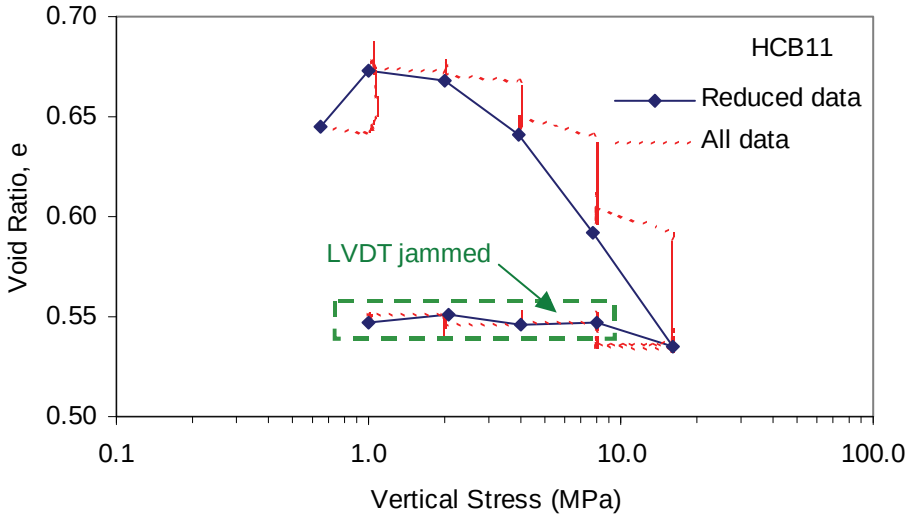

Figure A16: Void Ratio versus Vertical Stress of Specimen HCB11
(Reduced data = data point at the end of each load increment)

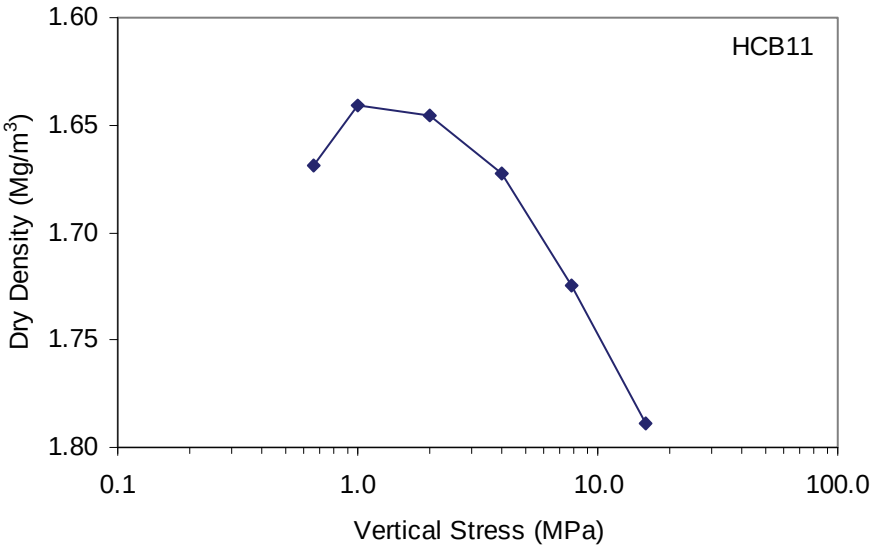

Figure A17: Dry Density versus Vertical Stress of Specimen HCB11

A4.3 COEFFICIENT OF CONSOLIDATION (C_V)

The coefficient of consolidation (c_v) can be generated from the results of 1D consolidation test from each load increment based on consolidation theory (Terzhagi 1943). The coefficient of consolidation (c_v) is a hydraulic-mechanical (H-M) parameter that couples the coefficient of hydraulic conductivity in vertical direction (K_v) and modulus of volume change (m_v). The formulation of the coefficient of consolidation (c_v) is limited to situations where the following assumptions apply (Budhu 2000).

1. The soil is saturated, isotropic, and homogeneous.
2. Darcy's law is valid.
3. Flow is only vertical.
4. The strains are small.

There are two common methods that can be used to calculate c_v.

1. The square root of time method (SQRT) (Taylor 1942).
2. The log time method (LogT) (Casagrande and Fadum 1940).

The procedures for determining the coefficient of consolidation can be found in most geotechnical engineering books (e.g., Budhu 2000, Craig 1992, Das 1998, etc.). The plots of displacement versus square root of time and displacement versus log of time for Specimens HCB7, 8, 9, 10, and 11 are shown in Figures A18 to A27, respectively.

Both methods were used to determine the coefficient of consolidation for each load increment. A comparison of the laboratory data and the calculated displacements based on the parameters determined by the two methods is shown in Figure A28 for Specimen HCB8 during compression under vertical stress of 16 MPa. There is only a slight difference in the coefficient of consolidation (c_v) determined using the two different methods as shown by Figure A28. The coefficient of consolidation (c_v) determined from the SQRT method is based on the matching of the data at the beginning of the primary consolidation, while c_v from the LogT method is based on the matching of the data at the end of the primary consolidation. The results of these analyses for Specimens HCB7 to HCB11 are shown in Tables A8 to A12, respectively.

The coefficient of consolidation (c_v) versus the void ratio (e) is shown in Figures A29 to A33 for Specimens HCB7 to HCB11 respectively. All specimens show that the coefficient of consolidation (c_v) during compression is greater than that during swelling.

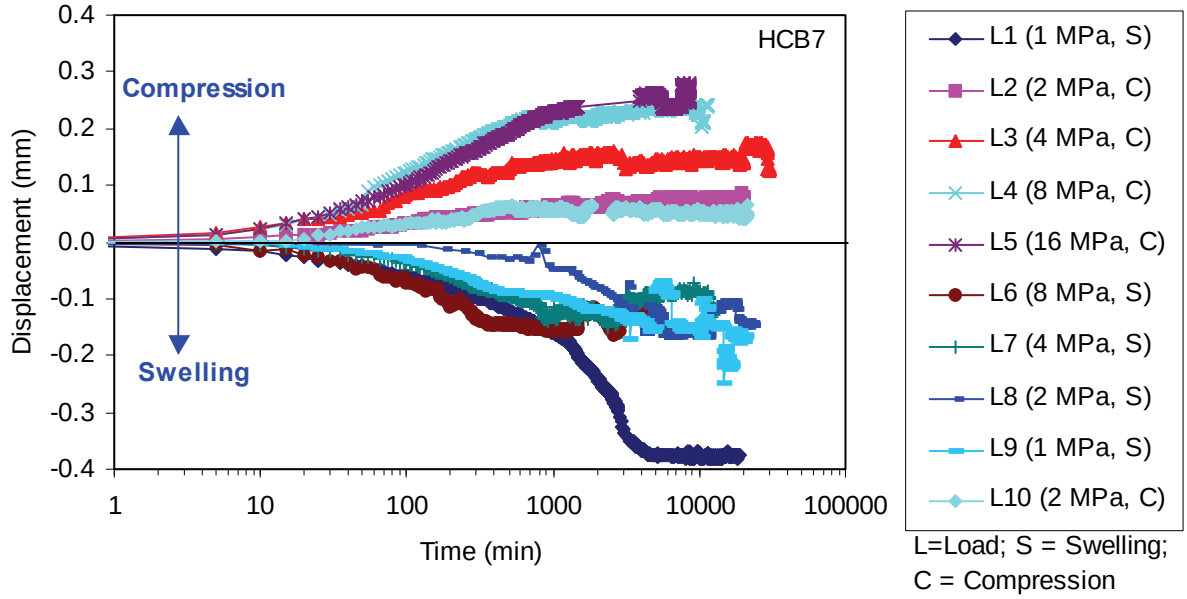

Figure A18: Displacement versus Time in Logarithmic Scale for Specimen HCB7

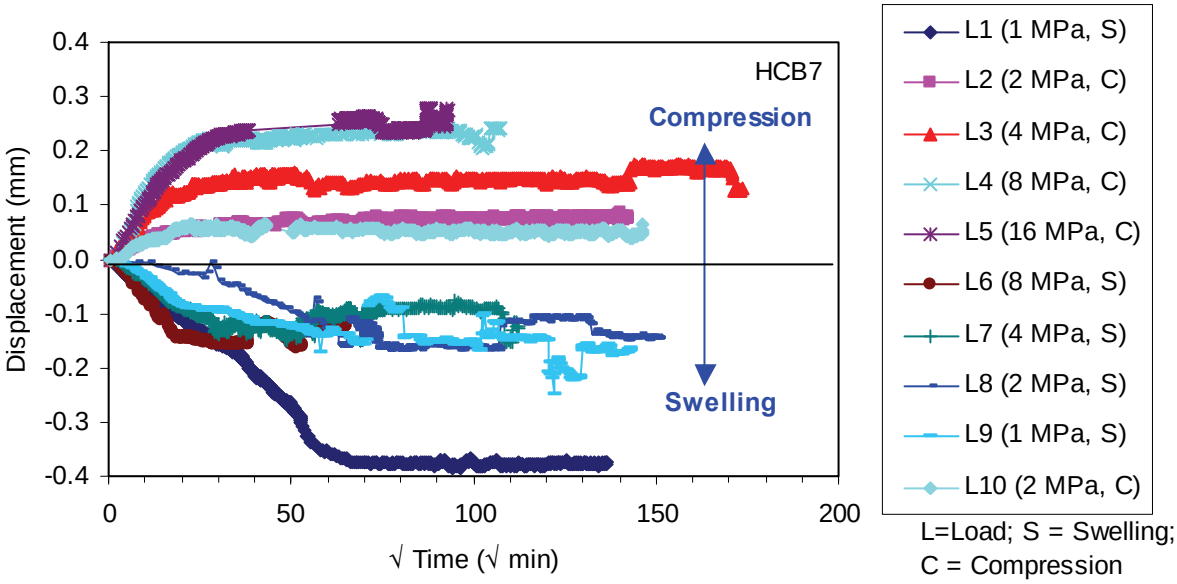

Figure A19: Displacement versus Square Root of Time for Specimen HCB7

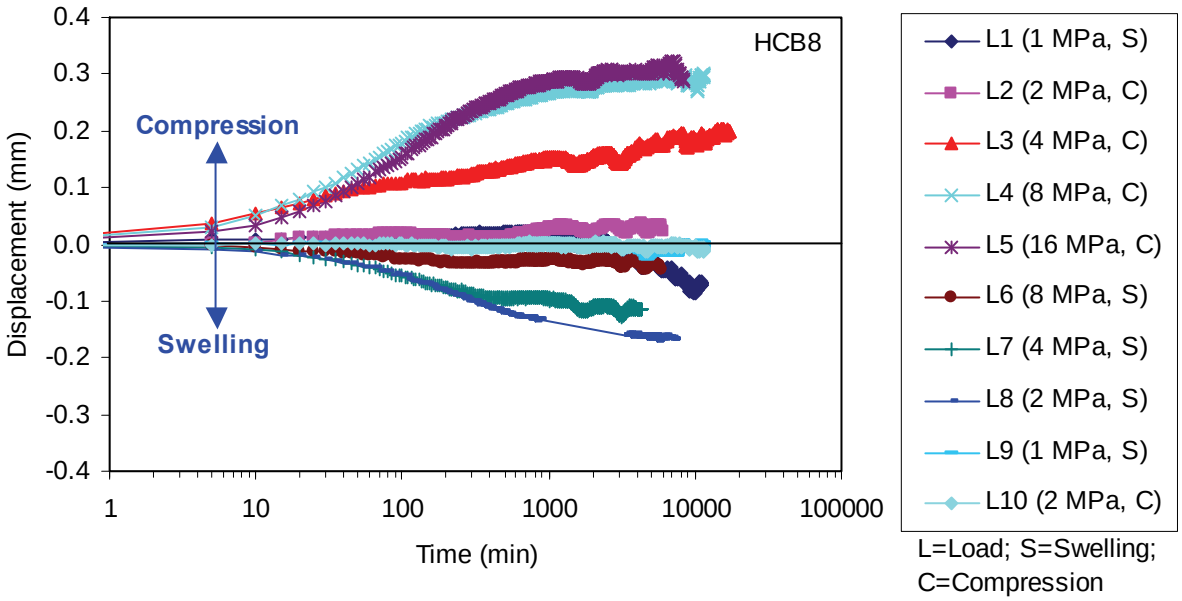

Figure A20: Displacement versus Time in Logarithmic Scale for Specimen HCB8

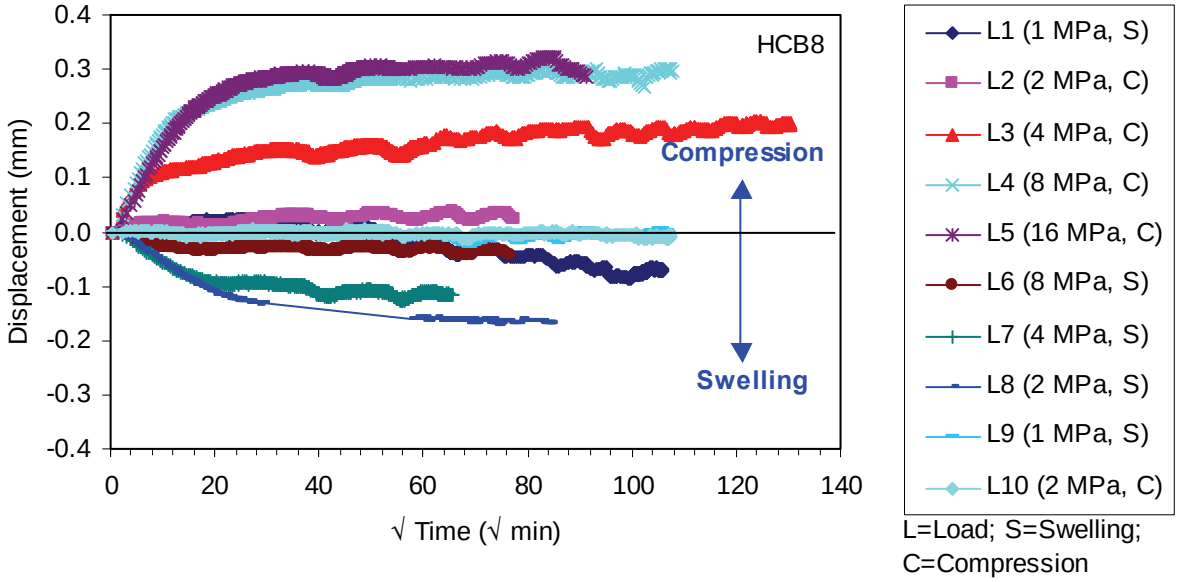

Figure A21: Displacement versus Square Root of Time for Specimen HCB8

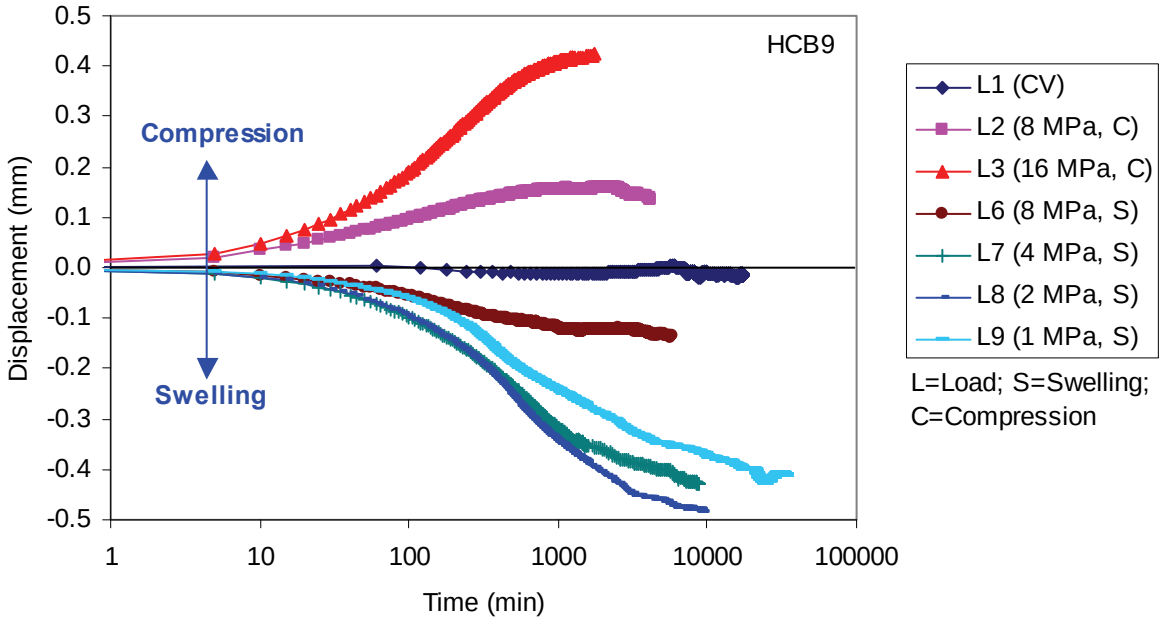

Figure A22: Displacement versus Time in Logarithmic Scale for Specimen HCB9

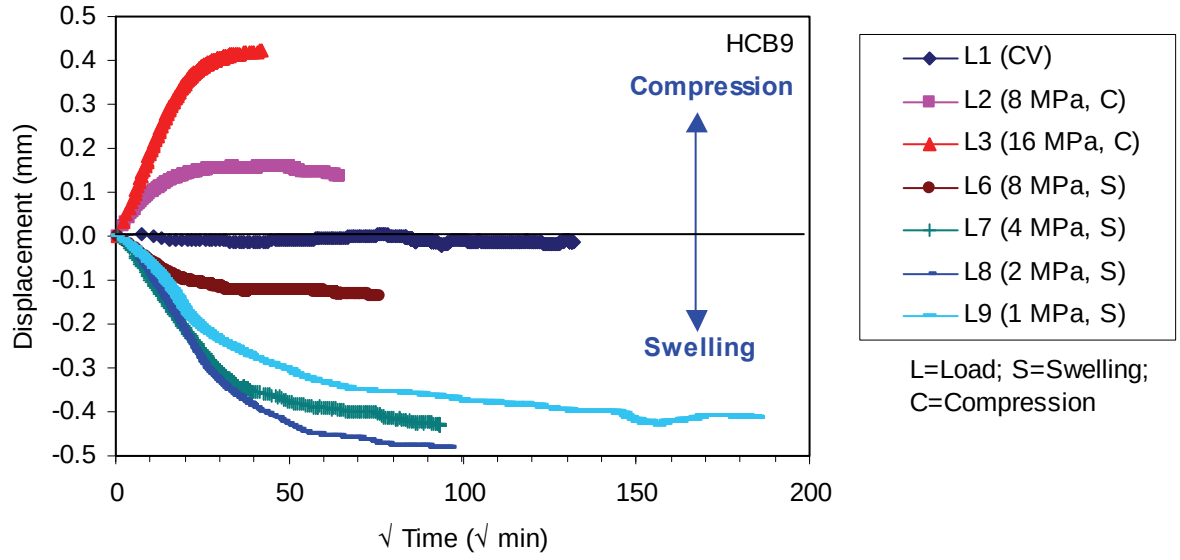

Figure A23: Displacement versus Square Root of Time for Specimen HCB9

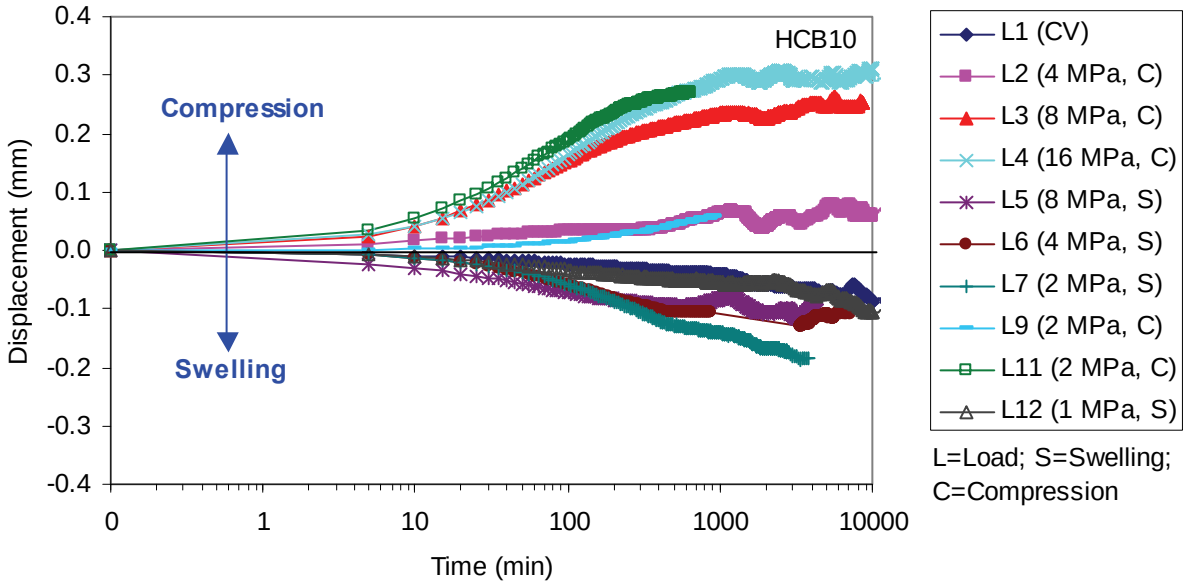

Figure A24: Displacement versus Time in Logarithmic Scale for Specimen HCB10

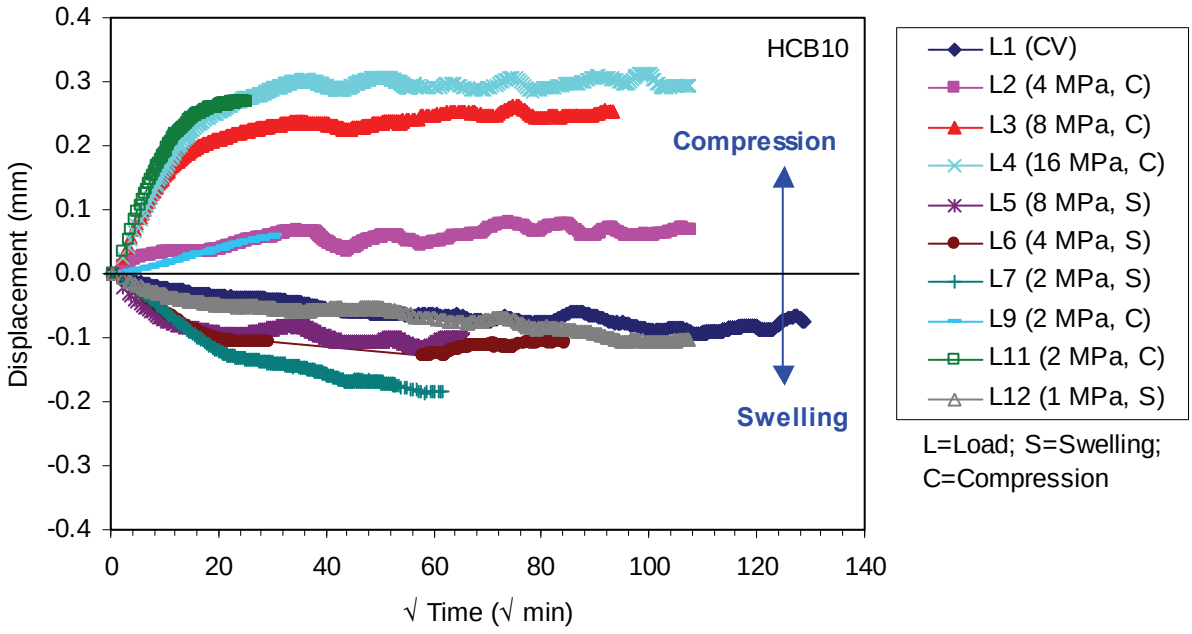

Figure A25: Displacement versus Square Root of Time for Specimen HCB10

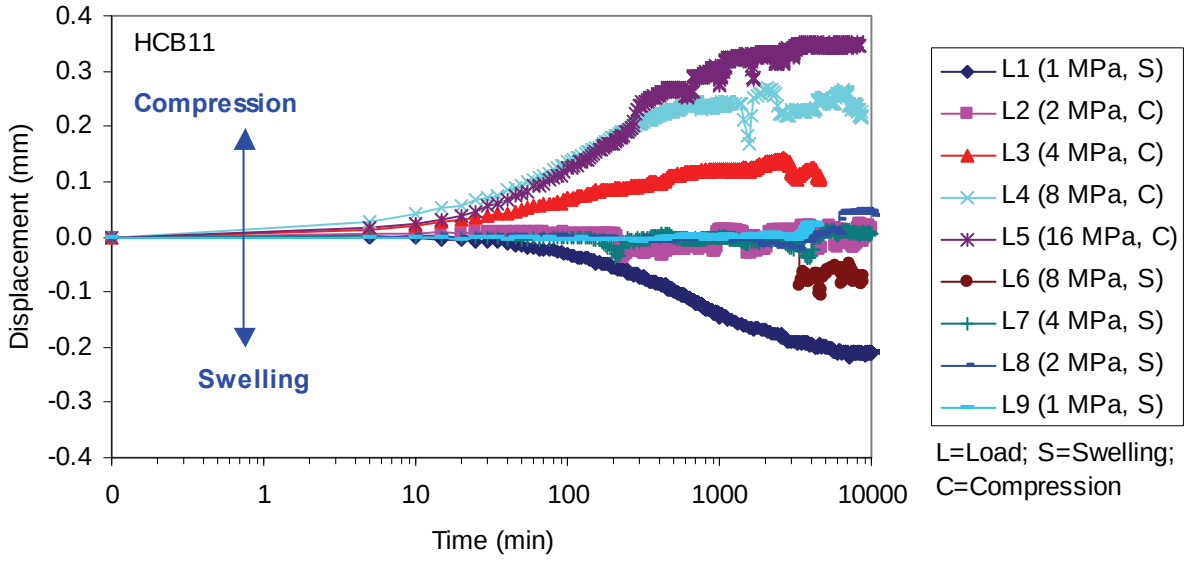

Figure A26: Displacement versus Time in Logarithmic Scale for Specimen HCB11

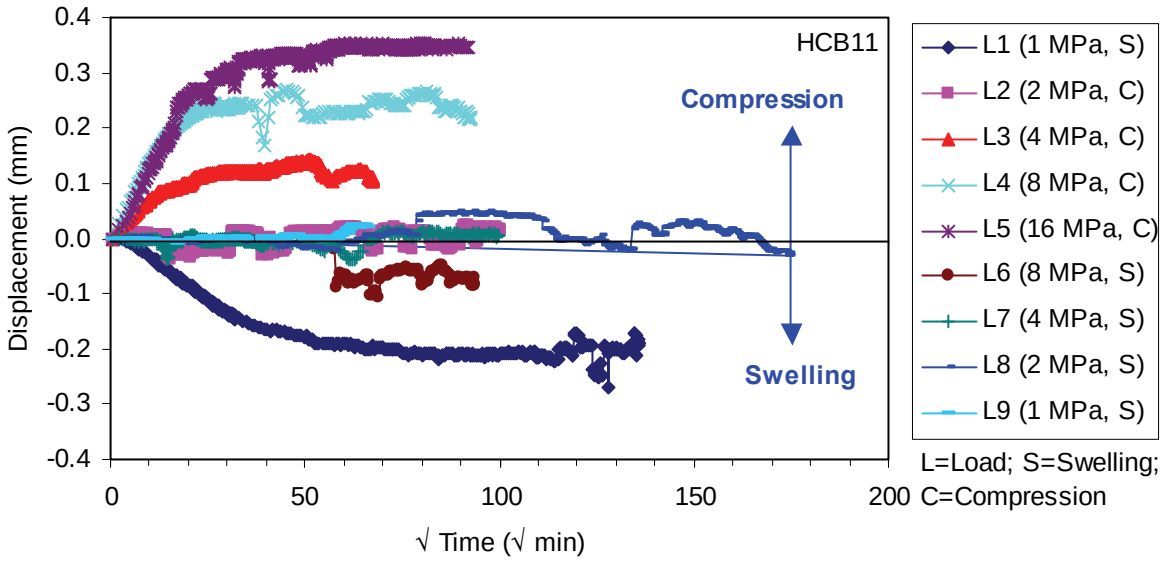

Figure A27: Displacement versus Square Root of Time for Specimen HCB11

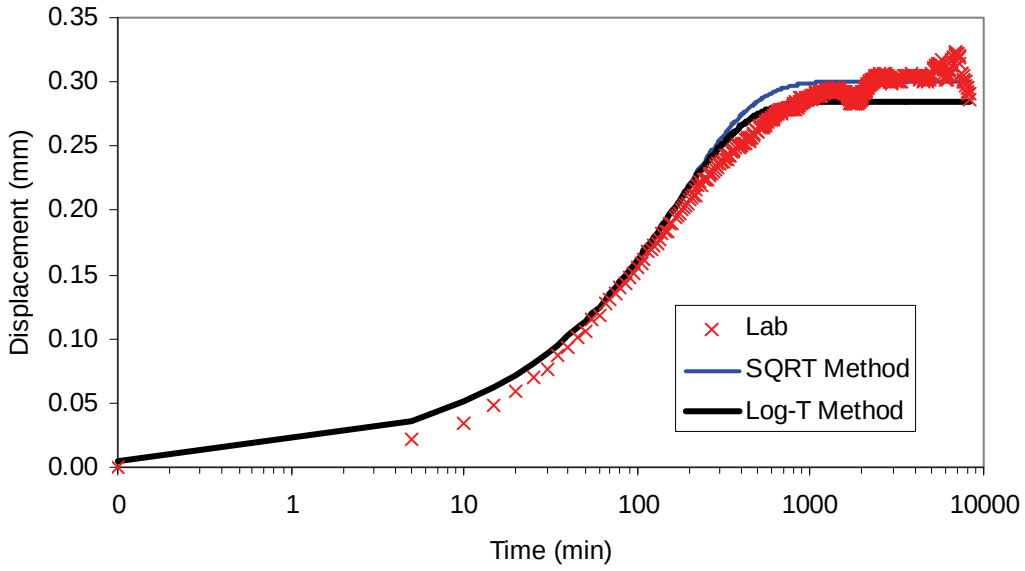

Figure A28: Displacement Calculated Using the Parameters Generated from SQRT and Log-T Methods Compared with the Laboratory Test Data for Specimen HCB 8, Load 5 (16 MPa, Compression)

Table A6: Coefficient of Consolidation (c_v) for Specimen HCB7

Stage	Vertical stress (MPa)	Thickness (mm)	Void Ratio	Dry density (Mg/m^3)	EMDD (Mg/m^3)	Coefficient of Consolidation (mm^2/min)					
						Compression			Swelling		
						Sqrt Time	Log Time	Average	Sqrt Time	Log Time	Average
Pre-Test	0	10.45	0.75	1.57	1.38						
1	1	10.53	0.76	1.56	1.37				0.006	0.004	0.005
2	2	10.43	0.74	1.57	1.39	0.040	0.036	0.038			
3	4	10.21	0.71	1.61	1.42	0.040	0.063	0.051			
4	8	9.89	0.66	1.66	1.48	0.041	0.057	0.049			
5	16	9.64	0.61	1.70	1.52	0.031	0.032	0.032			
6	8	9.80	0.64	1.67	1.49				0.036	0.038	0.037
7	4	9.96	0.67	1.65	1.46				0.020	0.023	0.021
8	2	10.12	0.69	1.62	1.44				0.003	0.002	0.003
9	1	10.28	0.72	1.60	1.41				0.015	0.016	0.016
10	2	10.22	0.71	1.61	1.42	0.066	0.065	0.066			
						Average					
						0.044	0.051	0.047	0.016	0.017	0.016

Table A7: Coefficient of Consolidation (c_v) for Specimen HCB8

Stage	Vertical stress (MPa)	Thickness (mm)	Void Ratio	Dry density (Mg/m^3)	EMDD (Mg/m^3)	Coefficient of Consolidation (mm^2/min)					
						Compression			Swelling		
						Sqrt Time	Log Time	Average	Sqrt Time	Log Time	Average
Pre-Test	0	10.27	0.68	1.63	1.44						
1	1	10.30	0.69	1.62	1.44						
2	2	10.23	0.68	1.64	1.45	0.043	0.116	0.079			
3	4	9.95	0.63	1.68	1.50	0.109	0.084	0.097			
4	8	9.57	0.57	1.75	1.57	0.109	0.084	0.097			
5	16	9.26	0.52	1.81	1.63	0.052	0.058	0.055			
6	8	9.36	0.54	1.79	1.61				0.089	0.114	0.102
7	4	9.50	0.56	1.76	1.59				0.050	0.061	0.055
8	2	9.67	0.59	1.73	1.55				0.030	0.025	0.027
9	1	9.68	0.59	1.73	1.55						
10	2	9.69	0.59	1.73	1.55						
						Average					
						0.078	0.085	0.082	0.056	0.067	0.061

Table A8: Coefficient of Consolidation (c_v) for Specimen HCB9

Stage	Vertical stress (MPa)	Thickness (mm)	Void Ratio	Dry density (Mg/m^3)	EMDD (Mg/m^3)	Coefficient of Consolidation (mm^2/min)					
						Compression			Compression		
						Sqrt Time	Log Time	Average	Sqrt Time	Log Time	Average
Pre-Test	0.1	9.60	0.61	1.71	1.53	N/A	N/A	N/A	N/A	N/A	N/A
1A	3.6	9.82	0.64	1.67	1.49	N/A	N/A	N/A	N/A	N/A	N/A
1B	5.0	9.84	0.65	1.67	1.49	N/A	N/A	N/A	N/A	N/A	N/A
2	8.0	9.73	0.63	1.69	1.51	0.058	0.081	0.069			
3	16.0	9.44	0.58	1.74	1.56	0.036	0.044	0.040			
5	16.0	9.26	0.55	1.77	1.60	0.048	0.061	0.055			
6	8.0	9.43	0.58	1.74	1.56				0.037	0.035	0.036
7	4.0	9.88	0.65	1.66	1.48				0.013	0.015	0.014
8	2.0	10.38	0.74	1.58	1.39				0.013	0.013	0.013
9	1.0	10.79	0.80	1.52	1.33				0.012	0.008	0.010
						Average					
						0.047	0.062	0.055	0.016	0.016	0.016

Table A9: Coefficient of Consolidation (c_v) for Specimen HCB10

Stage	Vertical stress (MPa)	Thickness (mm)	Void Ratio	Dry density (Mg/m^3)	EMDD (Mg/m^3)	Coefficient of Consolidation (mm^2/min)					
						Compression			Swelling		
						Sqrt Time	Log Time	Average	Sqrt Time	Log Time	Average
Initial	0.8	10.09	0.66	1.66	1.47						
	0.9	10.10	0.66	1.66	1.47						
1	2.6	10.17	0.67	1.64	1.46						
2	4.0	10.09	0.66	1.66	1.47	0.127	0.078	0.102			
3	8.0	9.78	0.61	1.71	1.53	0.101	0.083	0.092			
4	16.0	9.43	0.55	1.77	1.60	0.067	0.055	0.061			
5	8.0	9.53	0.56	1.75	1.58	0.142	0.125	0.134			
6	4.1	9.66	0.59	1.73	1.55				0.043	0.043	0.043
7	1.9	9.85	0.62	1.70	1.52				0.025	0.023	0.024
8	0.1	11.01	0.81	1.52	1.33						
9	2.0	10.26	0.68	1.63	1.44						
10	0.1	10.63	0.75	1.57	1.39						
11	2.1	10.25	0.68	1.63	1.45	0.117	0.109	0.113			
12	0.9	10.37	0.70	1.61	1.43				0.093	0.065	0.079
						Average					
						0.111	0.090	0.100	0.054	0.044	0.049

Table A10: Coefficient of Consolidation (c_v) for Specimen HCB11

Stage	Vertical stress (MPa)	Thickness (mm)	Void Ratio	Dry density (Mg/m^3)	EMDD (Mg/m^3)	Coefficient of Consolidation (mm^2/min)					
						Compression			Swelling		
						Sqrt Time	Log Time	Average	Sqrt Time	Log Time	Average
Initial	1	9.81	0.65	1.67	1.49						
1	1	9.98	0.67	1.64	1.46				0.007	0.008	0.007
2	2	9.95	0.67	1.65	1.46						
3	4	9.79	0.64	1.67	1.49	0.065	0.061	0.063			
4	8	9.49	0.59	1.72	1.54	0.057	0.059	0.058			
5	16	9.15	0.53	1.79	1.61	0.024	0.022	0.023			
						Average					
						0.048	0.047	0.048	0.007	0.008	0.007

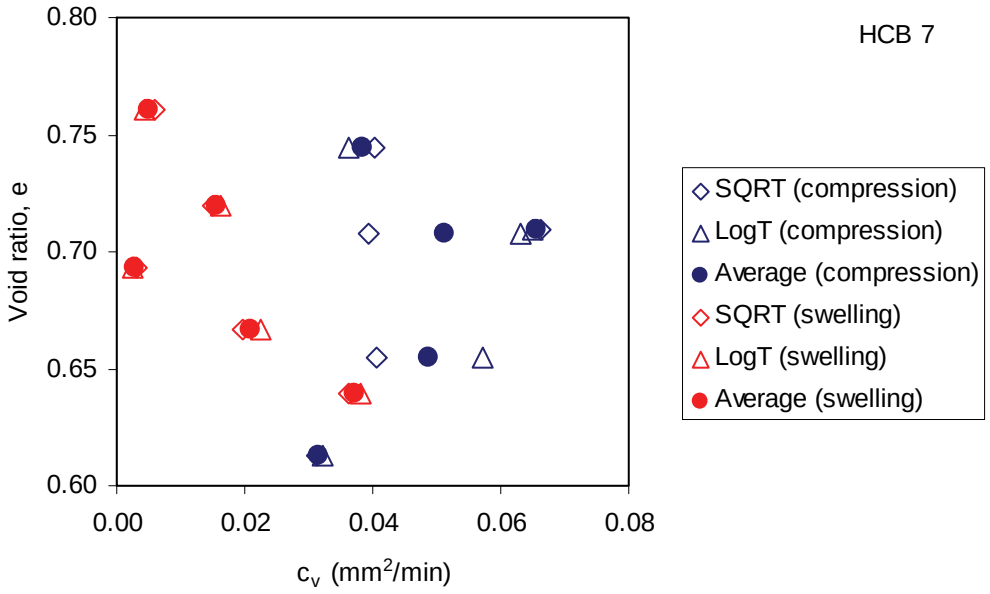

Figure A29: Void Ratio versus Coefficient of Consolidation (c_v) of Specimen HCB7

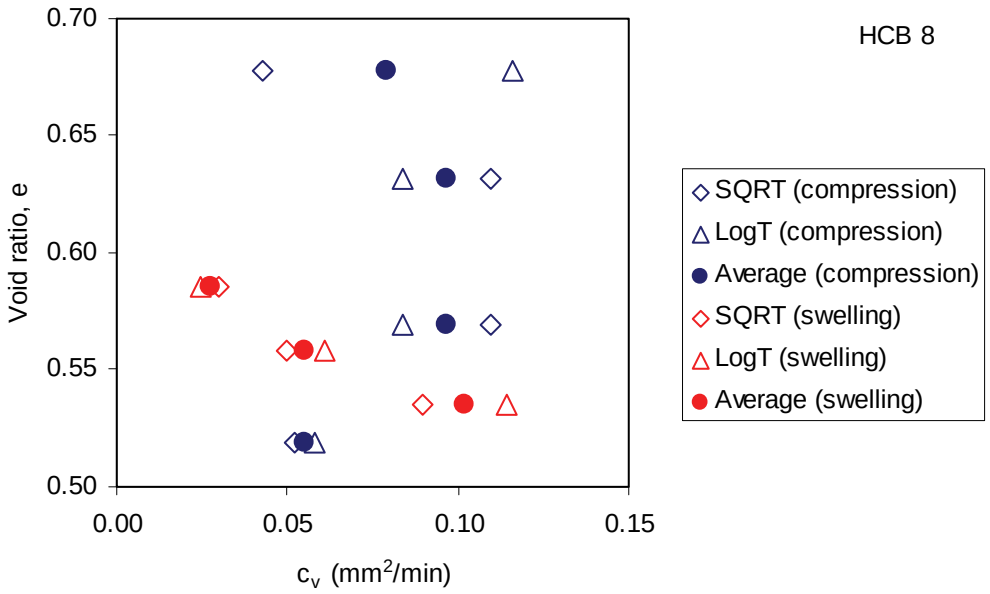

Figure A30: Void Ratio versus Coefficient of Consolidation (c_v) of Specimen HCB8

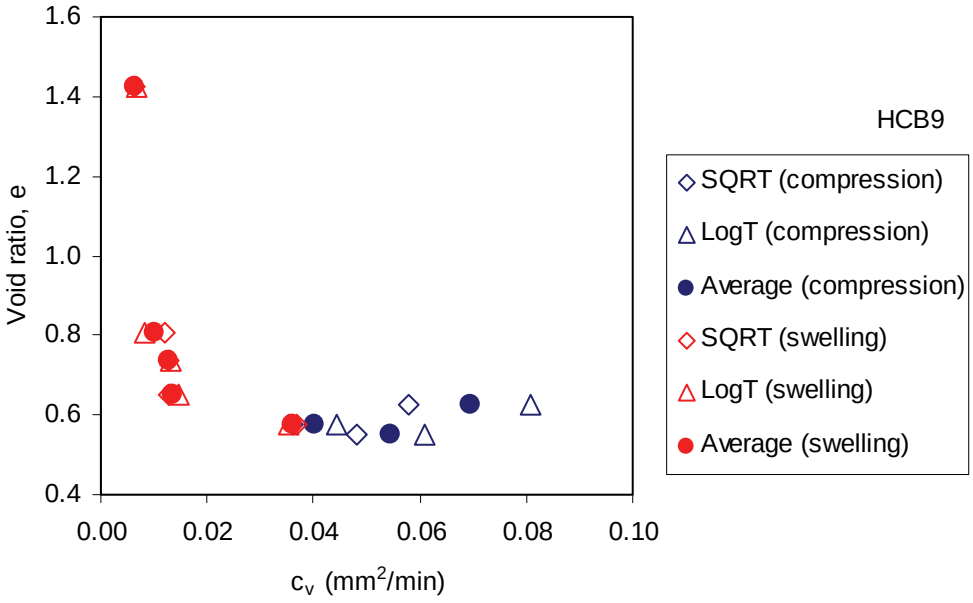

Figure A31: Void Ratio versus Coefficient of Consolidation (c_v) of Specimen HCB9

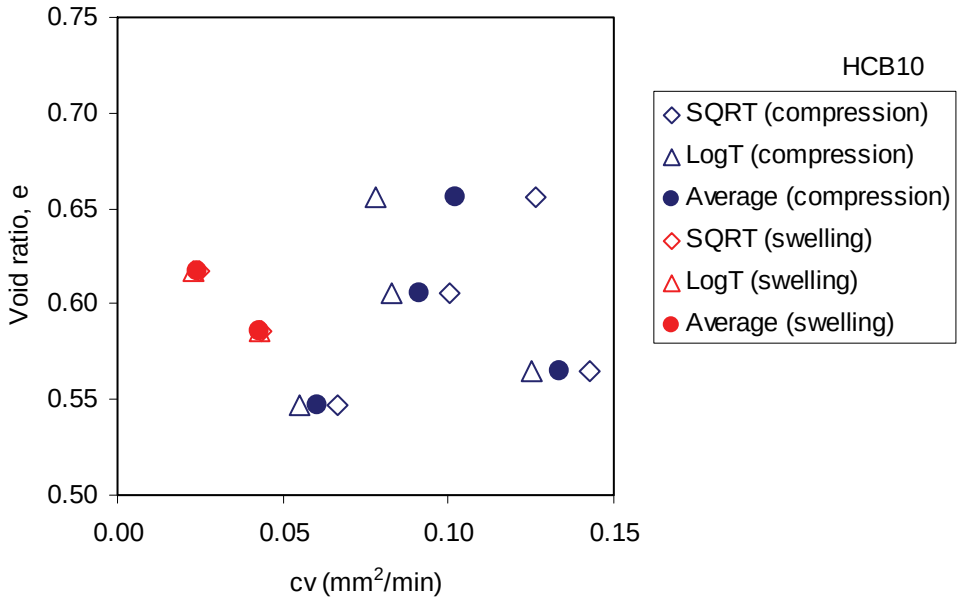

Figure A32: Void Ratio versus Coefficient of Consolidation (c_v) of Specimen HCB10

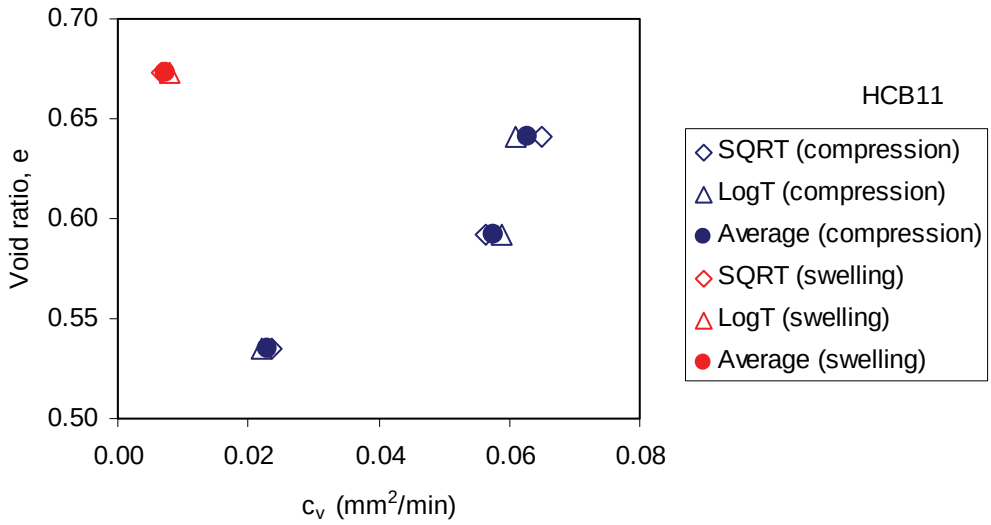

Figure A33: Void Ratio versus Coefficient of Consolidation (c_v) of Specimen HCB11

A4.4 HYDRAULIC CONDUCTIVITY (K)

The hydraulic conductivity (K) can be estimated from the coefficient of consolidation (c_v) by assuming that the soil is linear elastic for each load increment.

$$K = c_v \cdot m_v \cdot \gamma_w \qquad \text{(A4)}$$

where K - hydraulic conductivity (m/s);
m_v - coefficient of volume compressibility (Pa^{-1});
γ_w - unit weight of water (N/m^3)

The hydraulic conductivity (K) estimated from Equation A4 as a function of EMDD is shown in Figure A34. The hydraulic conductivity (K) calculated from the results of 1D consolidation tests is within the range of $1 \cdot 10^{-15}$ to $1 \cdot 10^{-11}$ m/s for EMDD within the range of 1.1 to 1.6 Mg/m^3; and it decreases with an increase of EMDD. This is comparable with the hydraulic conductivity (K) of the bentonite measured using hydraulic conductivity cells by Dixon et al. (1999) as shown in Figure A35.

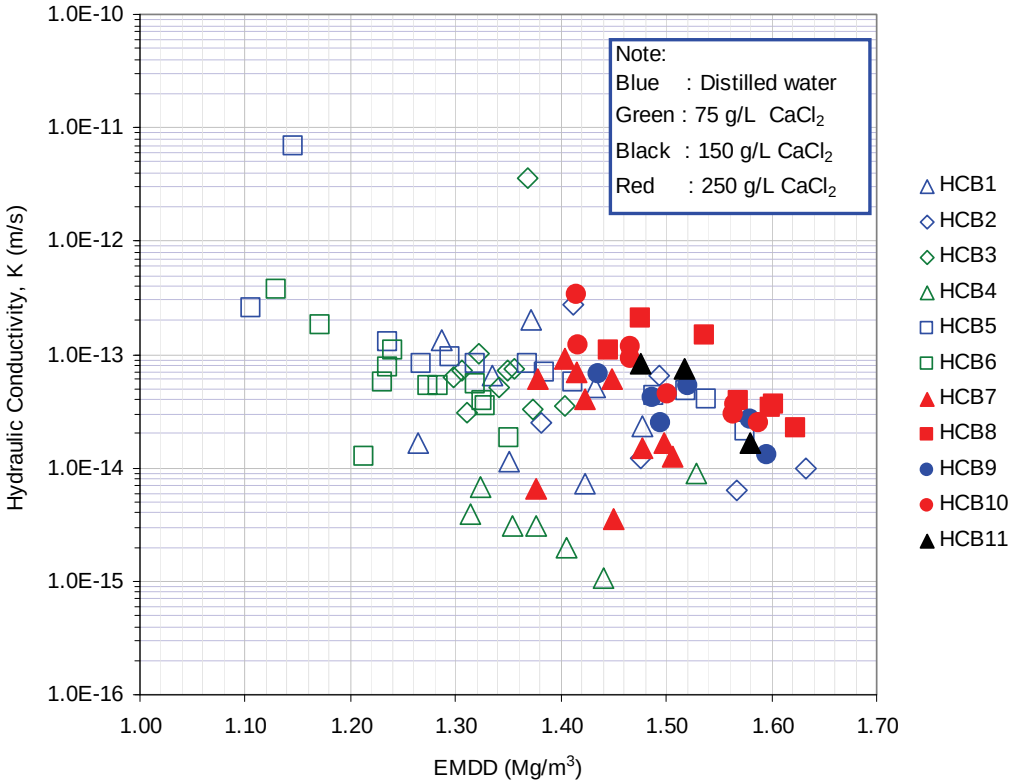

Figure A34: Hydraulic Conductivity Estimated from 1D-Consolidation Test for Highly Compacted Bentonite (HCB)

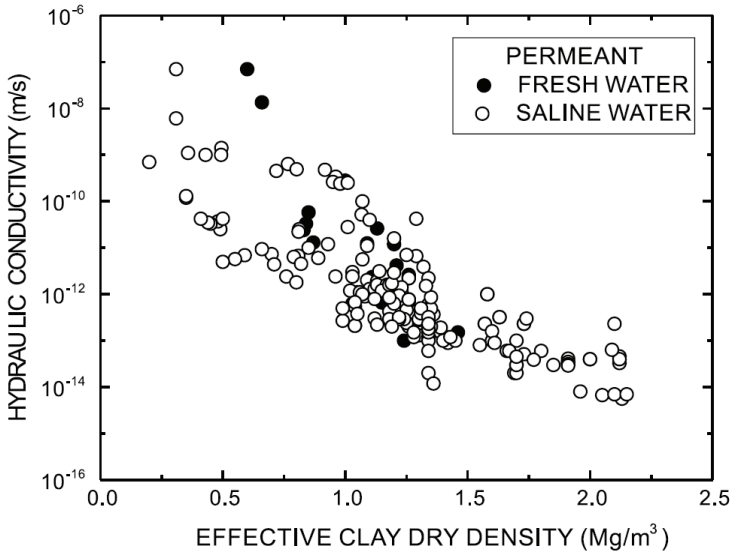

Figure A35: Hydraulic Conductivity (K) of Bentonite Measured using Hydraulic Conductivity Cell (Dixon et al. 1999)

A4.5 1D-MODULUS

The 1D consolidation tests only measure the displacement and stress in vertical direction. The horizontal stress during an oedometer test is unknown. Consequently only a 1D-constrained modulus (M) can be estimated from the results of these tests. The 1D-constrained modulus (M) of the soil can be calculated from the relationship of vertical strain (ε_v) and vertical stress increment (σ_v). The 1D-constrained modulus (M) for increasing loads is less than for decreasing loads. It should be recognized that the behaviour of soil is not linear elastic, especially for large strain changes. The soil can only be considered as a linear elastic material for a small strain increment. The mechanical behaviour of soils is also stress path dependent. The estimate values of 1D-constrained modulus (M) for Specimens HCB1 to HCB11 versus EMDD are illustrated in Figure A36, the data are shown in Tables A11 to A21.

Numerical modelling usually starts using the simplest constitutive model, such as linear elastic model. In two-dimensional modelling, the linear elastic model requires two parameters to describe the mechanical behaviour: Young's modulus (E) and Poisson's ratio (ν). The Young's modus (E) can be estimated from the 1D-constrained modulus (M) by assuming the value of Poisson's ratio (ν). Representative Poisson's ratio (ν) for soft clay is 0.15-0.25. For medium clay Poission's ratio (ν) is in the range of 0.2 to 0.5 (Das 1998). The Poisson's ratio (ν) of soil can be determined from the results of the triaxial test.

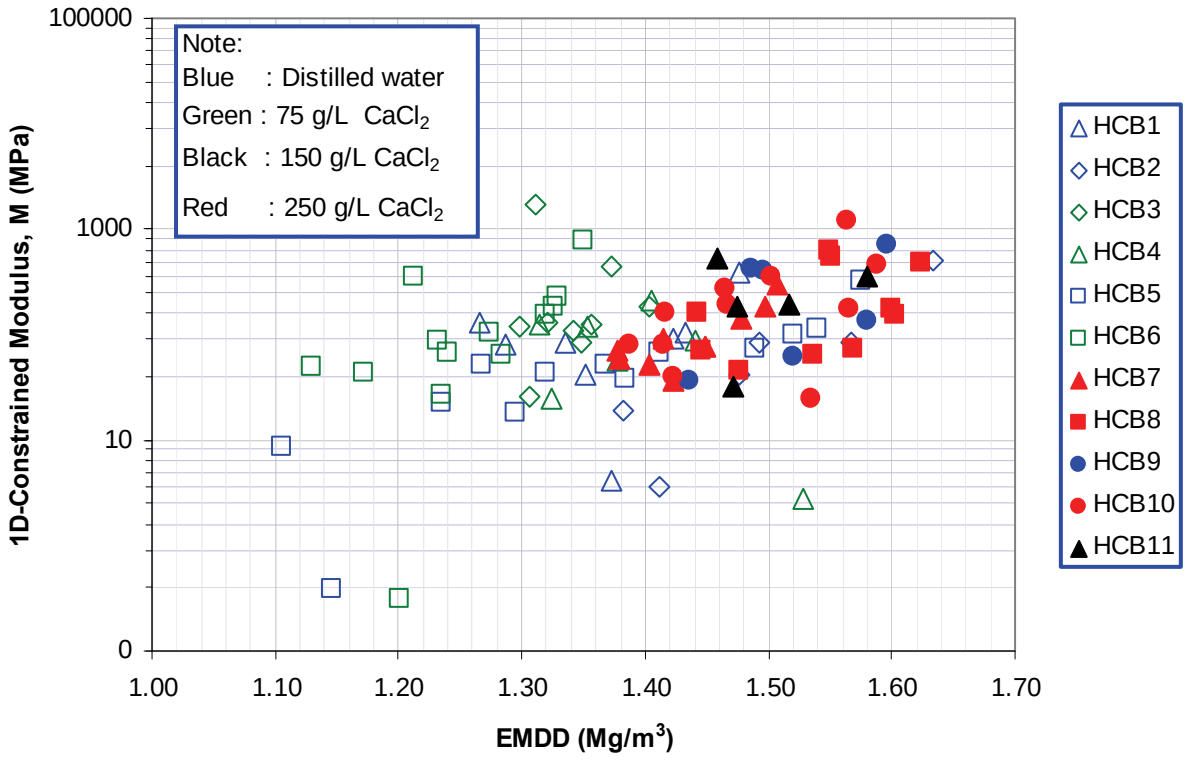

Figure A36: 1D-Constrained Modulus versus EMDD

Table A11: 1D-Constrained Modulus for Specimens HCB1

Stage	Vertical stress (MPa)	Vertical strain (%)	Vertical stress-mid value (MPa)	Void ratio-mid value, e	EMDD-mid value (Mg/m^3)	1D-Constrained Modulus (MPa)			
						All	Initial	Loading	Unloading
start	0.38	0.0							
1	0.99	15.0	0.7	0.77	1.37	4	4		
2	2.1	14.2	1.5	0.88	1.27	130		130	
3	3.98	11.8	3.0	0.86	1.29	79		79	
4	7.97	7.1	6.0	0.80	1.34	85		85	
5	15.93	-0.6	12.0	0.70	1.43	103		103	
6	8.01	1.5	12.0	0.65	1.48	383			383
7	4.02	5.9	6.0	0.70	1.42	90			90
8	2	10.8	3.0	0.78	1.35	42			42
		Max	12.0	0.88	1.48	383	4	130	383
		Min	0.7	0.65	1.27	4	4	79	42
		Average	5.5	0.77	1.37	115	4	99	171

Table A12: 1D-Constrained Modulus for Specimens HCB2

Stage	Vertical stress (MPa)	Vertical strain (%)	Vertical stress-mid value (MPa)	Void ratio-mid value, e	EMDD-mid value (Mg/m^3)	1D-Constrained Modulus (MPa)			
						All	Initial	Loading	Unloading
start	0.98	0.0							
1	1.31	9.2	1.1	0.72	1.41	4	4		
2	15.98	-8.4	8.6	0.65	1.49	83		83	
3	8.59	-6.9	12.3	0.52	1.63	506			506
4	4.27	-1.8	6.4	0.57	1.57	85			85
5	2.34	2.9	3.3	0.65	1.48	41			41
6	1.02	9.8	1.7	0.75	1.38	19			19
		Max	12.3	0.75	1.63	506	4	83	506
		Min	1.1	0.52	1.38	4	4	83	19
		Average	5.6	0.64	1.49	123	4	83	163

Table A13: 1D-Constrained Modulus for Specimens HCB3

Stage	Vertical stress (MPa)	Vertical strain (%)	Vertical stress-mid value (MPa)	Void ratio-mid value, e	EMDD-mid value (Mg/m^3)	1D-Constrained Modulus (MPa)			
						All	Initial	Loading	Unloading
start	1.02	0.0							
1	1.03	11.1	1.0	0.76	1.37	0.1	0.1		
2	2.07	11.1	1.6	0.83	1.31	1710		1710	
3	3.94	9.7	3.0	0.82	1.32	128		128	
4	8.05	6.4	6.0	0.78	1.36	125		125	
5	3.99	7.3	6.0	0.76	1.37	445			445
6	1.96	9.7	3.0	0.78	1.35	86			86
7	1	13.4	1.5	0.83	1.31	26			26
8	3.98	10.8	2.5	0.84	1.30	117		117	
9	7.97	7.1	6.0	0.79	1.34	108		108	
10	15.88	2.7	11.9	0.73	1.40	181		181	
		Max	11.9	0.8	1.40	1710	0.1	1710	445.0
		Min	1.0	0.7	1.30	0.1	0.1	108	25.9
		Average	4.2	0.8	1.34	292	0.1	395	185.5

Table A14: 1D-Constrained Modulus for Specimens HCB4

Stage	Vertical stress (MPa)	Vertical strain (%)	Vertical stress-mid value (MPa)	Void ratio-mid value, e	EMDD-mid value (Mg/m^3)	1D-Constrained Modulus (MPa)			
						All	Initial	Loading	Unloading
start	8.06	0.0							
1	8.22	5.8	8.1	0.61	1.53	3	3		
2	4.17	10.5	6.2	0.69	1.44	87			87
3	2.04	14.2	3.1	0.75	1.38	57			57
4	1.08	18.1	1.6	0.81	1.32	25			25
5	4.14	15.6	2.6	0.82	1.31	122		122	
6	7.95	12.4	6.0	0.78	1.35	119		119	
7	16	8.5	12.0	0.72	1.40	209		209	
		Max	12.0	0.8	1.53	209.3	3	209	87
		Min	1.6	0.6	1.31	2.7	3	119	25
		Average	5.7	0.7	1.37	88.9	3	150	56

Table A15: 1D-Constrained Modulus for Specimens HCB5

Stage	Vertical stress (MPa)	Vertical strain (%)	Vertical stress-mid value (MPa)	Void ratio-mid value, e	EMDD-mid value (Mg/m^3)	1D-Constrained Modulus (MPa)			
						All	Initial	Loading	Unloading
start	1.03	0.0							
1	0.96	17.9	1.0	1.07	1.15	0.4	0.4		
2	1.98	6.2	1.5	1.13	1.11	9		9	
3	4.06	-3.1	3.0	0.93	1.24	23		23	
4	8.11	-11.0	6.1	0.77	1.37	51		51	
5	15.85	-18.8	12.0	0.62	1.52	99		99	
6	8.12	-16.3	12.0	0.57	1.58	319			319
7	4.04	-10.7	6.1	0.64	1.49	72			72
8	2.02	-5.4	3.0	0.75	1.38	38			38
9	1.02	0.1	1.5	0.85	1.30	18			18
10	1.98	-1.8	1.5	0.88	1.27	52	52		
11	4.01	-6.5	3.0	0.82	1.32	43	43		
12	8.07	-12.4	6.0	0.72	1.41	69	69		
13	15.78	-19.2	11.9	0.60	1.54	114	114		
		Max	12.0	1.1	1.54	318.9	114.3	99.3	318.9
		Min	1.0	0.6	1.27	0.4	0.4	8.7	18.4
		Average	5.3	0.8	1.37	69.8	55.7	45.4	111.9

Table A16: 1D-Constrained Modulus for Specimens HCB6

Stage	Vertical stress (MPa)	Vertical strain (%)	Vertical stress-mid value (MPa)	Void ratio-mid value, e	EMDD-mid value (Mg/m^3)	1D-Constrained Modulus (MPa)			
						All	Initial	Loading	Unloading
start	1.01	0.0							
1	0.97	12.9	1.0	0.98	1.20	0.3	0.3		
2	1.99	10.8	1.5	1.08	1.13	50		50	
3	4.1	6.0	3.0	1.02	1.17	44		44	
4	7.94	0.3	6.0	0.92	1.24	68		68	
5	15.82	-4.7	11.9	0.82	1.32	158		158	
6	7.94	-3.7	11.9	0.78	1.35	771			771
7	3.99	-1.5	6.0	0.81	1.33	184			184
8	1.95	1.7	3.0	0.86	1.28	63			63
9	1.02	5.2	1.5	0.92	1.24	27			27
10	1.98	4.9	1.5	0.95	1.21	357		357	
11	4.04	2.6	3.0	0.93	1.23	89		89	
12	7.94	-1.0	6.0	0.87	1.27	107		107	
13	15.94	-4.6	11.9	0.81	1.33	225		225	
		Max	11.9	1.1	1.33	771.0	0.3	356.9	771.0
		Min	1.0	0.8	1.21	0.3	0.3	43.6	26.6
		Average	5.2	0.9	1.26	164.7	0.3	137.1	261.1

Table A17: 1D-Constrained Modulus for Specimens HCB7

Stage	Vertical stress (MPa)	Vertical strain (%)	Vertical stress-mid value (MPa)	Void ratio-mid value, e	EMDD-mid value (Mg/m^3)	1D-Constrained Modulus (MPa)			
						All	Initial	Loading	Unloading
Pre-Test	0	74.83							
1	1	76.11	0.56	0.75	1.38	72	72		
2	2	74.45	1.51	0.75	1.38	59		59	
3	4	70.81	2.94	0.73	1.40	52		52	
4	8	65.51	5.91	0.68	1.45	77		77	
5	16	61.28	11.92	0.63	1.50	188		188	
6	8	63.97	11.91	0.63	1.51	297			297
7	4	66.68	6.00	0.65	1.48	142			142
8	2	69.32	3.04	0.68	1.45	79			79
9	1	71.98	1.51	0.71	1.42	37			37
10	2	70.90	1.50	0.71	1.42	90		90	
				Max	1.51	297	72	188	297
				Min	1.42	37	72	52	37
				Average	1.46	109	72	93	139

Table A18: 1D-Constrained Modulus for Specimens HCB8

Stage	Vertical stress (MPa)	Vertical strain (%)	Vertical stress-mid value (MPa)	Void ratio-mid value, e	EMDD-mid value (Mg/m^3)	1D-Constrained Modulus (MPa)			
						All	Initial	Loading	Unloading
Pre-Test	0	68.47							
1	1	69.02	0.55	0.69	1.44	162	162		
2	2	67.74	1.45	0.68	1.45	71		71	
3	4	63.16	2.93	0.65	1.48	45		45	
4	8	56.96	5.96	0.60	1.54	64		64	
5	16	51.92	11.94	0.54	1.60	158		158	
6	8	53.55	11.94	0.53	1.62	489			489
7	4	55.79	5.99	0.55	1.60	176			176
8	2	58.56	3.01	0.57	1.57	73			73
9	1	58.74	1.50	0.59	1.55	546			546
10	2	58.90	1.50	0.59	1.55	617		617	
				Max	1.62	617	162	617	546
				Min	1.54	45	162	45	73
				Average	1.58	240	162	191	321

Table A19: 1D-Constrained Modulus for Specimens HCB9

Stage	Vertical stress (MPa)	Vertical strain (%)	Vertical stress-mid value (MPa)	Void ratio-mid value, e	EMDD-mid value (Mg/m^3)	1D-Constrained Modulus (MPa)			
						All	Initial	Loading	Unloading
Pre-Test	0.1								
1A	3.6	-34.79							
1B	5.0	-34.71	4.31	0.64	1.49	1823	1823		
2	8.0	-35.42	6.51	0.64	1.50	423		423	
3	16.0	-37.38	11.99	0.60	1.53	408		408	
5	16.0	-38.53	15.97	0.55	1.60				
6	8.0	-37.43	12.01	0.56	1.58	725			725
7	4.0	-34.41	6.02	0.61	1.52	133			133
8	2.0	-31.12	3.01	0.69	1.44	61			61
9	1.0	-28.37	1.51	0.77	1.36	36			36
				Max	1.60	1823	1823	423	725
				Min	1.36	36	1823	408	36
				Average	1.50	516	1823	416	239

Table A20: 1D-Constrained Modulus for Specimens HCB10

Stage	Vertical stress (MPa)	Vertical strain (%)	Vertical stress-mid value (MPa)	Void ratio-mid value, e	EMDD-mid value (Mg/m^3)	1D-Constrained Modulus (MPa)			
						All	Initial	Loading	Unloading
Initial	0.8								
	0.9	-34.67							
1	2.6	-34.20	1.73	0.66	1.47	368	368		
2	4.0	-34.74	3.30	0.66	1.47	273		273	
3	8.0	-36.75	6.01	0.63	1.50	197		197	
4	16.0	-39.02	11.97	0.58	1.56	350		350	
5	8.0	-38.36	11.98	0.56	1.59	1193			1193
6	4.1	-37.52	6.06	0.58	1.56	464			464
7	1.9	-36.26	3.03	0.60	1.53	173			173
8	0.1	-28.78	1.02	0.71	1.42	25			25
9	2.0	-33.62	1.06	0.75	1.39	40		40	
10	0.1	-31.24	1.06	0.71	1.42	80			80
11	2.1	-33.69	1.09	0.71	1.42	80		80	
12	0.9	-32.96	1.49	0.69	1.44	160		160	
				Max	1.56	1193	368	350	1193
				Min	1.39	25	368	40	25
				Average	1.44	284	368	183	387

Table A21: 1D-Constrained Modulus for Specimens HCB11

Stage	Vertical stress (MPa)	Vertical strain (%)	Vertical stress-mid value (MPa)	Void ratio-mid value, e	EMDD-mid value (Mg/m^3)	1D-Constrained Modulus (MPa)			
						All	Initial	Loading	Unloading
Initial	1	-34.85							
1	1	-33.74	0.83	0.66	1.47	32	32		
2	2	-33.93	1.49	0.67	1.46	530		530	
3	4	-35.00	2.97	0.65	1.48	185		185	
4	8	-36.95	5.87	0.62	1.52	195		195	
5	16	-39.22	11.86	0.56	1.58	360		360	
				Max	1.58	530	32	530	
				Min	1.46	32	32	185	
				Average	1.50	260	32	317	

A5. DISCUSSION

A5.1 BOUNDARY CONDITIONS DURING INITIAL SATURATION

Two types of boundary conditions are used in this test series: initial saturation under constant pressure (HCB7, HCB8, and HCB11) and constant volume (HCB9 and HCB10). In the case of swelling under constant pressure, the displacement of the soil increases with time and eventually equilibrates as shown in Figure A37 for specimen HCB7. Under constant volume boundary conditions, the vertical stress increases up to certain pressure level to maintain constant volume as shown in Figures A12 and A15 for Specimens HCB9 and HCB10. The swelling pressure for specimen with distilled water was higher (i.e., approximately 5 MPa) compared with the specimen with 250 g/L $CaCl_2$ (i.e., approximately 2.5 MPa).

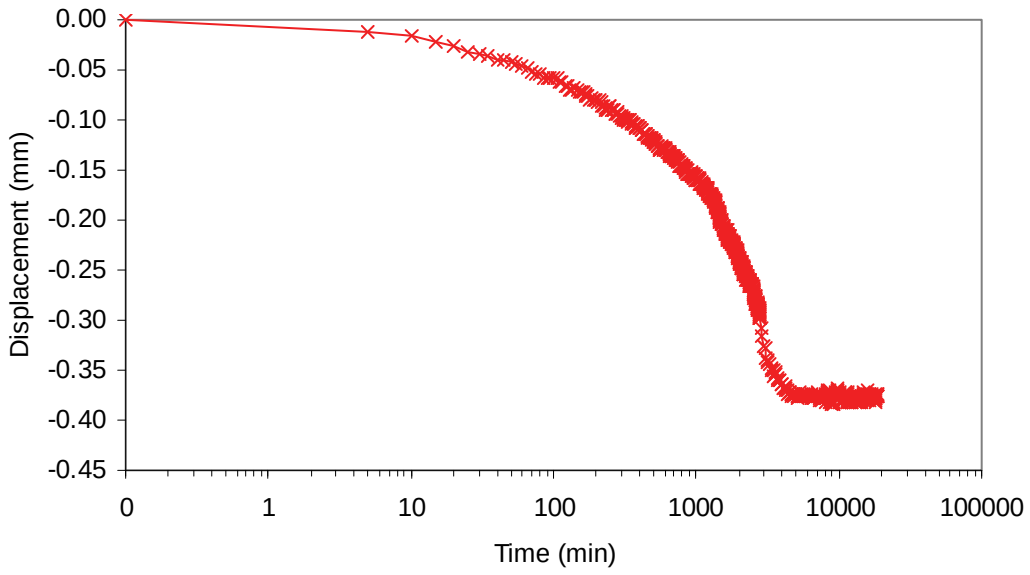

Figure A37: Displacement During Initial Saturation Under Constant Vertical Stress of 1 MPa for Specimen HCB7

A5.2 MECHANICAL CONSTITUTIVE MODEL

The results of 1D-consolidation tests of HCB are evaluated in the framework of two different mechanical constitutive models.

1. Model 1: Log-Linear Relationship;
2. Model 2: Modification of Model 1.

A5.2.1 Model 1: Log-Linear Relationship

The linear elastic constitutive model can only describe the mechanical behaviour of soil within small stress-strain increments. Alternatively, more rigorous constitutive models, such as the critical state model (e.g., Modified Cam-Clay (Roscoe et al. 1958, Roscoe and Burland 1968; Schofield and Wroth 1968)) may be used to define the mechanical behaviour of soil within larger range of stress-strain increments.

Log-linear relationships are used to interpret the results of the oedometer tests. This relationship is a component of a critical state model. In order to develop a complete critical-state model, the results of the oedometer tests need to be combined with the triaxial test results. However, a number of parameters can be determined from the oedometer tests alone, including: compression index (C_c); swelling index (C_s); and pre-consolidation pressure (σ_c). The parameters C_c, C_s, and σ_c are illustrated in Figure A38. These parameters can be determined from the relationship of void ratio (e) versus vertical stress (σ_v) (in log scale). The compression index (C_s) is the slope in the compression line; the swelling index (C_s) is the slope in the swelling line; and the consolidation pressure is the intersection of the swelling line and the compression line. It is recognized that the pre-consolidation pressure (σ_c) is not clearly observed from the results of the 1D-consolidation test. The initial pre-consolidation pressure (σ_c) is estimated from the changes of slopes defining C_c and C_s during the initial load increase.

The values of C_c, C_s, and σ_c for each specimen are summarized in Tables A22. The calculated response using these parameters (i.e., Calculated (model 1)) compared with the results of laboratory tests are illustrated in Figures A39 to A43. These figures show that the critical state model can be used to define the mechanical behaviour of the Highly Compacted Bentonite (HCB) when the vertical stress is greater than 1 MPa. The compression index (C_c) and swelling index (C_s) for all HCB specimens versus void ratio (e) are shown in Figures A43 and A44 respectively.

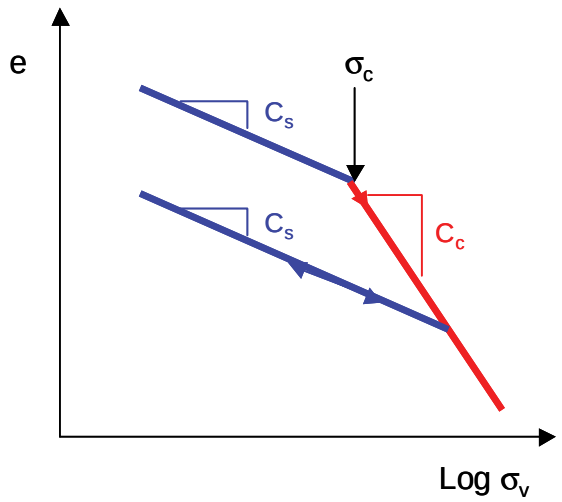

Figure A38: Model 1: Critical State Soil Mechanics Model for 1D-Consolidation

Table A22: Compression Index (Cc), Swelling Index (Cs), and Initial Consolidation Pressure of HCB Specimens

Speci-men No.		Void ratio, e	Dry density (Mg/m^3)	EMDD (Mg/m^3)	C_c	C_s	C_{sf}	Initial Consolidation pressure, σ_c (MPa)	Void ratio corresponds to consolidation pressure, e_c
HCB1	Min	0.63	1.45	1.26	0.42	0.11	0.25	4.00	0.84
	Mid-point	0.76	1.56	1.38	0.42	0.11	0.25	4.00	0.84
	Max	0.89	1.68	1.50	0.42	0.11	0.25	4.00	0.84
HCB2	Min	0.51	1.52	1.33	0.27	0.09	0.30	N/A	N/A
	Mid-point	0.66	1.67	1.49	0.27	0.09	0.30	N/A	N/A
	Max	0.81	1.82	1.65	0.27	0.09	0.30	N/A	N/A
HCB3	Min	0.69	1.47	1.28	0.15	0.09	0.21	4.50	0.83
	Mid-point	0.78	1.55	1.36	0.15	0.09	0.21	4.50	0.83
	Max	0.86	1.62	1.44	0.15	0.09	0.21	4.50	0.83
HCB4	Min	0.56	1.49	1.30	0.19	0.07	0.22	N/A	N/A
	Mid-point	0.70	1.62	1.44	0.19	0.07	0.22	N/A	N/A
	Max	0.84	1.76	1.58	0.19	0.07	0.22	N/A	N/A
HCB5	Min	0.54	1.22	1.04	0.57	0.30	0.00	NA	NA
	Mid-point	0.89	1.50	1.32	0.57	0.30	0.00	NA	NA
	Max	1.24	1.78	1.60	0.57	0.30	0.00	NA	NA
HCB6	Min	0.77	1.31	1.12	0.32	0.15	NA	2.34	1.05
	Mid-point	0.94	1.43	1.24	0.32	0.15	NA	2.34	1.05
	Max	1.10	1.55	1.36	0.32	0.15	NA	2.34	1.05
HCB7	Min	0.61	1.56	1.37	0.16	0.09	NA	4.01	0.74
	Mid-point	0.69	1.63	1.45	0.16	0.09	NA	4.01	0.74
	Max	0.76	1.70	1.52	0.16	0.09	NA	4.01	0.74
HCB8	Min	0.52	1.62	1.44	0.18	0.06	NA	2.35	0.67
	Mid-point	0.60	1.72	1.54	0.18	0.06	NA	2.35	0.67
	Max	0.69	1.81	1.63	0.18	0.06	NA	2.35	0.67
HCB9	Min	0.55	1.52	1.33	0.16	0.09	0.26	8.00	0.64
	Mid-point	0.68	1.65	1.46	0.16	0.09	0.26	8.00	0.64
	Max	0.80	1.77	1.60	0.16	0.09	0.26	8.00	0.64
HCB10	Min	0.55	1.52	1.33	0.19	0.06	0.15	4.13	0.65
	Mid-point	0.68	1.65	1.46	0.19	0.06	0.15	4.13	0.65
	Max	0.81	1.77	1.60	0.19	0.06	0.15	4.13	0.65
HCB11	Min	0.53	1.64	1.46	0.18	NA	NA	3.00	0.67
	Mid-point	0.60	1.71	1.54	0.18	NA	NA	3.00	0.67
	Max	0.67	1.79	1.61	0.18	NA	NA	3.00	0.67

*C_{sf} = slope during unloading under low pressure, see Figure A46.

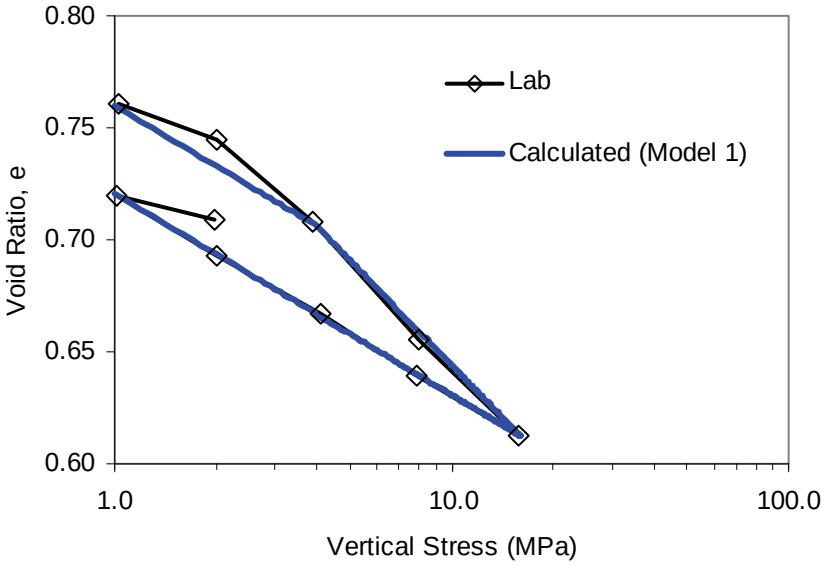

Figure A39: Calculated Response using Critical State Constitutive Model Compared with the Laboratory Results for Specimen HCB7

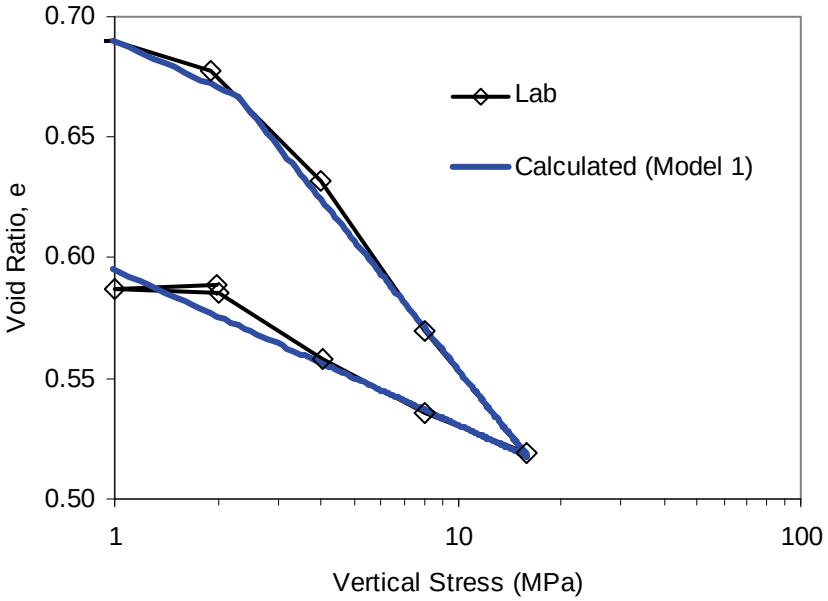

Figure A40: Calculated Response using Critical State Constitutive Model Compared with the Laboratory Results for Specimen HCB8

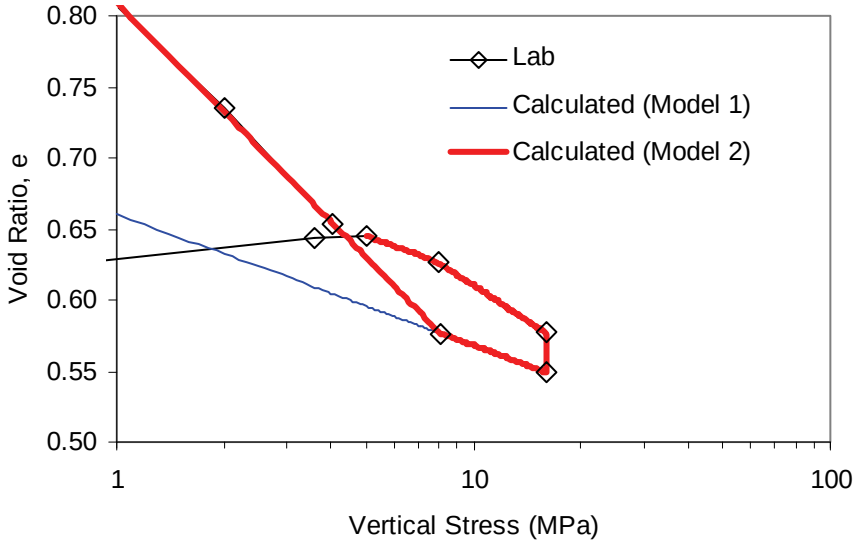

Figure A41: Calculated Response using Critical State Constitutive Model (Model 1) and Modified Model (Model 2) Compared with the Laboratory Results for Specimen HCB9

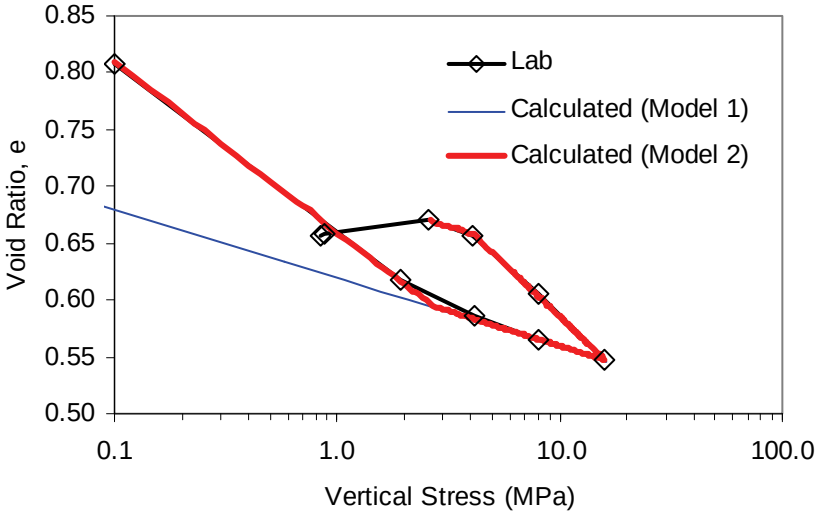

Figure A42: Calculated Response using Critical State Constitutive Model (Model 1) and Modified Model (Model 2) Compared with the Laboratory Results for Specimen HCB10

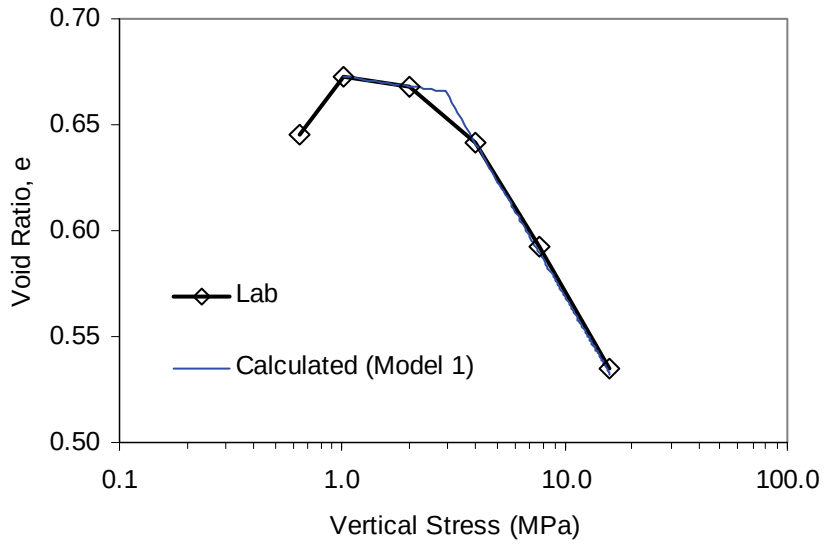

Figure A43: Calculated Response using Critical State Constitutive Model (Model 1) Compared with the Laboratory Results for Specimen HCB11

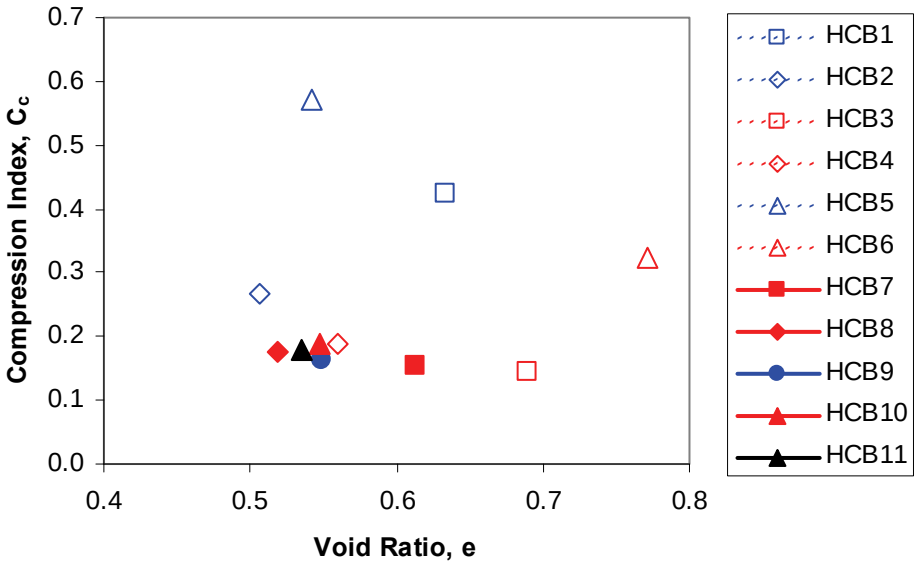

Figure A44: Compression Index (C_c) for HCB Specimens

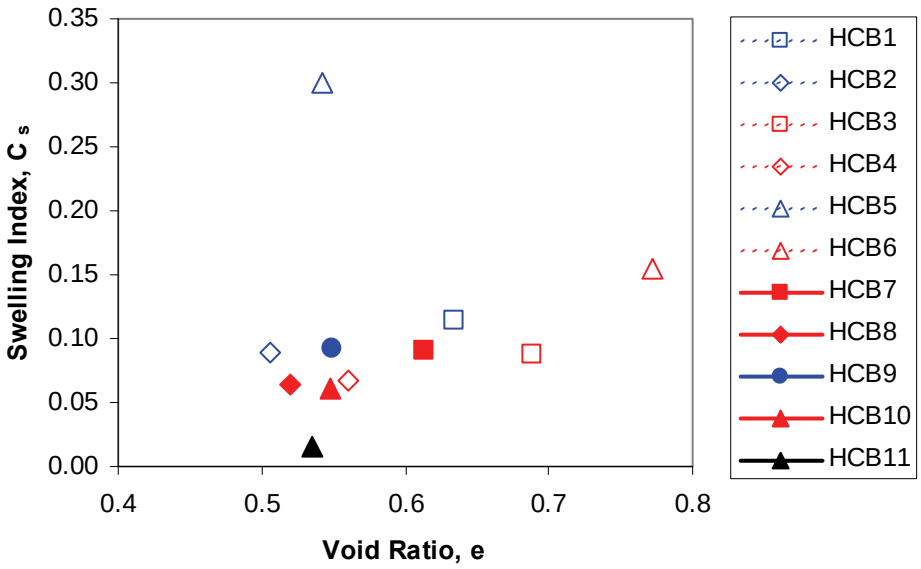

Figure A45: Swelling Index (C_s) for HCB Specimens

A5.2.2 Model 2: Modification Of Model 1

The 1D-consolidation test results of HCB9 and HCB10 (Figures A41 and A42) show that in log-linear scale the slope of the swelling curve under high vertical stress is less than that under low vertical stress. Similar behaviour was also observed on DBF materials with various sand contents (i.e., 70% to 85%) (N. A. Chandler, personal communication, 2007). The log-linear relationship (i.e., Model 1) described in section A5.2.1 underestimates the swelling under low vertical stress. This suggests the modification of model 1 in order to simulate the behaviour of the HCB under low pressure.

A possible modification of model 1 is shown in Figure A46. The vertical stress (σ_v^{cv}) that results in constant volume of the specimen is dependent on the void ratio (e). Assuming that σ_v^{cv} decreases with an increase of void ratio, the Constant Volume Line (CVL) can be created (Figure A46). When the vertical stress is less than this line, the swelling index (C_s) increases becoming the new swelling index (C_{sf}) (Figure A46).

The response calculated using this constitutive model compared to the laboratory data is shown in Figures A41 and A42 as Model 2 for Specimens HCB9 and HCB10 respectively. Further investigation to develop the Constant Volume Line (CVL) is still required. The work scope in 2008 discussed in Section 6.1 includes the investigation the HCB under low pressure.

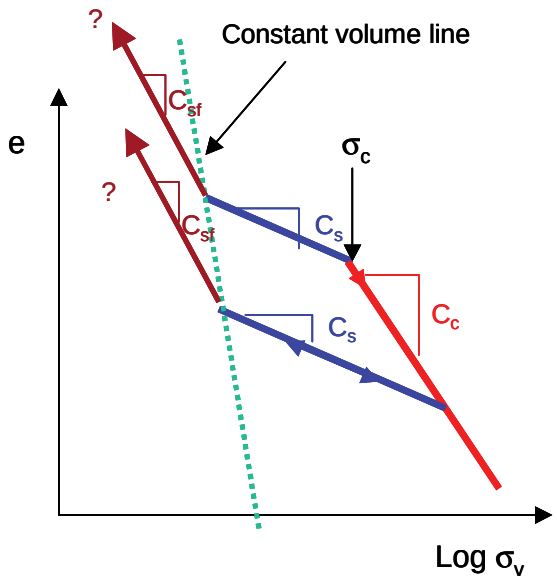

Figure A46: Model 2: Modification of Log-Linear Relationship (Model 1) for HCB Specimen

A5.3 APPLICATIONS OF PARAMETERS IN NUMERICAL MODELLING

The parameters from 1D consolidation results should be combined with the results of the triaxial tests (Blatz et al. 2008) to provide a complete critical state mechanical constitutive model. The parameters C_c and C_s are generated from the slope of void ratio (e) versus vertical stress (σ_v) results from the oedometer tests. This forms the critical state description in specific volume (V) – ln p' space. The triaxial test data provide the q-p' space description, which completes the critical state model. The combined oedometer and triaxial test derived critical state model can then be used directly in numerical modelling using Finite Element (FE) or Finite Different (FD) computer code.

A5.4 EFFECTS OF PORE LIQUID CHEMISTRY, LIQUID USED IN SPECIMEN PREPARATION, AND BOUNDARY CONDITIONS APPLIED DURING INITIAL SATURATION

A5.4.1 Effect Of Pore Liquid Chemistry

A5.4.1.1 Specimens Prepared with Distilled Water

Figure A47 shows comparison of the results of specimens prepared with distilled water (DW) having different pore liquid concentration in the oedometer reservoir (i.e., HCB1 (DW); HCB7 (250 g/L $CaCl_2$); and HCB11 (150 g/L $CaCl_2$). The reductions of void ratio (e) due to an increase in vertical stress from 1 MPa to 16 MPa are 0.27 for specimen HCB1 (DW), 0.14 for specimen HCB11 (150 g/L), and 0.15 for specimen HCB7 (250 g/L). The reduction of void ratio (e) for specimen with distilled water (i.e., HCB1) is greater than specimens with saline pore liquid (i.e., HCB11 and HCB7). The reductions of void ratio (e) for specimens HCB11(150 g/L) and HCB7 (250 g/L) are relatively similar (i.e., 0.14 versus 0.15). The different initial void

ratio (e) of specimen HCB7 and HCB11 prior to the load increase (i.e., 1 MPa) causes the reduction of void ratio (e) for specimens HCB7 (250 g/L) greater than HCB11 (150 g/L). Greater initial void ratio (e) means lower dry density (ρ_{dry}) and increases the compressibility of the specimen.

The slopes of compression index (C_c) and swelling index (C_s) illustrated in Figure A38 are calculated for each specimen. The compression index (C_c) and swelling index (C_s) versus pore liquid concentration are shown in Figures A48 and A49. The compression index (C_c) and swelling index (C_s) decrease with an increase in $CaCl_2$ concentration indicating that material becomes stiffer. For a concentration increase from 0 to 250 g/L, the compression index (C_c) decreases from 0.4 to 0.1 and the swelling index (C_s) decreases from 0.15 to 0.09.

The values of compression index (C_c) and the reduction of void ratio (e) for specimens HCB7 and HCB11 are relatively similar. It may indicate that the increase of the pore liquid salinity only decreases the compression index up to certain concentration (i.e, less than 150 g/L in this case). When the pore liquid concentration is greater than this value, the change of pore liquid concentration does not change the value of compression index (C_c). This relationship is illustrated in Figure A48 and A49 as "possible relationship". The relationships in Figures A48 and A49 can be used to incorporate the effect of pore liquid concentration on the mechanical behaviour in numerical modelling of HCB. This figure shows that the addition of saline pore liquid reduces the amount of swelling and reduces the slope of e-log σ_v curves.

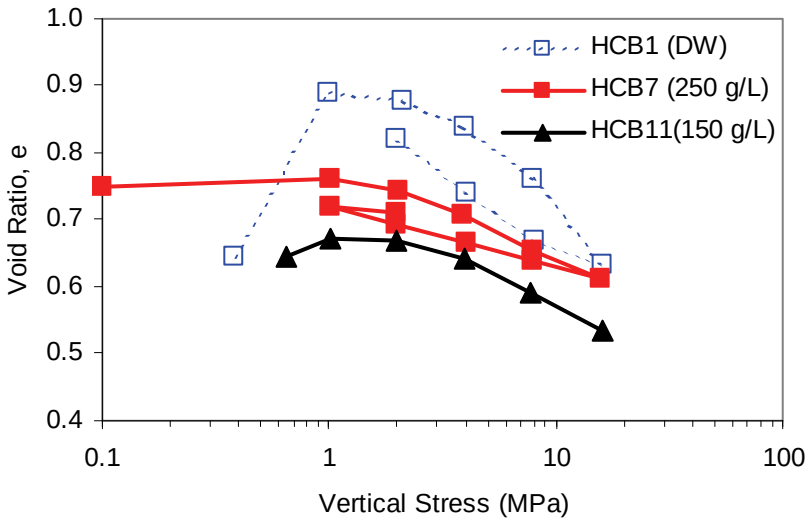

Figure A47: Void Ratio (e) versus Vertical Stress (σ_v) for Specimens Prepared with Distilled Water with Different Reservoir Liquid

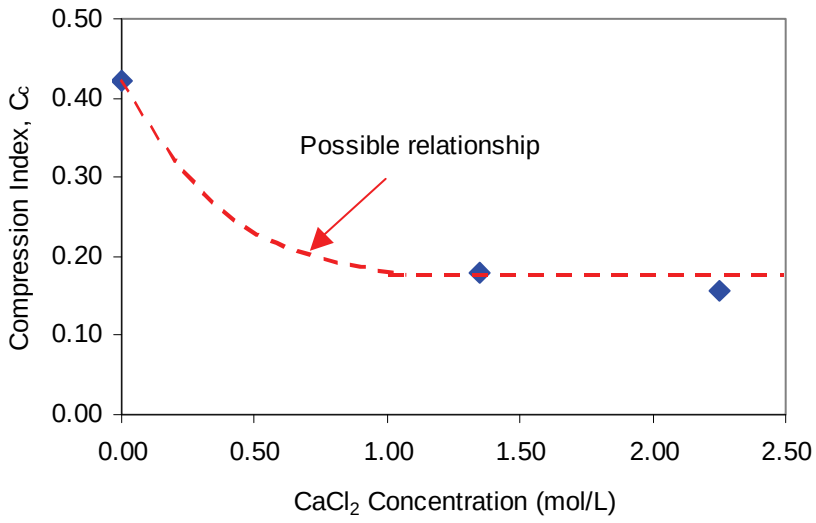

Figure A48: Compression Index (C_c) versus Concentration of $CaCl_2$ in Pore Liquid for Specimens Prepared using Distilled Water with Different Reservoir Liquid

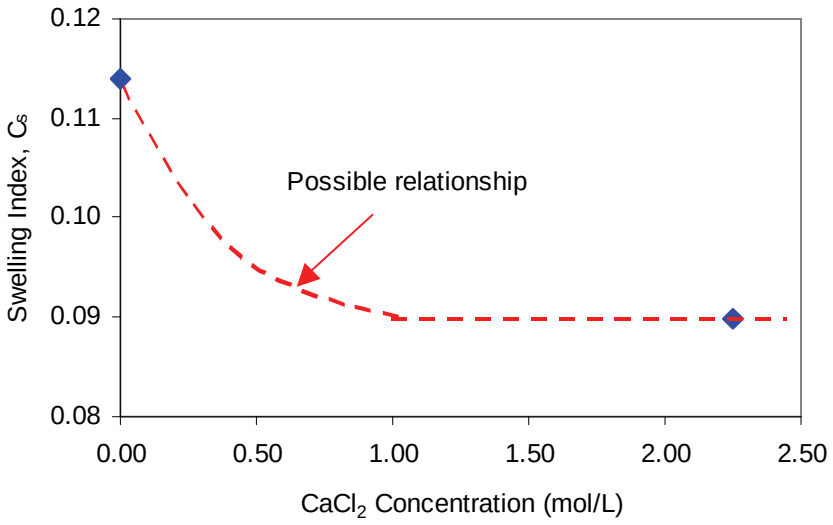

Figure A49: Swelling Index (C_c) versus Concentration of $CaCl_2$ in Pore Liquid for Specimens Prepared using Distilled Water with Different Reservoir Liquid

A5.4.1.2 Specimens Prepared with Salt Solution

Specimen HCB3 and HCB8 are prepared with 75 g/L and 250 g/L $CaCl_2$ respectively and similar liquids are added in the reservoir. Specimen HCB1 uses distilled water in specimen preparation and reservoir liquid. Comparison of the results of specimens HCB1, HCB3, and

HCB8 is used to examine the effect of pore liquid concentration. Specimens HCB1 and HCB3 have a higher void ratio compared to Specimen HCB8 due to different conditions applied during initial saturation. The compression index (C_c) and swelling index (C_s) versus pore liquid concentration are shown in Figures A51 and A52. The compression index (C_c) and swelling index (C_s) decrease with an increase of $CaCl_2$ concentration. The relationship in Figures A51 and A52 may be used to incorporate the effect of pore liquid concentration on the mechanical behaviour in numerical modelling of HCB.

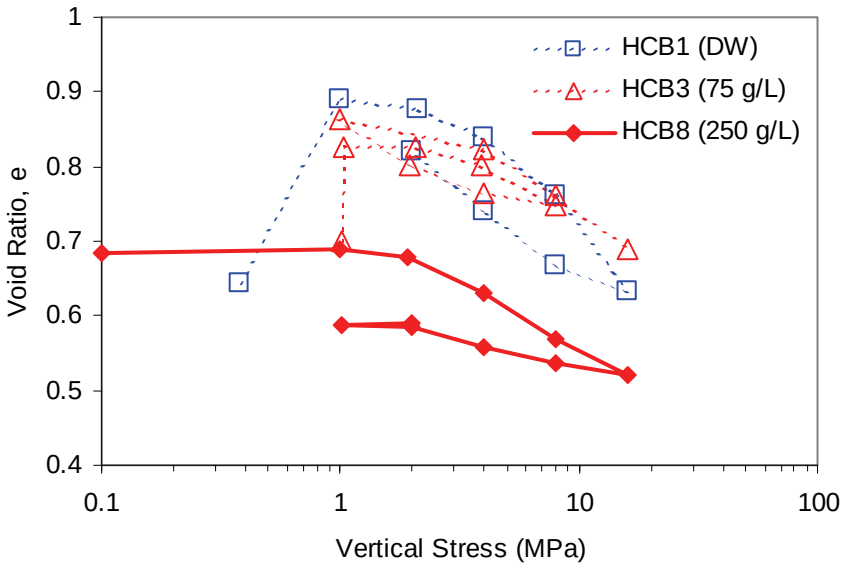

Figure A50: Void Ratio (e) versus Vertical Stress (σ_v) for Specimens Prepared with Different Mixing and Reservoir Liquid

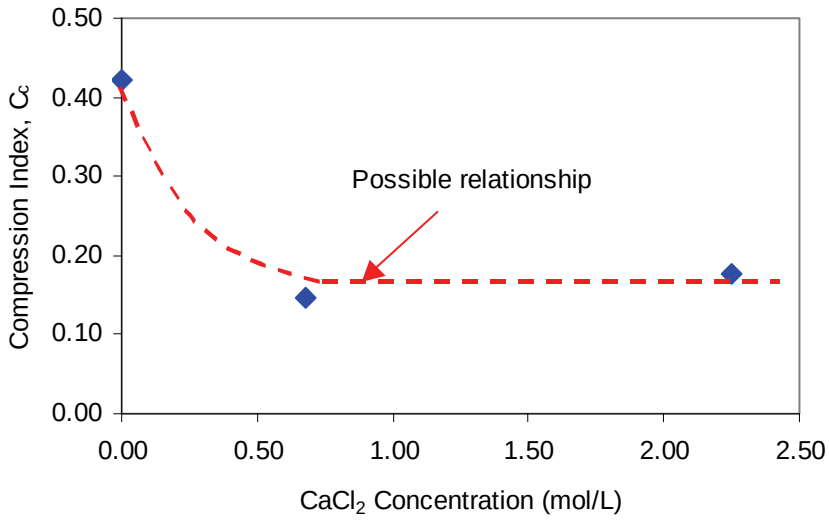

Figure A51: Compression Index (C_c) versus Concentration of $CaCl_2$ in Pore Liquid for Specimens Prepared with Different Mixing and Reservoir Liquid

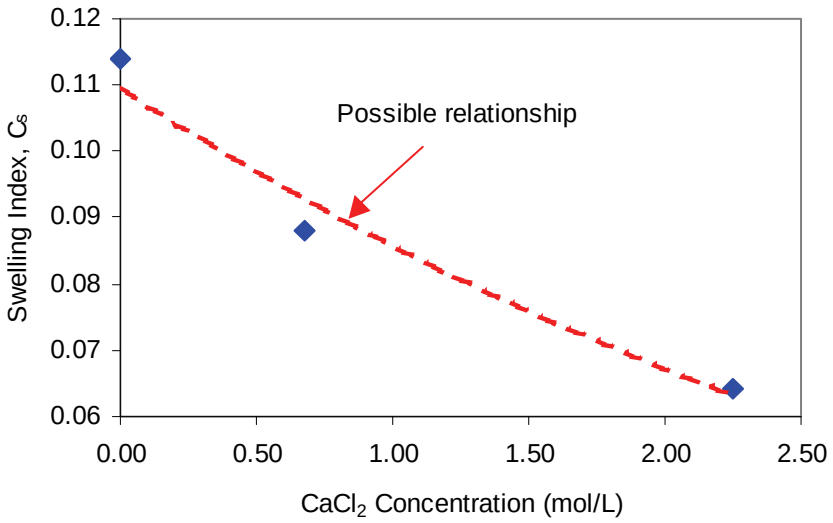

Figure A52: Swelling Index (C_s) versus Concentration of $CaCl_2$ in Pore Liquid for Specimens Prepared with Similar Mixing and Reservoir Liquid

A5.4.2 Effect Of Pore Liquid Used In Specimen Preparation

The effect of the liquid used in the specimen preparation can be examined by the comparison of specimens HCB1, HCB7, and HCB11 for specimens mixed with distilled water (Figure A47) and specimens HCB1, HCB3 and HCB8 for specimens mixed with salt solution with different concentrations (Figure A50). Distilled water is used in preparation of specimen HCB1 and provided in the reservoir during the test. Specimens HCB7 and HCB11 are prepared with distilled water, but $CaCl_2$ solutions with different concentrations are provided in the reservoir during the test. Specimens HCB3 and HCB8 are prepared with $CaCl_2$ solution with different concentrations and similar solutions are provided in the reservoir during the test.

The compression index (C_c) and swelling index (C_s) versus pore liquid concentration of these specimens are shown in Figures A53 and A54, which indicate that different liquids used in specimen preparation may only affect the swelling index (C_s) (Figure A54), but may not affect the compression index (C_c) (Figure A53).

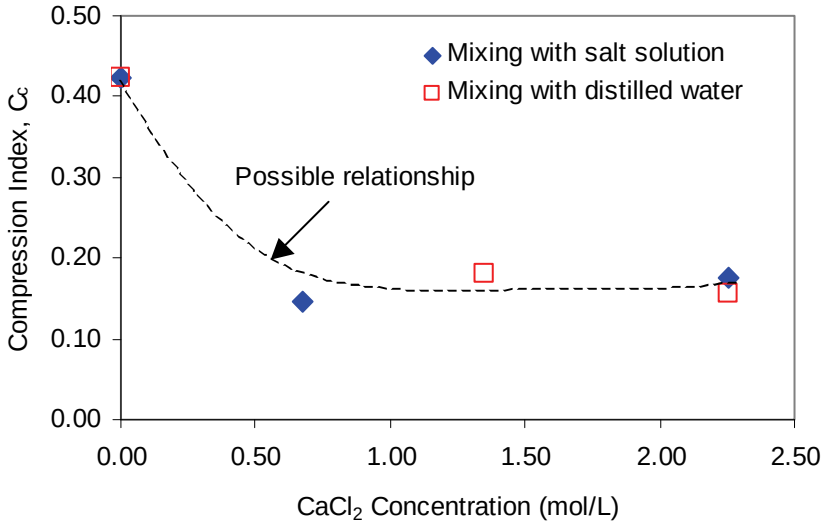

Figure A53: Compression Index (C_c) versus Concentration of $CaCl_2$ in Pore Liquid

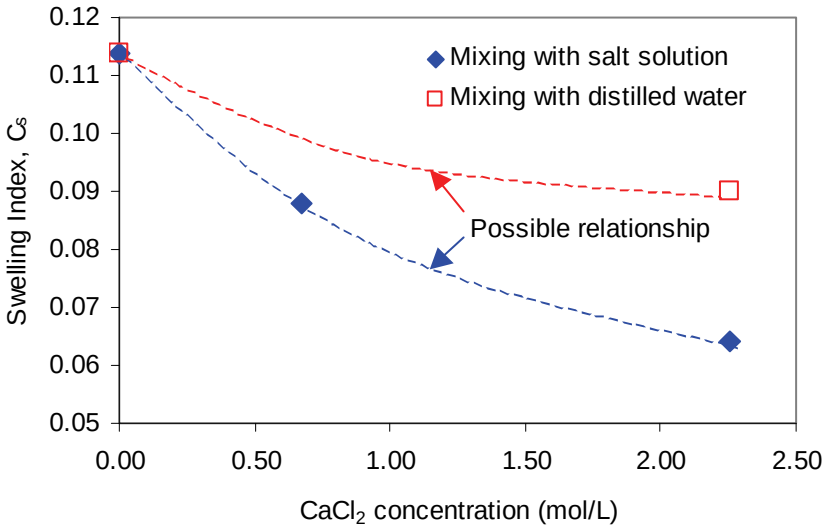

Figure A54: Swelling Index (C_s) versus Concentration of $CaCl_2$ in Pore Liquid

A5.4.3 Effect Of Boundary Conditions During Initial Saturation

The effect of boundary conditions applied during initial saturation can be examined by comparison of specimens HCB1 and HCB9 for specimens prepared with distilled water (DW) (Figure A55) and comparison of specimens HCB8 and HCB10 for specimens prepared with 250 g/L $CaCl_2$ (Figure A56). However, the compression index (C_c) and swelling index (C_s) versus pore liquid concentration of these specimens are shown in Figures A57 and A58. For specimens with 250 g/L $CaCl_2$, the initial boundary condition applied at initial saturation does

not affect the mechanical behaviour of HCB. However, the specimens prepared with distilled water with constant volume conditions has lower C_c and C_s values compared to the specimens with constant pressure conditions (Figures A57 and A58). This difference in C_c and C_s is likely due to the higher initial void ratio of specimens HCB1 than HCB9. The higher initial void ratios increase the value of C_c and C_s indicating that these parameters are stress path-dependent. Further investigation is required to better define the effect of boundary conditions.

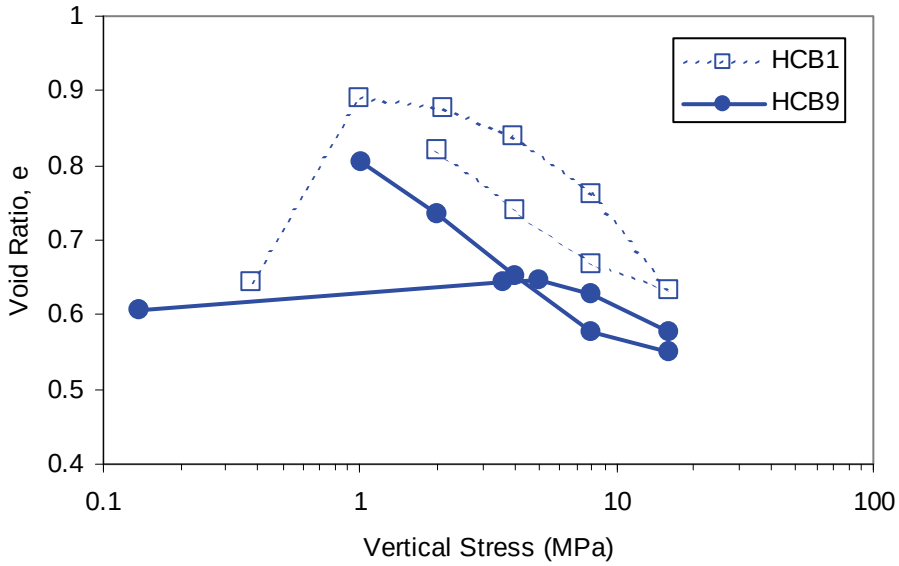

Figure A55: Void Ratio (e) versus Vertical Stress (σ_v) for Specimens having Distilled Water as Mixing and Reservoir Liquid with Different Boundary Condition during Initial Saturation (HCB1-Constant Pressure; HCB9 - Constant Volume)

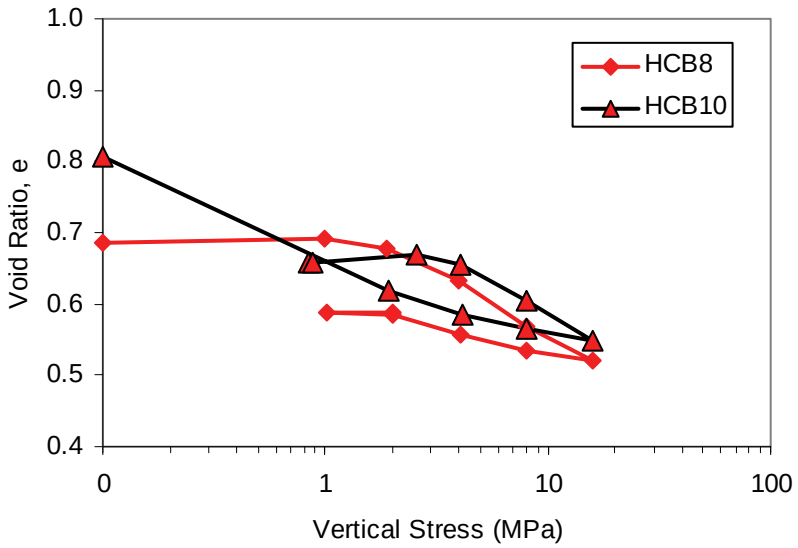

Figure A56: Void Ratio (e) versus Vertical Stress (σ_v) for Specimens having 250 g/L $CaCl_2$ as Mixing and Reservoir Liquid with Different Boundary Condition during Initial Saturation (HCB8-Constant Pressure; HCB10-Constant Volume)

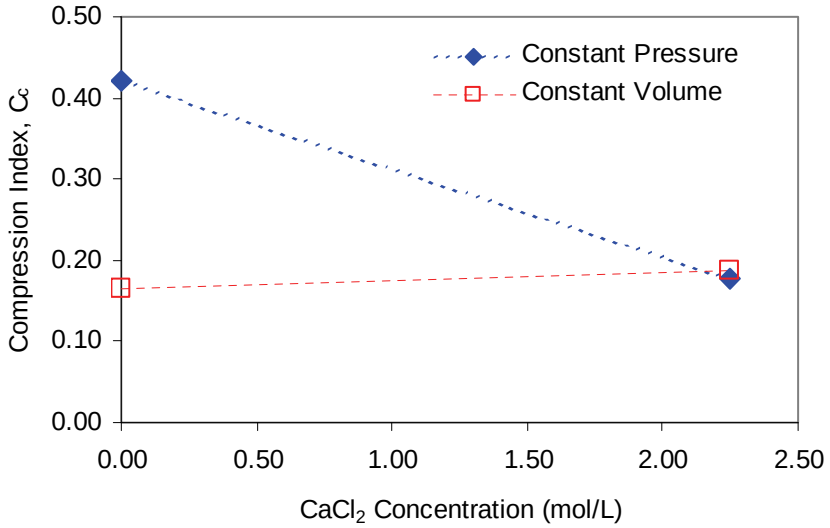

Figure A57: Compression Index (C_c) versus Pore Liquid Concentration for Specimens with Different Boundary Condition during Initial Saturation

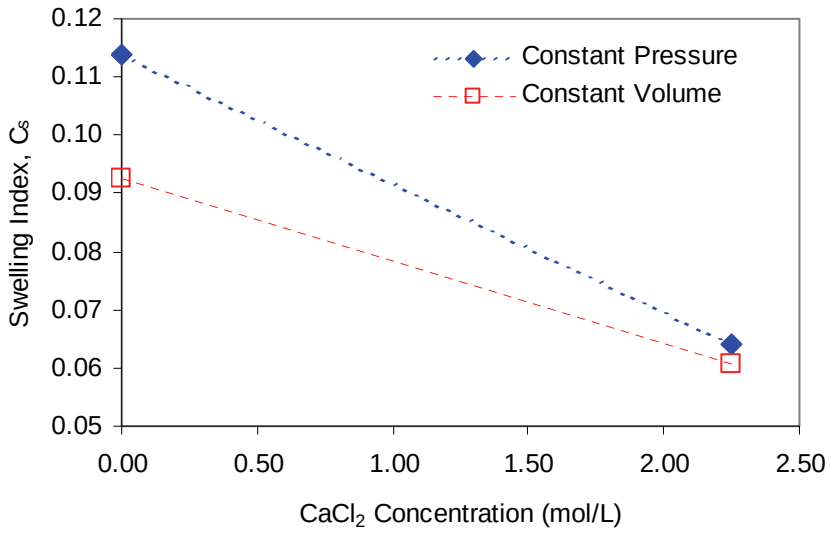

Figure A58: Swelling Index (C_s) versus Pore Liquid Concentration for Specimens with Different Boundary Condition during Initial Saturation

A6. CONCLUDING REMARKS

1. 1D-Constrained modulus (M) of HCB has been calculated from the stress-strain increments, which varies from 10 to 1000 MPa for EMDD within the range of 1.2 to 1.6 Mg/m^3. The results indicate that a linear-elastic model can only be used to describe mechanical behaviour of the HCB within small stress-strain increments. A more rigorous constitutive model (i.e., Modified Cam-Clay (Roscoe and Burland 1968)) should be used to define mechanical behaviour of HCB involving high range of stress-strain increments.

2. Mechanical constitutive model parameters including compression index (C_c), swelling index (C_s) and preconsolidation pressure (σ_c) were determined from the 1D consolidation tests on HCB. The range of the C_c and C_s parameters are 0.15 to 0.42 and C_s = 0.06 to 0.15, respectively. Combined with the results of triaxial tests, these parameters can be used to develop a modified cam-clay model (Roscoe and Burland 1968) to describe the behaviour of HCB.

3. The effects of the pore liquid concentration, liquid type used in the specimen preparation, and boundary conditions applied during initial saturation were examined and the following has been note.

    - The Compression Index (C_c) and the Swelling Index (C_s) of HCB decrease with an increase of the concentration of $CaCl_2$ as pore liquid. The relationship of these indices with the $CaCl_2$ concentration in pore liquid has been presented in this report. This relationship can be used to incorporate the effect of change in pore liquid chemistry to the mechanical behaviour of HCB.

- The liquid used in specimen preparation affects the value of swelling index (C_s), but it does not appear to affect the compression index (C_c).
- The boundary condition applied during the initial saturation establishes the initial void ratio or dry density of the specimen. It does not affect the behaviour of HCB specimens prepared with 250 g/L $CaCl_2$, but it affects the behaviour of specimens prepared with distilled water. Further investigation is still required to examine this effect.

4. The coefficients of consolidation (c_v) have been determined from the results of 1D consolidation tests. The hydraulic conductivity (K) calculated from c_v is within the range of 1×10^{-15} to 1×10^{-11} m/s for EMDD within the range of 1.6 to 1.1 Mg/m^3 respectively and it decreases with increasing EMDD. The results are comparable with the hydraulic conductivity (K) of the bentonite measured using hydraulic conductivity cells by Dixon et al. (1999).

5. The 1D consolidation result indicates that the swelling index (C_s) significantly increases for specimens under low vertical stress. A suggested modification of the existing constitutive model has been presented to incorporate this behaviour.

ACKNOWLEDGEMENTS

The authors gratefully acknowledge the technical support from P. Baumgartner, the careful and dedicated laboratory work by C.L. Kohle and D. Drew, and assistance of F. Johnston and T. Reimer during the laboratory tests.

REFERENCES

ASTM (ASTM International). 2004. Standard test methods for one-dimensional consolidation properties of soils using incremental loading. Standard D2435-04, ASTM International, West Conshohocken, Pennsylvania, USA.

ASTM (ASTM International). 2005. Standard Test Methods for Laboratory determination of water (moisture) content of soil and rock by mass. Standard D 2216-05, ASTM International, West Conshohocken, Pennsylvania, USA.

Baumgartner, P. and G.R. Snider. 2002. Seal Evaluation and Assessment Study (SEAS): Light backfill placement trials. Atomic Energy of Canada Limited Technical Record, TR-793.

Baumgartner, P., D. G. Priyanto, J. R. Baldwin, J. A. Blatz, B. H. Kjartanson, and H. Batenipour. 2008. Preliminary Results of One-Dimensional Consolidation Testing on Bentonite Clay-Based Sealing Components Subjected to Two Pore-Fluid Chemistry Conditions. Nuclear Waste Management Organization (NWMO) Technical Report No. TR-2008-04. Toronto, Canada.

Blatz, J.A., Siemens, G.A. and A. G. Man. 2008. Triaxial characterization of light and dense backfill to determine properties for use in numerical modeling. Nuclear Waste Management Organization (NWMO) Technical Report No. TR-2008-05. Toronto, Canada.

Budhu, M. 2000. Soil Mechanics and Foundations. John Wiley and Sons.

Cassagrande, A., and Fadum, R. E. 1940. “Notes on Soil Testing for Engineering Purposes.”Soil Mechanics Series, Graduate School of Engineering, Harvard University, Cambridge, MA, Vol. 8(268), p. 37.

Craig, R.F. 1992. Soil Mechanics, 5th Edition. E & FN Spoon, London.

Das, B.M. 1998. Principles of Geotechnical Engineering, 4th Edition. PWS Publishing Company, Boston, MA.

JNC (Japan Nuclear Cycle Development Institute). 2000. H12: Project to establish the scientific and technical basis for HLW disposal in Japan. Supporting report 2: Repository design and engineering technology. Japan Nuclear Cycle Development Institute Report, JNC TN 1400 2000-003.

Lide, D.R., ed. 2007. CRC Handbook of Chemistry and Physics, Internet Version 2007, (87th Edition), http://www.hbcpnetbase.com

Priyanto, D.G. 2007. Development and Application of New Constitutive Models to Simulate the Hydraulic and Mechanical Behaviours of Unsaturated Swelling Clay. Ph.D Thesis. Department of Civil Engineering, University of Manitoba, Canada.

Roscoe, K. H., Schofield, A. N., & Wroth, C. P. 1958. On the yielding of soils. *Géotechnique*, *8*, 22-53.

Roscoe, K. H., & Burland, J. B. 1968. On the generalized stress-strain behaviour of 'wet' clay. In J. Heyman & F. Leckie (Eds.), *Engineering Plasticity* (pp. 535-609). Cambridge:

Schofield, A. N., & Wroth, C. P. 1968. *Critical state soil mechanics*. London: McGraw Hill.

Taylor, D. W. 1942. Research on Consolidation of Clays. Serial No. 82, Massachusetts Institute of Technology, Cambridge.

Terzhagi, K. 1943. Theoretical Soil Mechanics. Wiley, New York.

APPENDIX B:
DENSE BACKFILL (DBF)

D. G. Priyanto[1], J. A. Blatz[2], and R. Offman[2]
[1]Atomic Energy of Canada Limited
[2]University of Manitoba

CONTENTS

LIST OF TABLES

Page

LIST OF FIGURES

Page

B1. DBF

Dense backfill (DBF) is a clay-based sealing-system component proposed for use in a nuclear fuel waste repository (Maak and Simmons 2005). The DBF proposed for repository use is composed of 5% bentonite, 25% glacial clay and 70% crushed granite aggregate by mass (Russell and Simmons 2003). It is to be compacted to a dry density of 2120 kg/m^3 at a water content of 8.5%, producing an initial degree of saturation of ~80%. For the consolidation tests, a DBF, composed of 75% crushed granite, 18.75% crushed illite clay (i.e., Sealbond) and 6.25% Avonlea bentonite, from a previous experiment in the URL (the BCE (Graham et al. 1997)), was supplied to the University of Manitoba's Geotechnical Laboratory by Atomic Energy of Canada Limited. This previously prepared material was used for two main reasons. Firstly, this material is well characterised and is consistent with DBF previously used in geotechnical testing and secondly, there is no commercial source of glacial lake clay. Any backfill material produced in an effort to match the reference DBF composition of Russell and Simmons (2003) would not necessarily be representative of backfill proposed for use in a repository. The bulk mechanical behaviour of the DBF used in the testing and the reference material is also anticipated to be similar. Therefore for consistency of testing and comparability of previous study results, the DBF used is the 75% granite – 25% clay blend material.

B2. TESTING MATRIX IN 2007

The testing plans for 1D consolidation tests in 2007 are shown in Table 1, which include two boundary conditions and two types of liquid used in sample mixing (i.e., distilled water (DW), and 250 g/L calcium chloride ($CaCl_2$) solution). Table 2 shows the loading sequence used in all four tests. Due to the low hydraulic conductivity and the large size of the DBF specimens, the tests took longer time than it was anticipated. Only two tests are shown in this report, the complete results of the tests will be presented in the technical report in the following year.

Table B1: Testing Matrix for 1D Consolidation Tests for DBF at the University of Manitoba in 2007

Test No.	Sample No.	Mixing Liquid	Reservoir Liquid	Swelling % on Initial Saturation	Loading Path □
1.	DBF1	250 g/L $CaCl_2$	250 g/L $CaCl_2$	20	Load to 4000 kPa after initial swelling
2.	DBF2	DDW	250 g/L $CaCl_2$	20	Load to 4000 kPa after initial swelling
3.	DBF3	250 g/L $CaCl_2$	250 g/L $CaCl_2$	Rigidly confined	Load to 4000 kPa after initial swelling
4.	DBF4	DDW	250 g/L $CaCl_2$	Rigidly confined	Load to 4000 kPa after initial swelling

* See Table 2

Table B2: Loading Sequence for the DBF Samples

Stage	Load Schedule Type 2
Step 1	Load to 1 MPa
Step 2	Load to 2 MPa
Step 3	Load to 4 MPa
Step 4	Unload to 2 MPa
Step 5	Unload to 1 MPa
Step 6	Unload to 0.5 MPa
Step 7	Load to 1 MPa
Step 8	Load to 2 MPa
Step 9	Load to 4 MPa

B3. PRELIMINARY RESULTS

Physical tests of Specimen DBF1 and DBF2 are current to December 2007. The next two tests (i.e., Tests No. 3 and 4) have been installed in the oedometer cells. These tests are expected to be complete in March 2008. The preliminary results up to December 2007 are shown in Figures B1 to B4. Figures B1 and B3 show the sample thickness and vertical stress versus time for Specimen DBF1 and DBF2. Figures B2 and B4 show the void ratio (e) versus vertical stress (σ_v) for Specimens DBF1 and DBF2. Specimens DBF1 and DBF2 were originally planned to experience 20% swelling on initial saturation, but 20% swelling did not occur during initial saturation. It may due to the initial load applied to the specimen was to high, the low montmorillonite content of the material, and low initial dry density of the specimens. Considering the length of initial saturation that required 35 days, the tests continued. The load applied on specimens DBF1 and DBF2 were increased from 0, 1, 2, and 4MPa. The load was decreased to 2 and 1 MPa. The specimens DBF1 and DBF2 were in the initial stage of 1 MPa load increment in December 2007.

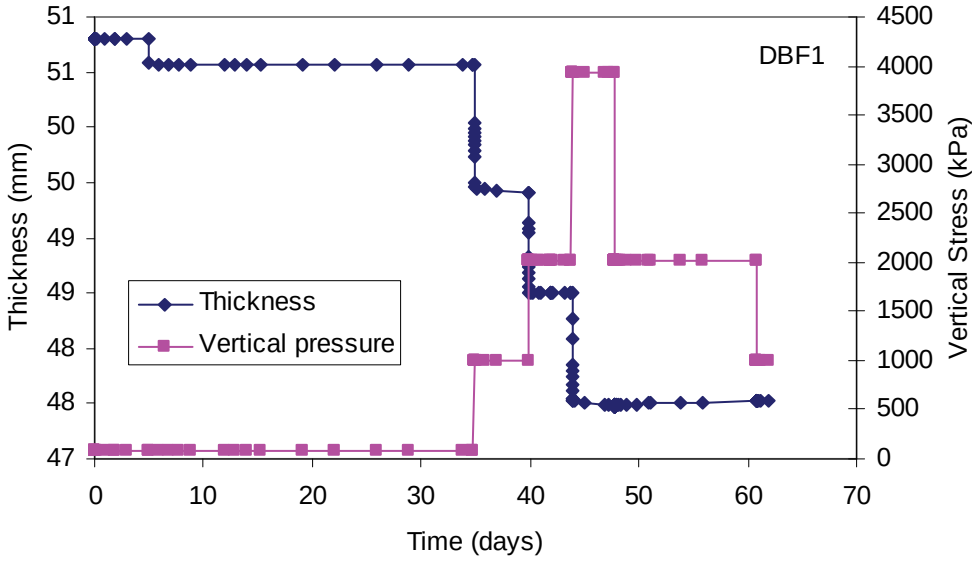

Figure B1: Sample Thickness and Vertical Stress versus Time for Test No 1 (Mixing Liquid: 250 g/L $CaCl_2$; Reservoir Liquid: 250 g/L $CaCl_2$) Results Current to December 2007

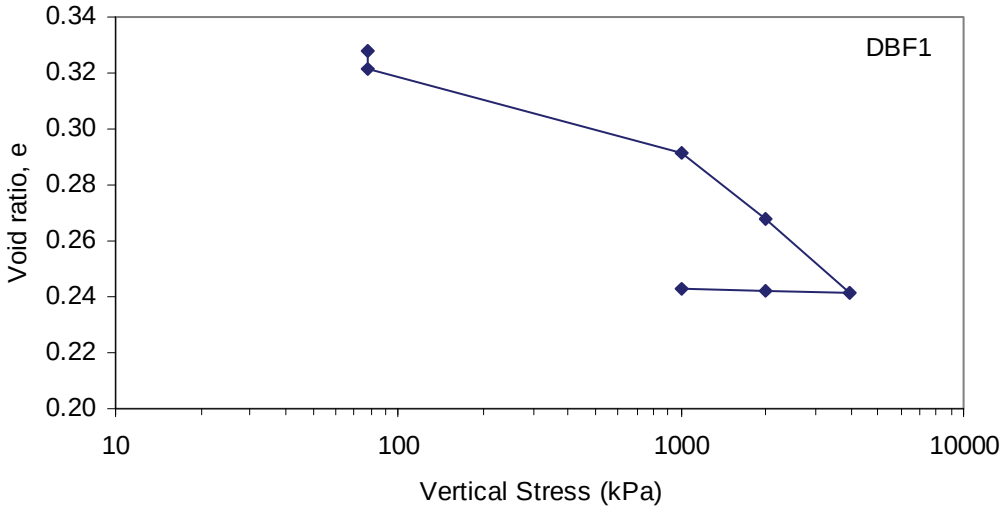

Figure B2: Void Ratio (e) versus Vertical Stress (σ_v) for Test No 1 (Mixing Liquid = 250 g/L $CaCl_2$; Reservoir Liquid = 250 g/L $CaCl_2$) Results Current to December 2007

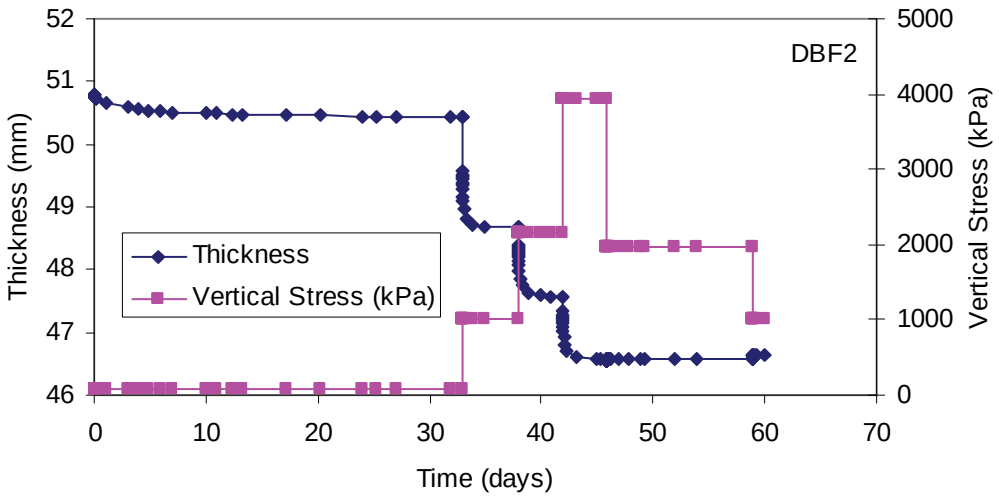

Figure B3: Sample Thickness and Vertical Stress versus Time for Test No 2 (Mixing Liquid = DDW; Reservoir Liquid = 250 g/L $CaCl_2$) Result Current to December 2007

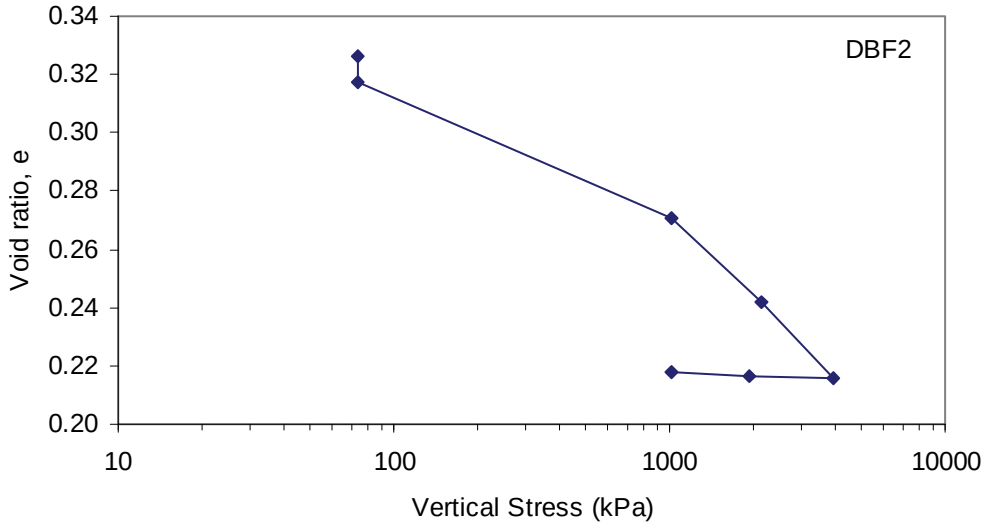

Figure B4: Void Ratio (e) versus Vertical Stress (σ_v) for Test No 2 (Mixing Liquid = DDW; Reservoir Liquid = 250 g/L $CaCl_2$) Result Current to December 2007

B4. COMPLETION OF TESTS

The final report will provide:

- parameters C_c and C_s interpreted from the 1D consolidation tests; and
- the discussions on the effects of pore liquid salinity used as mixing liquid in sample preparation and boundary condition applied during initial saturation.

REFERENCES

Maak, P. and G.R. Simmons. 2005. Deep geologic repository concepts for isolation of used fuel in Canada. In Proc. Canadian Nuclear Society conference Waste Management, Decommissioning and Environmental Restoration for Canada's Nuclear Activities: Current Practices and Future Needs. 2005 May 8-11, Ottawa.

Russell, S.B. and G.R. Simmons. 2003. Engineered barrier system for a deep geologic repository. Presented at the 2003 International High-Level Radioactive Waste Management Conference. 2003 March 30-April 2, Las Vegas, NV.